REPUBLIQUE ALGERIENNE DEMOCRATIQUE ET POPULAIRE

Ministère de l'Enseignement Supérieur et de la Recherche Scientifique

Université Hadj Lakhdar - BATNA 1

Faculté des Sciences de la Matière
Département de Physique

THÈSE

Présentée en vue de l'obtention du

Diplôme de Doctorat

Par :

Rahmouni Ibrahim

Thème :

Le biogaz comme combustible d'un moteur à combustion interne

Domaine	: Sciences de la Matière
Filière	: Physique
Spécialité	: Physique énergetique
Intitulé de la Formation	: Physique énergétique appliquée

Soutenue le 21/12/2023

Devant le jury :

Président:	Soudani Azeddine	Professeur	Université de Batna 1
Rapporteur:	Adouane Belkacem	Professeur	Université de Batna 1
Examinateurs:	Mameri Abdelbaki	Professeur	Université Larbi Ben M'hidi O.E.B
	Ferahta Fatima Zohra	MCA	Université de Batna 1

Democratic and Popular Republic of Algeria
Ministry of Higher Education and Scientific Research

University El-Hadj Lakhdar - BATNA 1
Faculty of Science of matter
Department of Physics

THESE

Submitted in order to obtain

Doctorate Diploma

by:

Rahmouni Ibrahim

Theme:

Biogas as a fuel for an internal combustion engine

Domain	: Science of matter
Sector	: Physics
Speciality	: Energetic Physics
Title of Training	: Applied Energetic Physics

Defended on 21/12/2023

In front of the jury:

Président:	Soudani Azeddine	Professor	University of Batna 1
Supervisor:	Adouane Belkacem	Professor	University of Batna 1
Examiners:	Mameri Abdelbaki	Professor	Université Larbi Ben M'hidi O.E.B
	Ferahta Fatima Zohra	MCA	University of Batna 1

To my Parents

ACKNOWLEDGEMENTS

Before proceeding, I express my gratitude to **ALLAH** for providing me with the strength and guidance to complete this study and research. Alhamdulillah.

Foremost, I extend my deepest gratitude to **Pr. Belkacem Adouane**, my supervisor, for his continual guidance and support during this study. His dedicated supervision and ongoing motivation in completing this thesis inspired me to give my best. His extensive knowledge and logical thinking have been exceptionally beneficial to me.

I extend my heartfelt gratitude to **Pr. Azeddine Soudani**, **Dr. Fatima Zohra Ferahta**, and **Pr. Abdelbaki Mameri**, for accepting being members of the thesis examination committee.

Furthermore, I am thankful for the collaboration between the LPEA laboratory of Batna 1 University and the Motor laboratory of Batna 2 University. This collaboration played a crucial role in the experimental aspect of this research study.

I also want to extend my thanks to my professors, lab mates, friends, and family for their consistent love, encouragement, and faith in me. My sincere gratitude also to all members of the Scientific Club of the Algerian Muslim Scholars Association, Batna.

Lastly, but certainly not least, throughout this work, I collaborated with numerous colleagues whom I hold in high regard. I extend my warmest thanks to all those who have assisted me in my work.

Ibrahim RAHMOUNI

الملخص

الهدف الرئيسي من هذه الأطروحة هو تحليل خصائص أداء محرك احتراق داخلي يعمل بالغاز الحيوي الخام. لهذا الغرض، تم إجراء تحقيق تجريبي على محرك بنزين من نوع هوندا GX140 أحادي الأسطوانة بقوة 5 احصنة مقترن بمقياس ديناميكي هيدروليكي TD115، يعمل بالغاز الحيوي الخام والبنزين. تم إنتاج الغاز الحيوي الخام في نظام مخبري في مختبر الفيزياء الطاقوية المطبقة (LPEA) في جامعة باتنة 1. تشير النتائج إلى أن جودة إنتاج الغاز الحيوي للركيزة المفردة (الهضم الأحادي) من روث البقر أفضل من جودة إنتاج الغاز الحيوي للهضم المشترك لروث البقر ومخلفات الطعام. من ناحية أخرى، تم تقييم اداء المحرك في مختبر المحركات بجامعة باتنة 2. تحت ظروف تحميل محركي؛ 0 و3.5 نيوتن متر، تم فحص خصائص أداء المحرك. لوحظت زيادة كبيرة في درجة حرارة غازات العادم ومعدل تدفق كتلة الوقود في حالة الغاز الحيوي الخام. أظهرت النتائج أيضًا أن الغاز الحيوي الخام أدى إلى زيادة الكفاءة الحرارية للكبح واستهلاك الوقود النوعي للكبح مقارنة بالبنزين. سيفتح هذا الباب أمام الغاز الحيوي ليحل محل الوقود الأحفوري جزئيًا وبجميع التأثيرات المجتمعية الإيجابية والسلبية التي من شانها ان تولد هذا الاستبدال.

الكلمات المفتاحية: الهضم اللاهوائي، الاحتراق، محرك احتراق داخلي، الغاز الحيوي.

Abstract

The main goal of this thesis is to assess the performance characteristics of an internal combustion engine when fueled with raw biogas. To achieve this objective, an experimental investigation was conducted using a Honda GX140 gasoline engine, 5HP single cylinder, coupled to the Hydraulic Dynamometer TD-115, functioning with both gasoline and raw biogas. Biogas was generated from a lab-made biogas setup at the LPEA laboratory of Batna 1 University. The results indicate that the quality of biogas production for the single substrate (Mono-digestion) of cow dung is better than the quality of biogas production for the co-digestion of cow dung and food waste. Additionally, the engine performance analysis was conducted at the Motor Laboratory of Batna 2 University, exploring two engine load conditions of 0 and 3.5 N.m. The experimental findings highlighted a substantial elevation in both exhaust gas temperature and fuel mass flow rate when utilizing biogas. Furthermore, these results indicated that biogas exhibited superior brake thermal efficiency but also recorded higher brake-specific fuel consumption in comparison to gasoline. These findings highlight the potential for raw biogas as a partial substitute for fossil-based fuels, with associated positive societal implications.

Keywords : Anaerobic digestion, Combustion, Internal combustion engine, Biogas.

Résumé

Le but principal de cette thèse est d'évaluer les performances d'un moteur à combustion interne alimenté au biogaz brut. A cet effet, une étude expérimentale a été menée sur un moteur à essence de type Honda GX140, monocylindre de 5 CV couplé à un dynamomètre hydraulique TD115, fonctionnant avec du biogaz brut et de l'essence. Le biogaz brut a été produit à partir d'une installation laboratoire de biogaz au laboratoire LPEA, de l'Université Batna 1. Les résultats indiquent que la qualité du biogaz produit avec le substrat unique (mono-digestion) de la bouse de vache est meilleure que celle du biogaz produit par la codigestion du la bouse de vache et des déchets ménages. D'autre part, les performances du moteur ont été analysées au laboratoire Moteur de l'Université Batna 2 ; sous deux conditions de charge du moteur ; 0 et 3,5 N.m, les performances du moteur ont été étudiées. Une augmentation significative de la température d'échappement et du le débit massique de carburant ont été observées dans le cas du biogaz brut. Les résultats ont également révélé que le biogaz brut générait une efficacité thermique des freins et une consommation de carburant spécifique aux freins plus élevées que l'essence. Cela ouvrira la porte au biogaz pour substituer partiellement aux combustibles d'origine fossile et avec tous les effets sociétaux positifs que générerait cette substitution.

Mots clés : Digestion anaérobie, Combustion, Moteur à combustion interne, Biogaz.

TABLE OF CONTENTS

LIST OF TABLES

LIST OF FIGURES

GENERAL INTRODUCTION

1 Overview

Energy security has emerged as a highly contested global concern, with a focus on the sustained and dependable availability of energy supplies. Two crucial factors impact this issue significantly. Firstly, recent events such as the Russia-Ukraine conflict underscore the importance of diversifying energy suppliers to enhance energy security. Secondly, the COVID-19 pandemic has underscored the necessity of ensuring a reliable and continuous supply of electricity for consumers and businesses alike.

Projects focused on alternative fuels aim to facilitate the transition from conventional motor fuel sources like gasoline and diesel to alternative options such as biodiesel, ethanol, biogas, compressed natural gas, partially electric vehicles, hydrogen fuel cells, or liquefied petroleum gas. These alternative fuels can be employed either as a single-fuel solution or in hybrid systems alongside other fuels, including hybrid-electric or flexible fuel cars.

Using biogas as a fuel within an internal combustion IC engine is a way amongst others to generate electricity from biogas. Therefore, analyzing the engine's behavior when converted to biogas is very important. The development of this type of projects will generate benefits, among which, is the generation of electrical energy in isolated areas. In addition, the engines operated with biogas can cover the energy needs of farms, contingent upon the farm's size. The use of biogas will influence activities such as lighting small areas and be incorporated into the food cooking processes of families in small production units.

2 Objective

2.1 Main objective:

This present work aims to investigate an IC engine's performance using raw biogas as an alternative fuel.

2.2 Specific objectives:

- To compare the effect of mono-digestion of cow dung and co-digestion of cow dung and food waste on raw biogas composition.

- To measure the engine characteristics with the help of the hydraulic dynamometric bench, such as; speed, torque, fuel consumption, and exhaust gas temperature.
- To determine the engine performances with gasoline and biogas as a fuel to compare the temperature of exhaust gas, fuel mass flow rate, brake-specific fuel consumption, and brake thermal efficiency for both fuels.
- To analyze the results obtained in the tests carried out on the engine with the two fuels (Gasoline - Biogas).

3 Thesis Plan

The thesis comprises five parts, with the initial section serving as a general introduction. It provides an overview of the significance of utilizing biogas as a fuel for internal combustion (IC) engines. Additionally, the main objectives explored and discussed in the thesis are outlined in this section.

The first chapter focuses on the anaerobic digestion process and reviews the literature on biogas as a fuel in internal combustion engines, particularly spark-ignition engines.

The second chapter discusses various experimental investigations on the producing of raw biogas from cow dung and food waste. The third chapter involves an experimental investigation of the SI engine test rig performance characteristic variations under two engine loading conditions using raw biogas.

The fourth chapter describes the experimental results in two parts. The first part concerns the mono-digestion of cow dung and co-digestion (cow dung + food waste) on biogas-produced composition. In the second part, the focus is on the variations in engine performance parameters, including exhaust gas temperature (T_{ex}), fuel mass flowrate ($\dot{m}_f$), brake-specific fuel consumption (BSFC), and brake thermal efficiency (BTE). The experiments were carried out using two fuels: raw biogas and gasoline.

CHAPTER 1:

LITERATURE REVIEW

CHAPTER 1

1 Introduction

This chapter provides a concise outline of the anaerobic digestion process and a review of the literature on biogas as a fuel in internal combustion engines, particularly spark-ignition SI engines.

2 Anaerobic Digestion (AD)

The biological production of gaseous fuels is effectively accomplished through Anaerobic Digestion (AD), recognized as a viable biomass conversion method. AD proves to be a promising option for treating diverse biomass and waste materials, including energy crops, agricultural remnants, various types of biowaste and municipal waste, industrial byproducts (such as from food and beverage sectors), livestock and poultry residues, sewage, and algae. Beyond its bioenergy advantages, AD aligns with the principles of a circular economy, embodying the "Reduce - Reuse - Recycle" concept.

The number of AD plants in the world has grown steadily in recent years. It is a significant capital investment, and, like any commercial decision, it will be based on thorough research and driven by several factors. In this section, we ask the question: what are the drivers for AD, and why do we need to know the drivers?

2.1 Anaerobic Digestion Drivers

The three critical drivers for AD are energy production, waste management, and nutrient recycling, depending on the needs and motivations of individual sites. Let us start by looking at each in turn.

2.1.1 Energy Production

The first thing that comes to mind for many people is the possibility of producing renewable energy that can substitute fossil fuels. However, it is also worth describing the simple combustion of biogas, in which vehicles powered by gas give emissions of nitrogen and particles that are only a couple of percent of the corresponding emissions from vehicles powered by fossil fuels. The benefit for the climate is vast, and CO_2

emissions from the complete lifecycle are seldom more than 20% of the corresponding values for petrol and diesel. When dung is digested, the positive effects on the climate are double since methane emissions from the dung are eliminated, while at the same time, the gas produced can replace fossil-based fuels.

2.1.2 Waste Management

A second significant advantage that AD contributes to is the treatment of waste. The society produces a great deal of problematic and wet waste that is unsuitable for incineration and cannot be released into the environment. Such waste comes from, e.g., slaughter-houses, dairy facilities, breweries, wastewater treatment plants, and household food waste. Some of the waste is hazardous for health and the environment and must be sanitized. AD contributes to this while at the same time preserving the nutrient value of the waste.

2.1.3 Nutrient Recycling

AD also creates another renewable product – biofertilizer. This fertilizer can replace mineral-based fertilizers derived from fossil resources, with extensive positive effects on the climate and the environment. Not only do biofertilizers contain vital plant nutrients; nitrogen, phosphorus, and potassium, but using them also supplies micronutrients and organic material to the soil. In this way, the long-term productivity of the soil is secured, and more carbon can be sequestered in the soil – which also has a beneficial effect on the climate [1]. With the increasing cost of manufactured fertilizers and the associated environmental issues, it is easy to see why valuable recycling nutrients in digestate is another driver for developing an AD plant [2]. For example, an AD plant will help manage the slurry using digestate when the crop requires it and also enhance nutrient availability.

To fully understand the AD process, we have to delve into the biological process. What exactly is happening during AD? We all know what digestion is, but what does anaerobic mean? It is essential to understand the simple facts at the heart of the process, because it will help us to make better day-to-day judgments relating to the efficiency of our operation.

2.2 What is the AD?

Anaerobic digestion (AD) is a natural, not a mechanical process.

In the AD process, microorganisms from the Bacteria and Archaea domains thrive without oxygen (O_2). Fungi also contribute to the process of degradation. Within this microbial community, there are both versatile and specialized organisms cooperating to create a diverse population. This collective plays a crucial role, breaking down substantial organic molecules into smaller compounds, ultimately producing methane. (CH_4) [3].

CH_4 percentage within the biogas is one of the best indicators of the health of the biological process. The natural AD sequence produces carbon dioxide (CO_2) in the first phase and CH_4 in the final and most sensitive stage. The AD process occurs naturally in various environments, and it can be intentionally applied for regulated production, regardless of the scale, whether small or large [4].

2.3 Anaerobic Digestion Phases

The complete digestion process can be segmented into four stages of complex biochemical reactions: Hydrolysis, Acidogenesis, Aceto-genesis, and Methanogenesis. This series involves the cooperation of three distinct categories of microorganisms: hydrolytic-acidogenic bacteria (potentially including fungi), syntrophic acetogenic bacteria, and methanogenic archaea [3].

2.3.1 Hydrolysis

The depolymerization process involves breaking down insoluble organic hydrocarbons into soluble monomers. This process breaks down carbohydrates, lipids, and proteins, the primary substrate compounds, into respective low molecular weight forms: monosaccharides from carbohydrates, long-chain fatty acids from lipids, and amino acids from proteins. The timeframe for this breakdown varies, with carbohydrates taking a few hours, proteins and lipids taking a few days, and lignin and lignocellulose taking several days [5].

2.3.2 Acidogenesis

Following depolymerization, the breakdown products, including Amino-acids and sugars, undergo a transformation into various compounds such as volatile fatty acids (VFAs) like acetic, butyric, and propionic. Furthermore, the process yields organic acids, Ammonia (NH_3), Hydrogen gas (H_2), Carbon Dioxide (CO_2), Hydrogen Sulfide (H_2S), and low Alcohols. It's important to note that the concentration of H_2 generated at this stage can influence the final product of the digestion process. The organic

materials produced, such as VFAs, are not immediately suitable for transformation into CH_4 by methanogens [5].

2.3.3 Acetogenesis

Transforms the VFAs, particularly acetic and butyric acids, into acetate, H_2, and CO_2. Approximately 65–95% of CH_4 originates directly from acetic acid. Conversely, propionic acid largely remains unconverted due to its less favorable thermodynamic degradation compared to butyric acid, as indicated by the relationship between hydrogen partial pressure and VFA degradation [5].

2.3.4 Methanogenesis

CH_4 is produced in the last stage of AD through the activity of three categories of methanogens microorganisms: Acetotrophic, Hydrogenotrophic, and Methylotrophic. Acetotrophic transforms the acetate into CH_4 and CO_2 (The majority of the CH_4 is produced), Hydrogenotrophic converts both H_2 and CO_2 into CH_4 (around 30% of CH_4 may be made), and Methylotrophic microorganisms convert the methyl or trimethylamine constituents present in a particular feedstock into CH_4, with some CH_4 being potentially produced in this process as well [5].

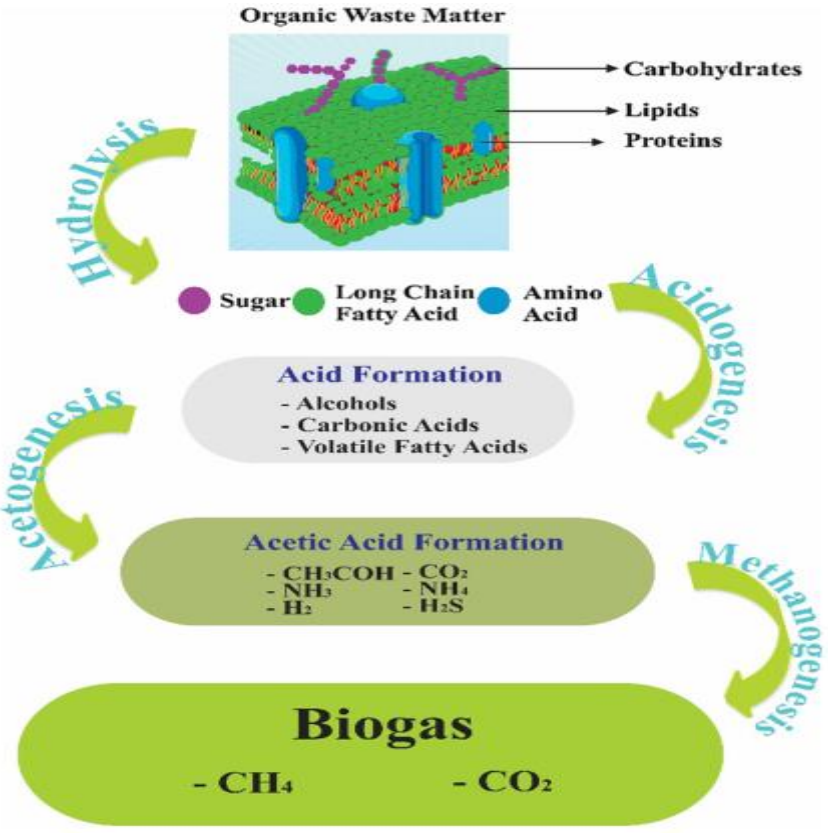

Figure 1-1 The pathway of the AD process originating from a specific substrate [6].

2.4 The Operating Parameters of AD:

The process of biogas generation entails a sequence of successive metabolic reactions that rely on the cooperation of diverse microorganism groups possessing varying metabolic abilities and growth requirements [7]. Several factors, such as the complexity of the process, inadequate stability, low biodegradability, intricate substrate composition, and reduced productivity, hinder CH_4 production and digestate yield in AD.

2.4.1 Feedstock

2.4.1.1 Substrate Composition

The biogas production, CH_4 content, biodegradability, and degradation rates are influenced by the chemical composition of the substrate material. The Boyle theoretical calculation formula is employed to estimate the actual yield [8]:

$$C_aH_bO_cN_dS_e + \left(a - \frac{b}{4} - \frac{c}{2} + \frac{3d}{4} + \frac{e}{2}\right) H_2O \rightarrow \left(\frac{a}{2} + \frac{b}{8} - \frac{c}{4} - \frac{3d}{8} - \frac{e}{4}\right) CH_4 + \left(\frac{a}{2} - \frac{b}{8} + \frac{c}{4} + \frac{3d}{4} + \frac{e}{4}\right) CO_2 + dNH_3 + eH_2S \quad (1\text{-}1)$$

Substrates can be broadly classified into three categories based on their state: wet, semi-solid, or solid. This classification is determined by the total solids (TS) content present in the substrate, with the wet substrates having <10% of TS, semi-solid substrates having 10–15% of TS, and solid substrates having >15% of TS [9]. The material introduced into digesters needs to maintain a suitable equilibrium of both macro and micronutrients to establish a stable and efficient biogas generation process [3]. The effectiveness of biodegradation depends on the substrate chemical and physical compositions that create favorable conditions for biological degradation.

Feedstocks	Total Solids (% dissolved solids (DS))	Volatile solids (% DS)	Retention time (days)	Biogas Yields (m^3/kg VS)	CH_4 content (%)
Pig slurry	3-81	70-80	20-40	0.25-0.50	70-80
Cow slurry	5-12	75-85	20-30	0.20-0.30	55-75
Chicken slurry	10-30	70-80	>30	0.35-0.60	60-80
Whey	1-5	80-95	3-10	0.80-0.95	60-80
Leaves	80	90	8-20	0.10-0.30	NA
Straw	70	90	10-50	0.35-0.45	NA
Garden wastes	60-70	90	8-30	0.20-0.50	NA
Grass silage	15-25	90	10	0.56	NA
Fruit wastes	15-20	75	8-20	0.25-0.50	NA
Food remains	10	80	10-20	0.50-0.60	70-80

Figure 1-2 Biogas and methane yields from various feedstocks [10].

2.4.1.2 Inoculum

Ensuring sufficient microbiological activity might demand the process additives inclusion like trace metals, buffering agents, iron, anti-foaming agents, etc., especially for certain materials or material combinations [11]. Using a large inoculum volume or a low substrate to inoculum (S:I) ratio may result in the instability of the process and low biogas yield [12].

2.4.1.3 Pre-treatment

Usually, the material undergoes preliminary treatment before entering the biogas process. Several reasons support this pre-treatment:

- Sanitization to eliminate pathogenic microorganisms.
- Removal of non-degradable materials that could interfere with the process.
- Thickening to concentrate the organic material content.
- Enhancing the availability of organic matter by reducing particle size or increasing solubility [13].

There are four primary pretreatment methods for increasing feedstock utilization for AD:

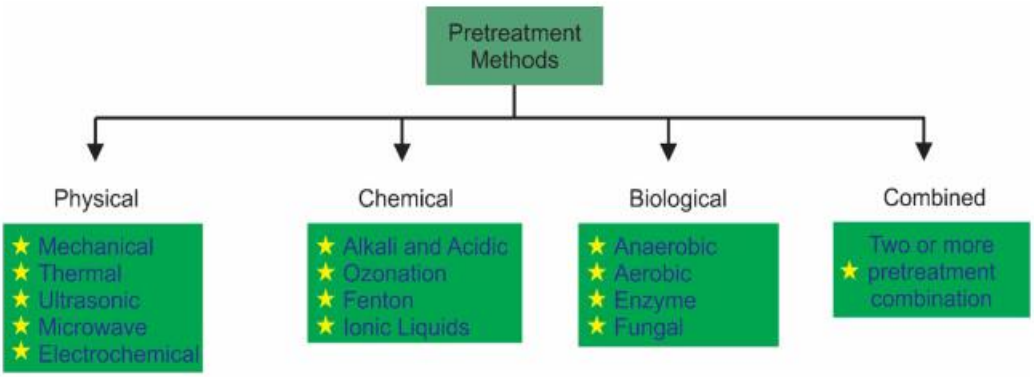

Figure 1-3 Pretreatment methods for the AD process improvement [6].

2.4.1.4 Co-Digestion

Certain materials function effectively as sole substrates, while others require mixing with complementary substrates in co-digestion. Blending different materials helps maintain sufficient trace element concentrations, enhances buffering capacity, and optimizes the carbon-to-nitrogen ratio (C/N). In addition, Co-digestion increases handling substrates likelihood containing toxic components [14].

The primary objective is to establish the ideal levels of macronutrients and micronutrients, enhancing biogas yield through various combinations and fractions during anaerobic digestion (AD). This approach can lead to favorable nutrient and water level, along with the concentration of potential inhibitors. Co-digestion frequently produces an optimal nutrient composition, known as the "priming effect" [15].

2.4.1.5 Carbon to Nitrogen Ratio (C/N)

Within the organic matter decomposition in a biogas procedure, the C/N (carbon-to-nitrogen) ratio holds significant importance. It is imperative to maintain a balanced ratio, ensuring that nitrogen does not significantly exceed carbon. Otherwise, the process is susceptible to Ammonia (NH_3) inhibition [16]. Pinpointing the exact optimal ratio proves challenging due to its variability across different substrates and varying process conditions.

2.4.2 Reactor

2.4.2.1 Configuration

There are three main types of digesters:

- **Batch Reactors** also known as discontinuous reactors, are initially filled with fresh substrates. Once the biogas or CH_4 production ceases, signifying the completion of the digestion process, the entire digestate is emptied, and the process restarts. One advantage of batch reactors is their comparatively low initial investment cost.
- **Continuous-Flow Digester** involves continuously feeding digesters with new substrates, resulting in a constant and predictable production. Continuous digesters can adopt different configurations, including vertical, horizontal, or multiple tank systems, depending on the selected method for stirring the substrate. They can exist in two primary types: completely mixed or plug-flow. Typically, completely mixed digesters are in a vertical orientation, while plug-flow digesters are horizontal.
- **Semi-Batch Digesters**: they are well-suited for co-digestion processes, especially when digesting straw and dung together. In this setup, the biogas digester functions on a semi-batch basis. The straw-type material, which digests slowly, is introduced twice a year, while the dung is consistently added and removed [17].

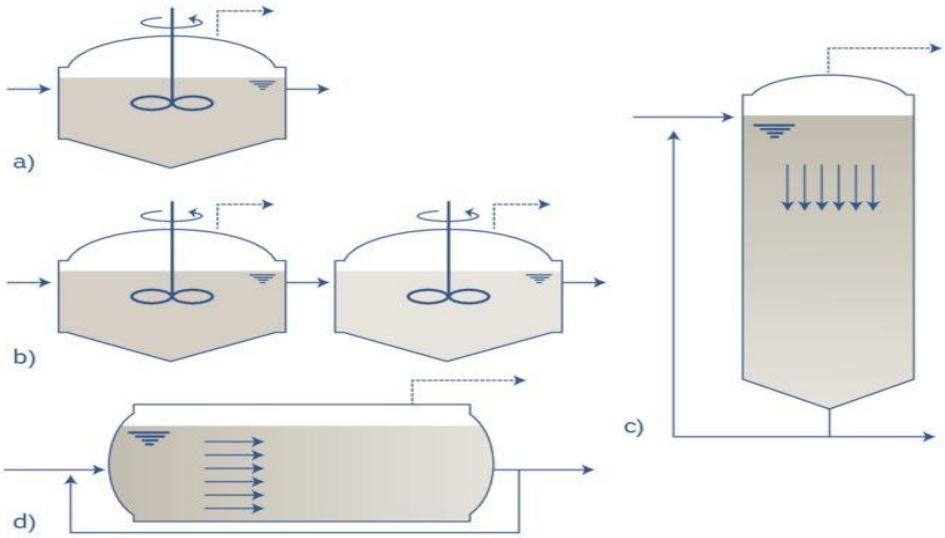

Figure 1-4 CSTR (Continuous stirred tank reactors)/ plug–flow reactors, to semi-solid and solid waste. a) CSTR. b) CSTRs in series. c) Vertical plug–flow digester. d) Horizontal plug–flow digester [18].

2.4.2.2 Mixing

The stirring of the reactor holds significance as it enhances the interaction between the substrate and microorganisms, thereby influencing the degradation rate. This process fosters better engagement among substrates, bacteria, and nutrients while ensuring an even distribution of temperature throughout the digester [19].

Creating mixing in digesters can be achieved through mechanical methods (employing a mixer), hydraulic techniques (recirculating liquid), and pneumatic approaches (recirculating gas). These methods can be applied at various frequencies, such as continuous or intermittent mixing for extended periods or multiple times per hour during the day, and at different intensities, ranging from gentle to intermittent to rigorous rotation speeds [20].

2.4.3 Temperature

Temperature and substrate are critical parameters that determine process stability and performance in anaerobic digestion. Temperature plays a significant role not only in shaping the structure of the microbial community but also in affects diversity, degradation pathways, and the rate of degradation [21]. Particularly, methanogens within the microbial community exhibit sensitivity to temperature. Insights from large-scale operations suggest that temperature variations should ideally remain within 2–3°C to ensure optimal outcomes and minimize instability [22].

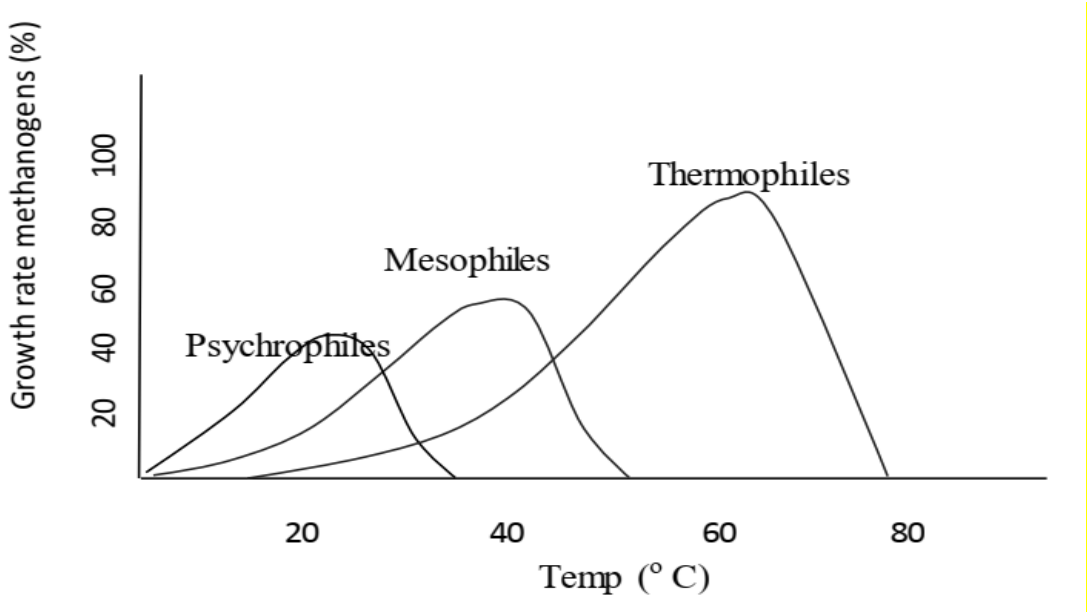

Figure 1-5 Relative growth rates of methanogens [23].

Raising the temperature increases metabolic rates and biochemical reactions. Thermophilic conditions (ranging from 50–70 °C) have shown to accelerate decomposition rates and raw biogas production from various substrates compared to mesophilic conditions (ranging from 30–42 °C).

The features of thermophilic temperature are a high methane production rate, a short hydraulic retention time (HRT), a higher load, the excellent killing of pathogens, a less stable process, and low viscosity. In contrast, the features of mesophilic temperature are good stability, lower energy consumption, high microbial diversity, and more efficient degradation [24].

2.4.4 PH

PH reflects the health of anaerobic bacteria as well as the functioning of the AD system. The optimal range for CH_4 generation falls between 6.5 and 7.5. Methanogens exhibit high sensitivity to pH variations and typically thrive at a pH nearing 7. pH levels below 6.3 or above 7.8 could potentially impede methanogenesis, elevating the risk of process failure [25].

The extent of pH variation is determined by the available alkalinity (buffering capacity) within the reactor, which in turn controls how quickly the pH returns to optimal levels. Partial alkalinity (PA) indicates the buffering capacity of the carbonate system, including the ammonium-ammonia system as well [26]. Process stability can be

assessed by measuring the IA/PA ratio, where 0.3 value or less indicates a steady process [27].

2.4.5 Hydraulic & Solid Retention Time

Retention Time (RT) serves as a crucial factor in the design and optimization of an AD plant. It must be sufficiently extended to facilitate the effective degradation of specific materials within defined operating conditions. Materials abundant in fiber and cellulose, indicative of plant materials, undergo a more prolonged microbial breakdown. On the contrary, substrates abundant in sugar and starch generally undergo quicker breakdown and require a shorter RT [28]. There is no need for hydrolysis for the deterioration of these materials, and the decomposition begins immediately at the second phase, fermentation.

Hydraulic retention time (HRT) describes the RT of the liquid. HRT type used depends on the feedstock, reactor capacity, procedures, and temperature. Reducing the HRT raises the risk of bacterial movement, leading to the buildup of higher molecular weight VFAs and subsequently placing greater strain on the methanogens.

Solid retention time (SRT) refers to the duration for which the microbial culture remains within the digester. Shorter SRT was purposefully employed to regulate VFA synthesis by moving microbial populations from one production pathway to another [28].

2.4.6 Organic Loading Rate

The Organic Loading Rate (OLR) describes the raw material quantity introduced to a digester on a daily basis per unit volume. It's denoted by measuring the organic material quantity introduced per volume of the active reactor per day. Maintaining a stable operation requires that the OLR not be excessively high. The ideal load is contingent on various factors, such as substrate traits and the operational temperature.

There's often a preference for a high OLR because it encourages the proliferation of specialized bacterial species, allows for smaller reactor sizes, reduces heating requirements, and ultimately lowers the overall investment costs.. Heightened OLR levels usually correlate with reduced RT, potentially leading to a swift microbial wash-out and less efficient degradation if the duration becomes excessively short [28].

The load introduced to the digester can be a single daily quantity, distributed across multiple instances, or continuously fed into the reactor. How the material is fed impacts

the kinetics of degradation, the generation of intermediates, and the production of biogas, although it typically has little effect on the ultimate methane yield. Additionally, the feeding pattern has demonstrated an impact on microbial community activity, structure, and functional stability [29].

2.4.7 Inhibitory Components

Inhibition of one or several groups of organisms results in an imbalance between the different degradation steps, creating instability or even collapse of the process [30].

2.4.7.1 Ammonia (NH_3)

The level of NH_3 plays a significant role in shaping the structure of the microbial community. NH_3 stems from nitrogen-rich components in the feedstock, primarily generated during the hydrolysis phase [31]. A high ammonium content contributes alkalinity to the process and enhances the digestate's value as a fertilizer. However, it can also inhibit the process, particularly affecting the methanogenic community [32].

Ammonia exists in two forms: Ammonium Ions (NH_4^+) and Free Ammonia (FA) or Unionized Ammonia (NH_3), collectively known as total ammonia nitrogen (TAN). The temperature and pH indirectly influence the degree of inhibition by shifting the balance among ammonium (NH_4^+) and ammonia (NH_3), when the latter being the primary cause of inhibition [33].

2.4.7.2 Volatile Fatty Acids (VFAs)

These critical intermediates consist of acetic acid/acetate, propionic acid/propionate, butyric acid/butyrate, valeric acid/valerate, caproic acid/caproate, and enanthic acid/enanthate [34].

Most VFAs breakdown primarily to acetate and further to CH_4 through the methanogenesis, involving both acetoclastic and hydrogenotrophic pathways. However, excessive levels or specific types of accumulated VFAs can become toxic and, in extreme situations, inhibit the process [35].

Improving VFA conversion efficiency is typically preferred, as it contributes to increased stability in CH_4 production and balance across various production stages. Accumulating high concentrations of VFAs, regardless of type, is discouraged as it can reduce the potential for CH_4 production and subsequently lower AD efficiency.

2.5 The Anaerobic Digestion Outputs

The outputs of AD consist of biogas, containing a high energy content and suitable for various subsequent conversion technologies, and a liquid residue rich in macro and micronutrients. This residue serves as an organic fertilizer or soil enhancer, catering to agricultural needs.

2.5.1 Biogas

We now move our focus to outputs. In this section, we look at biogas. Again, detailed knowledge of factors such as the biogas quality, the biogas use, dealing with biogas contaminants, and biogas storage, are critical if an AD plant is to be run effectively.

2.5.1.1 Biogas Quality

The primary constituents of biogas are CH_4, CO_2 and H_2S. The proportion of each gas provides a plant operator with critical information as to the health of the process. It also relies on the feedstock and the health of the system, but typically the breakdown is 50-60% CH_4, 40-50% CO_2, and 0-2,000 ppm (0-0.2%) H_2S [36].

The percentage of CH_4 has a direct impact on the energy value of the biogas, so biogas with a high CH_4 concentration has more energy value than one with a lower CH_4 concentration. The higher CH_4 content, the less biogas is required to run a boiler or combined heat and power (CHP) at its total output.

2.5.1.2 Biogas Contaminants

Biogas contains contaminants that can harm humans, plants, and equipment. Understanding these contaminants and implementing effective management strategies is essential to ensure the safety and the biogas production process efficiency.

- **Water (H_2O)**

Biogas is a saturated gas that comes off the digester at around 38°C. As the biogas cools in the gas lines, moisture drops out as condensate. If condensed moisture enters the biogas consumers – CHP, boiler or compressors - then it can cause damage to the equipment.

The condensate can successfully be removed from the gas lines through condensate pots located at low points of the gas lines. In addition, inline biogas chillers can further increase the moisture drop-out to create a drier biogas [37].

- **Hydrogen Sulfide (H_2S)**

Feedstocks high in sulphates, such as chicken and pig dung, will create a higher concentration of H_2S [38]. H_2S is toxic to humans and corrosive to operational plants due to the condensing of moisture from within the biogas, into which the H_2S dissolves and becomes sulphuric acid. This sulphuric acid can cause the pipework corrosion and damage CHPs and boilers [39].

Biogas is typically malodorous, although the CH_4 is odorless. It is the H_2S that generates the typical biogas smell. H_2S disables the olfactory nerve, our sense of smell, so we cannot use this to detect its concentration. This is why personal gas monitors must be worn to alert you to a dangerous level of H_2S, which can be deadly.

There are a number of ways of reducing the H_2S content in the biogas, which include:

- Air injection: An air pump is used to inject oxygen into the digester head space, which inhibits the bacteria that produce H_2S and promotes the growth of bacteria, which in turn convert the H_2S to sulfur. A net hanging within the digester head-space allows the sulfur-fixing bacteria to attach themselves and can be seen as a layer of white or pale-yellow material.
- Iron fixing: Ferric chloride or ferrous hydroxide reacts with the H_2S to produce ferric sulfide and hydrochloric acid. The iron product is pumped or fed directly into the digester, and the resultant chemicals are discharged within the digestate.
- Biogas scrubbing: Biogas is scrubbed through chemical or carbon scrubbers. This is done in the gas line to the biogas consumer [40].

- **Siloxanes**

Siloxane is a chemical compound derived from silicone. Siloxanes are typically found in biogas produced from sewage sludge. If siloxanes get into an internal combustion engine, they are oxidized to silicon dioxide, which very quickly deposits within the engine, causing damage to the components.

There are many ways of removing siloxanes from biogas. The most common way is activated carbon, which is done in the gas line to the biogas consumer [41].

2.5.1.3 Biogas Storage

Biogas produced by the AD process is usually consumed in real-time but requires buffer storage for fluctuating production and usage rates. It's commonly stored in a double membrane or bell-over-water gas holder, either integrated into the digester's roof or as a separate vessel. These storage units often feature level detectors to automatically regulate biogas consumption.

- **Double-Membrane Gas Holder**

A double membrane can be positioned on the floor near process tanks or integrated into the digester or digestate storage tank's roof.

- The outer membrane is consistently inflated using an air blower, maintaining pressure on the inner membrane.
- the inner membrane expands and contracts accordingly as biogas production and consumption vary.
- A weighted outlet on the outer membrane regulates air release, controlling system pressure. Monitoring air quality at this outlet helps detect potential biogas leaks within the membrane [42].

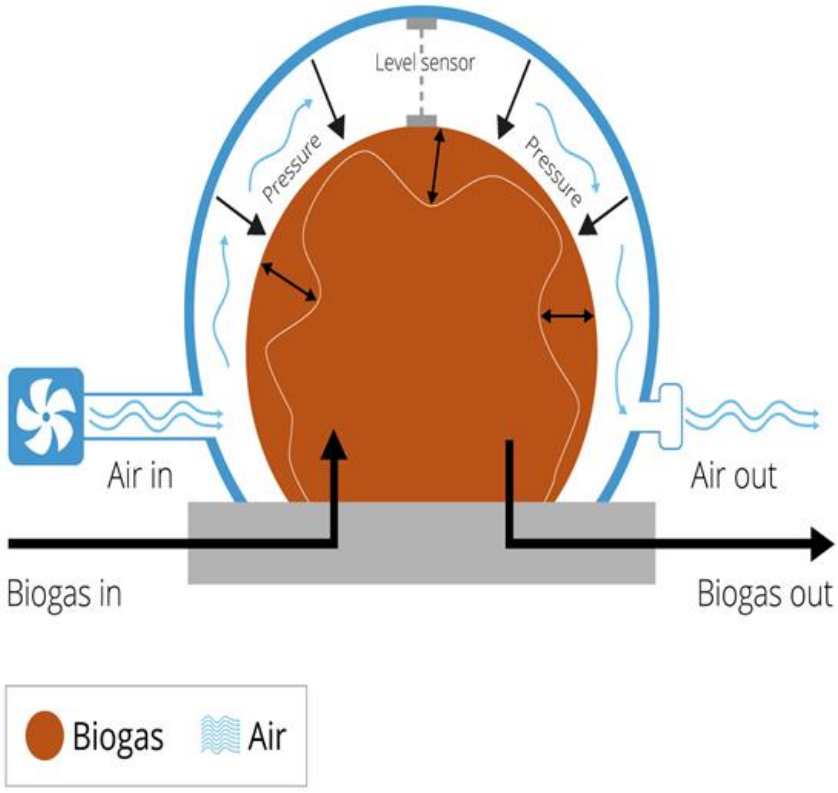

Figure 1-6 The Gas Double-Membrane Holder

- **Bell-Over-Water Gas Holder**

A bell-over-water can be a floor mounted, stand-alone unit, or the bell can float on top of the digesting sludge as an integral part of the digester.

- Rollers on the side of the tank guide the bell up and down, keeping it stable and upright.
- The bell floats on a liquid tank, rises, and falls as biogas is produced and consumed.
- The bell weight puts pressure on the system. The height difference between the water or sludge levels inside and outside of the bell is generally the operating gas pressure, usually measured in a water gauge [43].

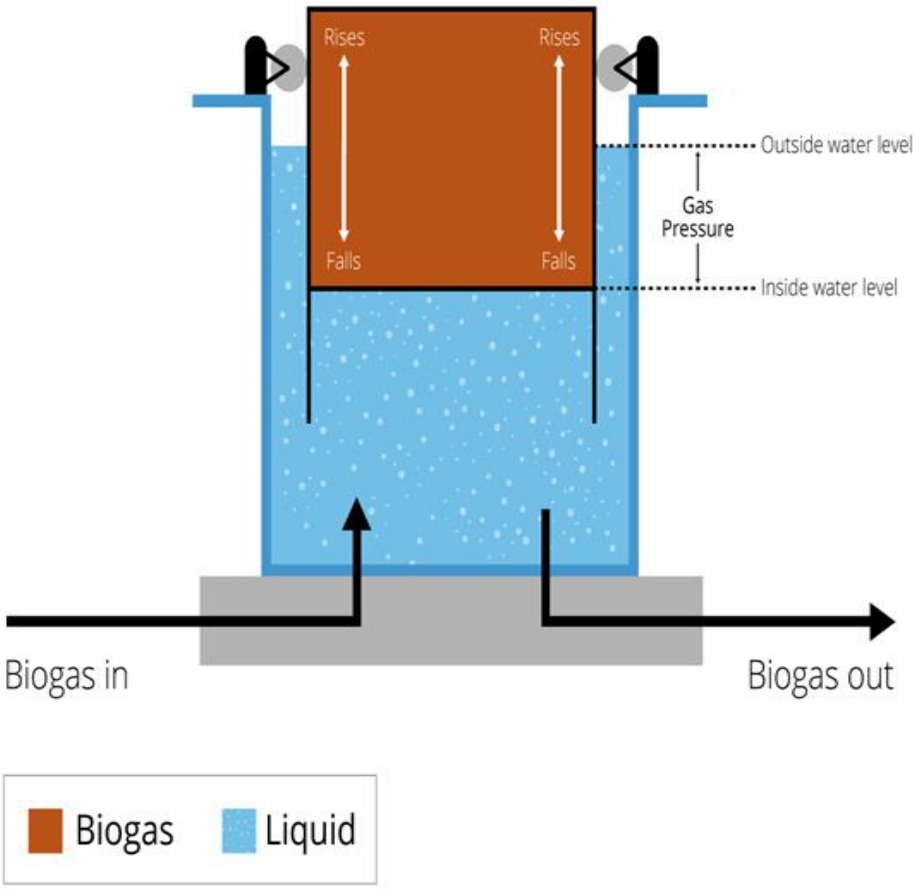

Figure 1-7 Bell Over Water Gas Holder

2.5.1.4 Biogas Applications

In this section, we examine how biogas can be utilized in various ways and how it is treated, depending on its end use.

Biogas needs to be consumed continually as the digestion process produces it, unless the site has additional biogas storage for operational, economic, or environmental reasons. Biogas can be consumed in several ways, including through boilers and CHP units. It's also possible to refine it into biomethane, suitable for use as a vehicle fuel or for injection into the national gas grid.

- **Combined Heat & Power Unit**

CHPs generate electricity and heat. Depending on the CHP's size, The process of converting biogas into both electricity and heat is 40% and 42% respectively, with 18% losses. The smaller the CHP, the lower the electrical conversion and the higher the heat conversion [44].

- **Boilers**

Biogas boilers typically convert 85% of the biogas energy into heat, with the remainder lost throughout the process. Therefore, most AD plants will have a boiler to provide a backup heat supply when the CHP is not generating. Heat is key to the AD process, especially during the cooler months, when heat requirement is most significant [45].

- **Biogas Upgrade for National Gas Grid Injection**

Biogas can undergo purification and then be introduced into the national gas grid as biomethane. All contaminants must be scrubbed, including H_2S, siloxanes, CO_2, O_2, nitrogen (N_2), NH_3, and H_2O. Although the loss of energy through biogas upgrade is 1.5%, some upgrade processes can have a high electrical parasitic requirement [45].

National grid gas requires a calorific value of 38-41MJ/m^3. Biomethane has a calorific value of 35.7MJ/m^3, so propane is added to the biomethane to increase energy content. It then goes through a continuous testing process before entering the grid [46].

For safety reasons, biomethane is required to smell within the national grid to detect leaks. Therefore, an odorant must also be added prior to compression and injection to the grid. The compression level depends on whether the biomethane is going to a local line (low pressure), branch line (medium pressure) or regional line (high pressure).

- **Biomethane for Vehicle Fuel**

When transformed into biomethane, biogas can serve as a vehicle fuel option. The resulting biomethane is then compressed and stored ready for use.

The biomethane can be used Natural Gas Vehicles or dual-fuel vehicles, where the liquid fuel tank is retained, and the biomethane is ignited by a small amount of the liquid fuel. In addition, many vehicles can run on biomethane, including trains, buses, lorries, cars and vans [46].

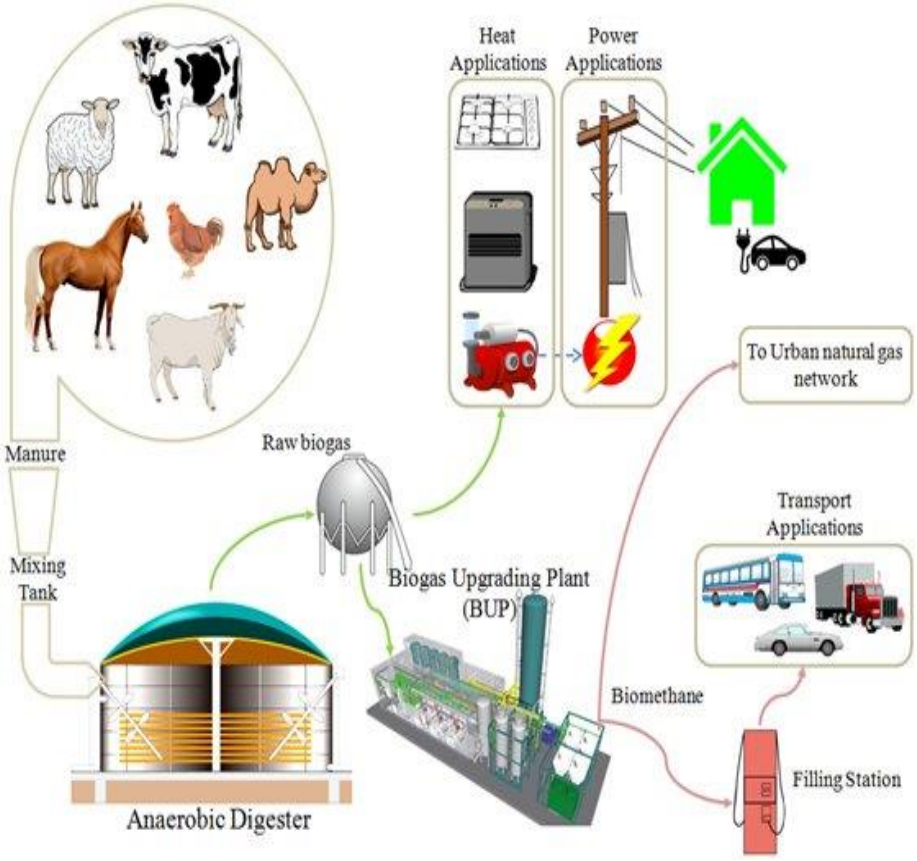

Figure 1-8 Summary of biogas production and Applications [47].

2.5.2 Digestate

The amount of digestate produced from different feedstocks relies on the conversion of organic dry matter into biogas and the water content of the feedstocks. The majority of which will pass through the AD process and into the digestate.

Residues from digestion, resulting from the breakdown of organic matter in AD, comprise crucial plant nutrients and organic material. When used as soil amendments, they enhance soil quality by improving its physical and chemical properties. These residues can contribute significantly to crop production, offering comparable benefits to those derived from artificial fertilizers. [48].

This section takes a closer look at the digestate characteristics and ways of storing it and applying it to land.

2.5.2.1 Digestate Characteristics

The mass of the digestate and biogas depends upon the amount of biogas produced by the original feedstock.

Digestate can be handled as a whole product as it is discharged from the digester or separated into liquid and solid fractions. In this section, we are referring to the whole digestate.

- **Mass Balance**

The concept of Mass balance is very straightforward. Everything that enters the digester will come out as either biogas or digestate so a mass balance can be calculated.

The mass of raw feedstock = the mass of biogas + the mass of digestate [49].

- **Nutrient Content**

Most nutrients present within the original feedstock are retained within the digestate, which is usually stored on site until it is appropriate to use as a fertilizer for growing crops and soil conditioner.

The primary nutrients retained digestate are Nitrogen, Phosphorous and Potassium (N, P, K). These elements were initially present in the original feedstock but are now in a more accessible form within the digestate.

Most AD plants are fed a mix of feedstocks so that the digestate nutrient content will reflect the variety of feeds. Therefore, it is essential to analyze for digestate nutrient content to ensure the correct application rate to land.

2.5.2.2 Digestate Storage & Application

Digestate requires storing before it is applied to the land, so process and environmental factors must be considered when designing digestate storage facilities.

Digestate is usually stored throughout the winter months and applied to the land as crops require it to maximize the uptake of nutrients. However, it can be spread once ground conditions are suitable and during the times that environmental regulations allow this.

Either the raw digestate or just its liquid component is stored in a digestate storage tank or a lagoon. Separated fiber would be stored in a building or a clamp. Digested sewage

sludge is dewatered into a ‘cake’ and stored as a solid, with liquors returning to the sewage works [50].

- **Digestate Storage Considerations**

- Mixing

Digestate stores require a method of mixing the contents, including a submersible mixer or a tractor-driven mixing system. It is vital to ensure the digestate in the storage vessel is thoroughly mixed before spreading it onto the land for even nutrient application.

- Covers

Digestate stores and lagoons can have covers to prevent rainwater ingress and reduce odors and emissions. Some covers are specifically designed to be gas tight and provide a way of capturing residual biogas from the digestate. Media such as clay balls can also be used to prevent odors and emissions.

- Separators

Numerous AD Plants are equipped with separators that divide the entire digestate into liquid and solid fractions before it enters the ultimate storage container. The benefits of separation are:

- It separates the fibrous material and reduces the amount of liquid digestate that requires storing.
- Improves the application of digestate to the land, as the liquid and solid fractions can be handled separately.
- Reduces problems with solids build up within the digestate storage vessel [50].

3 State of the Art on Biogas as a Fuel:

3.1 The Engine Definition

Engines are essential devices that convert energy from one form to another. In particular, the efficiency of this conversion process is crucial. Commonly known as "heat engines," most engines are designed to convert thermal energy into mechanical work. These engines operate by converting chemical energy derived from a fuel to thermal energy, which is subsequently utilized to perform useful work.

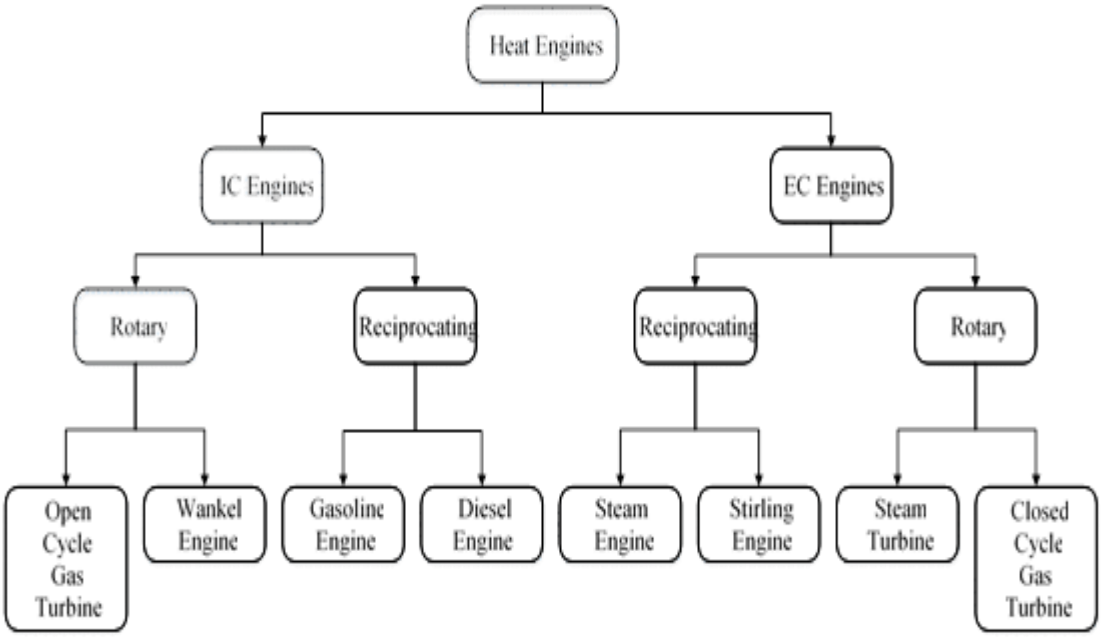

Figure 1-9 Classification of heat engines [51].

3.1.1 External Combustion Engines

External combustion engines (ECEs) are engines where combustion happens outside of the engine. This term covers engines that obtain their heat from a source separate from the fluid used for engine propulsion.

3.1.2 Internal Combustion Engines

Internal combustion engines (ICEs) convert heat produced by combustion into mechanical energy. They are categorized into two primary types: spark ignition (SI) engines, which utilize gasoline, and compression ignition (CI) engines, which function on diesel. Gasoline engines are commonly used in automobiles and motorcycles, while diesel engines are employed in trucks, ships, and off-road vehicles due to their superior energy efficiency and power density relative to gasoline engines [52].

3.2 Biogas as a Fuel in the IC Engines

Biogas, containing a significant portion of CH_4, is usable in ICEs due to its combustible nature. However, the presence of non-combustible gases like CO_2 within biogas reduces its lower heating value. Consequently, the combustion speed of the mixed gas slows down, elongating the highest pressure duration and reducing the maximum pressure achieved during combustion [53].

When incorporating fuel into an engine, there are several operational modes: utilizing a single type of fuel, employing a choice between two fuels (like gasoline and an alternative such as biogas in spark-ignition systems), or blending two fuels, usually diesel and an alternative fuel like biogas in CI systems. Moreover, the fuel delivery to the combustion chamber differs, ranging from basic venturi gas mixers that combine air and fuel to more sophisticated pressured injection systems that provide controlled and efficient fuel delivery at higher pressures [54].

Even though biogas can be utilized in CI engines, its higher autoignition temperature, which is approximately 15% to 25% greater than that of diesel, and its lower ignitability prevent it from being the sole primary fuel in these engines. Hence, CI engines require a supplementary injection of diesel fuel to ignite the biogas [55].

When utilized in SI engines, biogas doesn't encounter similar issues. The spark plugs designed for igniting the petrol-air blend can readily ignite the biogas mixture. Minimal adaptations are necessary in standard spark plug designs to accommodate biogas combustion for generating the requisite energy. Moreover, owing to its high octane rating (MON=130), biogas allows for increased compression ratios in engines without causing knocking, ultimately improving overall engine performance [56].

The pivotal aspect when employing fuels in engines revolves around the Wobbe Index (WI), deemed the primary criterion for gas interchangeability. When Wobbe indices are comparable, it signifies that a fuel can be substituted, maintaining similar power outputs, at designated pressure and valve settings. WI serves as a standardized gauge for fuel traits and their interchangeability within engines, encompassing power providers and Original Equipment Manufacturers (OEMs). Initially conceived to characterize various compositions of natural gas (NG) [57].

$$WI = \frac{HHV_{fuel,Vol}}{\sqrt{\rho_{fuel}/\rho_{air}}} \qquad MWI = \frac{LHV_{fuel,Vol}}{\sqrt{T_{gas}\,\rho_{fuel}/\rho_{air}}} \qquad (1\text{-}2)$$

In our context, WI is described as higher heating value (HHV) of the gas divided by the ratio of fuel density to air density. The Modified Wobbe Index (MWI) encompasses the lower heating value (LHV) and fuel temperature. Various WI classifications are well-documented in literature. Table 1-1 illustrates WI values for biogas and other singular fuels, including pure H_2, syngas (CO), liquefied petroleum gas (LPG), and CH_4 [57].

Table 1-1 The ranges of Wobbe index at normal condition [57].

Fuel Category	*Wobbe Index Range (MJ/Nm^3)*
Biogas ($0.9CH_4$-$0.1CO_2$)	44.41
Biogas ($0.6CH_4$-$0.4CO_2$)	24.64
Syngas Type	24-29
Natural gas Type	48-53
LPG Type	72-87
Methane	47-53
Hydrogen	40-48

3.3 Previous Works on Biogas Use in SI engines

Numerous researchers are actively exploring ways to optimize the utilization of this alternative fuel in SI engines. Strategies such as elevating compression ratios (CR), optimizing spark timing, investigating CO_2 content adjustments, upgrading biogas quality, exploring biogas-gasoline blends, and enrichment of H_2 enrichment are some of the focal points within the biogas research domain. Subsequent sections will delve into several noteworthy studies on these topics.

3.3.1 Increasing the Compression Ratio

Hotta et al. [58] explored a single cylinder SI engine performance fueled by both biogas and gasoline. They conducted experiments at a CR of 10, examining a spectrum of conditions from wide open to part throttle across speeds ranging from 1450 to 1700 rpm, resulting in distinct findings. When fueled by biogas, the engine exhibited an 18% decrease in brake power (BP), a 66% rise in brake-specific fuel consumption (BSFC), and a 12% decline in brake thermal efficiency (BTE). Notably, emission components like nitrogen oxide (NOx) and carbon monoxide (CO) showed significant reductions by 81.5% and 40%, respectively. However, there was an increase of 6.8% in unburnt hydrocarbon (UHC) emissions and a 40% increase in CO_2 emissions. Additionally, the cylinder pressure observed when using biogas was lower compared to that recorded with gasoline.

Porpatham et al. [59] performed experiments using a single cylinder diesel engine converted to SI, at 1500 rpm. The engine was tested at throttle openings of 100% and 25%, exploring multiple equivalence ratios spanning from lean to rich limit. Within a CR of 15:1, they achieved a power output of 4.8 kW. Furthermore, when increasing the CR from 9.3:1 to 15:1, they observed a rise in peak BTE from 23% to 26.8%.

Simultaneously, there was an increase in NOx levels from 2125 to 2650 ppm and for HC levels from 1184 to 2000 ppm.

Simsek et al. [60] investigated experimentally on a four stroke, single cylinder SI engine running with LPG, biogas, and gasoline at both half (HTO) and full (FTO) throttle openings. Results indicated adverse effects on BSFC, BTE, and cylinder pressure values when fueling with LPG and biogas. At FTO, there was a considerable 75.52% and 34.19% increase in BSFC versus gasoline usage, while BTE showed reductions of 16.04% and 8.95%. At HTO, BSFC increased by 85.2% and 45.51%, and BTE decreased by 33.43% and 20.22% with biogas and LPG, respectively. Cylinder pressure values also saw declines of about 17.76% and 24.41% with biogas and LPG. However, emissions showed significant improvements. With biogas and LPG in FTO, CO emissions decreased by 15% and 62.03%, HC emissions by 23% and 63%, and CO_2 emissions by 6.77% and 56.42% compared to gasoline. At HTO, reductions of 15.97% and 47.65% in CO emissions, 21.19% and 62.38% in HC emissions, and 6.84% and 69.54% in CO_2 emissions were observed for biogas and LPG, respectively.

Sudarsono et al. [61] studied the CR varying impact on a generator of 3 kW powered by biogas. Their aim was to determine the ideal CR for the generator's optimal operation within biogas. They evaluated the engine's efficiency -specifically, BP, torque, BSFC, and BTE- across compression ratios of 7.5, 8.5, 9.5, and 10.5. Their findings indicated that the most efficient CR for the generator running on biogas was 9.5. At this optimal CR, the engine displayed maximum values of 450.37 W for BP, 1.66 Nm for brake torque, 46.93% for BTE, and 0.59 Kg/kWh for BSFC.

3.3.2 Advancing Spark Timing:

Samanta et al. [62] investigated the spark timing (ST) impact on a SI engine model in their study. Their findings revealed that the most optimal performance was achieved at 27° before top dead center (BTDC). At this ST, BTE reached 24%, while BSFC measured 0.29 m^3/kWh. Rossetto et al. [63] conducted an assessment on an Otto cycle engine using a dynamometer, examining its performance while fueled by biogas. They derived torque and power characteristic curves for the engine and determined that the greatest power using biogas was achieved within these specific conditions: a CR of 12.5:1, an elongated gas mixer, and a spark advance of 45°. These circumstances

resulted in achieving peak power that surpassed the original biogas power output by 100%.

Sendzikiene et al. [64] explored the effects of bio-methane gas containing 65% of CH_4 and 35% of CO_2 on a SI engine's (Nissan Qashqai HR 16DE) performance and emissions under specific conditions: a 15% open throttle, consistent stoichiometric fuel mixture, and varied advance angles of ignition versus gasoline. They discovered that optimizing thermal efficiency required ignition advancement angle of 4°CA. Moreover, their observations indicated that CO_2 within biogas hampers combustion, driving to increased CO content in the exhaust gas. However, this resulted in reduced NOx emissions and lower HC concentration.

Chandra et al. [65] conducted experiments on a modified 5.9 kW CI to SI engine running on compressed natural gas (CNG), biogas, and biomethane. The CR was fixed at 12.65 while the ignition timing at TDC was varied at 300, 350, and 400. Advancing the spark to 350 resulted in the highest recorded brake power, but also exhibited substantial power losses compared to the engine's original fuel. The losses were 31.8%, 35.6%, and 46.3% for natural gas, biomethane, and biogas, respectively. Interestingly, biomethane showcased analogous values for specific gas consumption, engine performance, thermal efficiency, and BP output when compared to NG.

3.3.3 CO_2 Content Variations

Kim et al. [66] explored various compositions of biogas fuels within a micro co-generation engine system, regulating the fuel flow rates and intake air to alter the equivalence ratio. Their findings indicated higher CO_2 content led to increased ignition delay and reducing the combustion speed at a given engine load. Although fuel consumption showed a slight increase with CO_2 content, implementing a lean burn strategy notably improved thermal efficiency, resulting in reduced NOx emissions. Furthermore, utilizing biogas with a stoichiometric air/fuel ratio effectively lowered NOx emissions and enhanced fuel economy, particularly at higher loads.

Huang and Crookes [67] conducted simulations involving biogas with varied CO_2 concentrations (0%-40%) in an Otto cycle engine Ricardo E6 model across four different speeds. They identified the optimal compression ratio as 13:1 for all gas mixtures, observing instances of knocking at a 15:1 compression ratio with certain biogas compositions. Additionally, they noted a 3% reduction in BTE with an increase

in CO_2 to 40%. Moreover, elevating the compression ratio beyond 13:1 resulted in increased emissions of CO, HC, and NOx.

In a comparable study, Jawurek et al. [68] observed a decrease in power output by 10-20% when replacing gasoline with methane in an engine. While overall performance remained satisfactory, engines faced challenges at higher CO_2 concentrations typical of raw biogas, displaying issues such as starting difficulties, uneven performance, and power reduction. Engines ran harshly at CO_2 concentrations of 42% and above but operated more smoothly at 23% and below. At 41% CO_2, there was a 45% power reduction compared to petrol. Ignition solely on biogas was feasible only at concentrations of 31% and lower, requiring the assistance of petrol at higher CO_2 concentrations for ignition.

Porpatham et al. [69] examined the impact of decreasing CO_2 percentages using a constant-speed engine. They achieved reduced CO_2 levels via a lime water scrubber, achieving concentrations of 21%, 30%, and 41%. Employing a modified valve enhanced swirl, maintaining a fixed compression ratio at 13:1, while the equivalence ratio varied from lean to rich at a constant speed of 1500 rpm. Reducing CO_2 levels directly enhanced performance, expanded the range for lean operation, lowered emissions-particularly HC in lean mixtures-and showcased an augmented thermal efficiency. Retarding spark timing by 50 at a 10% CO_2 level resulted in significant HC reduction and a minor elevation in NOx levels.

Kriaučiunas et al. [70] examined the impact of varied biogas compositions of 0%, 20%, 40%, and 50% CO_2, on a four-cylinder NISSAN HR16DE SI engine. They conducted experiments using two ST (fixed/optimal) at 2000 rpm, employing a stoichiometric biogas and air mixture. Their findings revealed that elevating CO_2 concentration alongside fixed ST notably extended the mass burned fraction combustion duration by 90%, leading to reduce in cylinder pressure, BTE, and NOx emissions. Conversely, the selection of optimal ST increased BTE, HC, and CO_2 emissions, as indicated by the authors.

Karagoz et al. [71] explored the impact of CO_2 content in biogas on spark ignition performance and engine vibration using a modified four-cylinder diesel engine, equipped with a spark plug. They conducted experiments with composition of biogas containing 49% and 13% CO_2 across power levels ranging from 1.5 kW to 9 kW, in

increments of 1.5 kW, while maintaining a steady 1500 rpm engine speed. Their findings revealed an increase in engine vibration across all axes with higher CO_2 content and increased engine load. Moreover, they observed a rise in cylinder pressure with reduced CO_2 ratios and higher engine loads. For instance, at 1.5 kW, The peak in-cylinder pressure with 13% CO_2 biogas was roughly 24% higher than with 49% CO_2 biogas, whereas at 9 kW, it was 14% higher. This led to a decrease in BSFC; the BSFC for 49% CO_2 was 30% higher at 1.5 kW and 15% higher at 9 kW compared to 13% CO_2 biogas.

Mokrane et al. [72] studied numerically the impact of biogas composition on NOx and CO emissions in an SI engine. Their findings indicated a major reduction in NOx emissions with a rise in CO_2 content within the biogas. CO emissions remained low and were observed only at higher concentrations of CH_4. Their study suggested that a biogas mixture comprising 60% CH_4 and 40% CO_2, burning at approximately ϕ = 0.9 (stoichiometry), and employing an advanced ST ranging between 10 to 20°, represents a practical and promising combination concerning biogas composition, stoichiometry, and spark timing.

3.3.4 Biogas Upgrading

Prakash et al. [73] undertook an effort to enhance biogas quality with eliminating CO_2 and H_2S, thereby elevating its CH_4 content to NG levels. Their study involved analyzing a four-stroke SI engine performance fueled with this upgraded biogas as the primary source, evaluating its emission characteristics. The engine exhibited superior performance with the upgraded biogas compared to the raw version. BP for raw and upgraded biogas was respectively 38% and 12% lower than that of gasoline, while the BSFC averaged 19.5% lower. Additionally, there was a significant reduction in CO, NOx, HC, and CO_2 emissions by 82%, 69%, 75%, and 12% respectively.

Putrasari et al. [74] conducted an assessment of an SI engine's performance and emissions when fueled by CNG (Compressed Natural Gas) under varied load conditions. The engine under study was the Honda L15A, featuring four cylinders with a displacement of 1,497 CD^3, equipped with an electronic control unit. The experiments were conducted at throttle openings of 25% and 80%, maintaining an engine speed exceeding 4800 rpm. Results indicated that at a 25%, the engine utilizing a commercially available CNG conversion kit exhibited nearly equivalent maximum

brake power (19.00 kW) compared to the suggested CNG kit (19.68 kW). Conversely, at an 80%, the SI engine equipped with the proposed CNG conversion kit showcased higher maximum BP (38.67 kW) in contrast to the commercially available CNG kit (34.29 kW). Furthermore, the HC and CO emission levels at an 80% were observed to be lower than those at a 25% throttle opening for both the commercially available and proposed CNG conversion kits.

3.3.5 Blending Biogas with Gasoline

Simsek et al. [75] investigated the biogas and gasoline blend effect at various volumetric ratios on a Honda GX390 (single cylinder) SI engine. They conducted experiments with an increased CR at six different loads while maintaining a constant speed. The research assessed emission levels, performance metrics, and combustion indicators relative to the operation on gasoline. Results indicated that the utilization of 100% biogas resulted in the lowest BTE and the highest BSFC. Versus gasoline, there was an increase of 75.52% in BSFC and a decrease of 16.04% in BTE and observed with 100% biogas. However, using biogas improved overall emissions, with the top emission values noted for 100% biogas. In comparison to gasoline, NOx, HC, and CO emissions decreased by 48.96%, 63%, and 56.42% respectively. Additionally, operating with 100% biogas yielded lower pressure compared to gasoline, resulting in approximately a 24.69% reduction.

Peter et al. [76] investigated into performance and emissions while operating engines with enriched and compressed biogas blends (B10, B20) compared to gasoline at a constant speed. Their findings highlighted a notable increase in BSFC and a reduction in BTE of the engine. Additionally, the study observed a decrease in exhaust emissions such as CO_2, CO, and HC for biogas blends. However, in the case of NOx, the trend was reversed for biogas blends.

Awogbemi et al. [77] studied experimentally on a Honda GX 140 (single cylinder) SI engine, utilizing a 80:20 petrol-biogas blend across a speed range from 1000 rpm to 3500 rpm in 500 rpm increments. The study uncovered that the biogas-petrol blend displayed heightened torque, BP, indicated power, BTE, and brake mean effective pressure in comparison to petrol. Additionally, it demonstrated reduced fuel consumption and exhaust gas temperature in contrast to pure petrol.

3.3.6 Hydrogen Enrichment:

Mathai et al. [78] explored the impact of augmenting CNG with 18% H_2 by volume, aiming to create a higher fuel than NG for a dual fuel gasoline generator. Their examination encompassed various aspects such as power output, emissions, engine parts conditions, and the quality of lubricating oil, comparing CNG against HCNG. Over a 60-hour duration, HCNG exhibited reduced BSFC, as well as lower emissions of CO and HC, but notably elevated levels of NOx. Iron deposits were visibly present on spark plugs and cylinder liners when using HCNG, resulting in significant reductions in kinematic viscosity and Total Base Number (TBN) in the lubricating oil. Additionally, there were heightened concentrations of wear metals.

Chen et al. [79] found that elevating H_2 concentration augments the heat release rate and enhances flame speed propagation. Additionally, with higher H_2 concentrations, the overall calorific value of the gas mixture decreases, facilitating temperature reduction and lowering NOx emissions. Increased CO_2 dilution leads to heightened variability in engine cycles, but augmenting the rate of H_2 can mitigate this cycle variability.

Park et al. [80] highlighted that introducing H_2 into the mixture improves combustion stability and widens the low temperature spectrum by reducing H_2 and HC emissions while increasing NOx emissions. However, the rise in H_2 content correlates with increased heat transfer losses, thereby reducing thermal efficiency. Although H_2 enhances the stability of biogas combustion, it also leads to higher adiabatic flame temperatures, resulting in elevated NOx emissions.

3.4 Biogas Compared to Other Fuels

Beyond its efficacy in spark ignition engines, several compelling factors support the use of biogas: sustainability stemming from diverse, abundant, and long-lasting sources, cost competitiveness relative to petrol, safety in usage, and environmental friendliness.

Unlike LPG, another eco-friendly fuel, biogas isn't finite, being sourced from renewable and widely available raw materials. Its potential to harness vast waste reserves makes it a versatile supplement to fossil fuel-based natural gas, enabling seamless integration into existing systems and reducing overall production costs [81].

Compared to ethanol, which commonly serves as octane number booster rather than a primary fuel, biogas stands out as a more viable and versatile fuel option. Its cost-effective production from waste and indigestible food crops diminishes concerns about using arable land solely for energy crops. Despite ongoing discussions about this issue, there are other acceptable production methods available for biogas [82].

Despite its effectiveness in fuel cell systems, the biogas high production costs have hindered its widespread adoption, positioning it more as a futuristic fuel. Comparatively, hydrogen, another fuel garnering interest, outshines both gasoline and biogas in dedicated engines. In a classical SI system, H_2 offers potential for enhanced fuel economy and reduced emissions owing to its lean burn characteristics and noncarbon composition. Currently, the focus remains on incorporating hydrogen optimally to strike a balance between performance, emissions, and cost [83].

4 Conclusion

The experimental endeavors of multiple researchers exploring the use of biogas in SI engines. Building on this extensive literature review, our study delves into the performance dynamics of SI engines under two distinct loading conditions utilizing raw biogas.

The subsequent chapter will detail the experimental exploration of raw biogas production sourced from diverse feedstocks.

CHAPTER 2:

THE EXPERIMENTAL BIOGAS PRODUCTION SETUP

CHAPTER 2

1 Introduction

This chapter comprises two parts. The first one provides a concise overview of the potential for harnessing cow dung (CD) and food waste as sources for biogas production. The second part delves into the setup and methodology employed in the experimental production of biogas.

2 Cow Dung as Substrate

It is critical to provide a clean energy source free of pollution. Biogas emerges as a technology that holds promise in mitigating various negative socio-economic, health, and ecological implications linked to the conventional use of biomass energy in Algeria. Its utilization stands as a pivotal solution in addressing energy challenges in rural areas, notably benefiting marginalized communities.

An important benefit of biogas production lies in its ability to utilize wet biomass feedstock with a moisture content exceeding 60–70%, such as sewage sludge, animal slurries, and food waste [84]. Approximately one ton of organic waste generates an output of 100-160 m^3 of biogas, equating to 60-100 liters of petrol [85].

2.1 Biogas Potential from Animal Dung

When cattle slurry/dung is anaerobically stored, it also contributes to atmospheric CH_4. The entire global methane generation from dung is estimated to be 35.2 million tonnes annually, accounting for around 9% of total biogenic output [86].

Mitigation solutions against CH_4 emissions from animal dung have three key advantages. Firstly, less animal methane means lower greenhouse gas concentrations in the atmosphere. The second benefit is that it increases farmer revenue since less methane implies more efficient animal output. A third significant advantage arises from converting livestock dung to biogas [87].

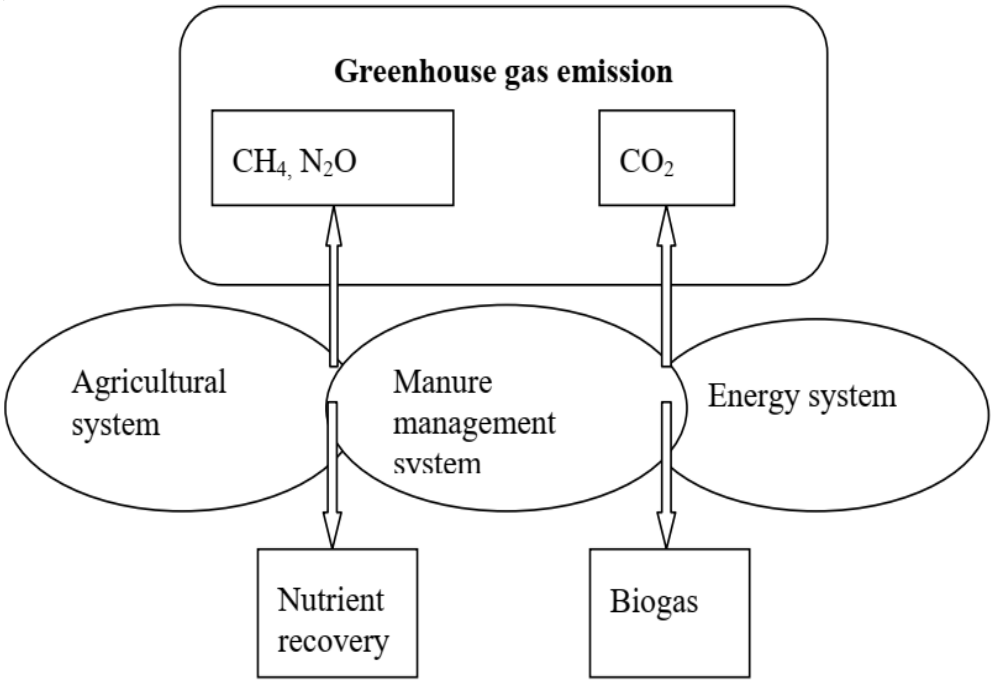

Figure 2-1 Environmental advantages of the dung/biogas/digestate system [88]

Dung is an excellent starting substrate for biogas plants because of its availability and accessibility, comprises all essential nutrients required by anaerobic bacteria and possesses a significant buffering capacity. All animal dung types may be used to generate biogas, according their quantity, features, and design. The CH_4 generation capacity of dungs varies depending on dung type (Table 2.1) and case specific factors such as animal diet and housing methods, dung TS content, and the type of bedding material used [89].

Table 2-1 Potential biogas production from specific livestock dung [89]

Animal	*Total dung (Kg/head/day)*	*Total solid TS (Kg/head/day)*	*Biogas yield factor (m^3/Kg of dry matter)*	*C/N ratio*	*VS (% of fresh dung)*
Cow	20	4.0	0.20-0.50	18-25	13
Buffalo	25	4.5	0.15-0.32	18-25	-
Pigs	1-5	0.6	0.56-0.65	13	12
Sheep	1.8	0.6	0.37-0.61	29	-
Poultry	0.1	0.03	0.31-0.54	-	17
Horses	24	7.1	0.20-0.30	24-25	-

2.2 Composition of Cow Dung

According to the ministry of agriculture and rural development, Algeria had a cow population of 942,828 heads in 2016 [90].

The biogas composition, including the ratio of CO_2 to CH_4, is influenced by the characteristics of the dung. CD, for instance, consists of various constituents in different proportions (Table 2.2). Typically, biogas derived from cow dung contains approximately 55-65% CH_4 and 35-45% CO_2. Additionally, N_2 and H_2S traces are present in the resulting biogas [91].

Table 2-2 Composition of cow dung [91]

Components	Dry Matter (%)
Volatile Solids	83.0
Ether Extract	2.6
Cellulose	31.0
Hemicellulose	12.0
Lignin	12.2
Starch	12.5
Crude Protein	12.5
Ammonia	0.5
Acids	0.1

2.3 Mono-digestion of Cow Dung

Using CD in exclusive processes proves advantageous for biogas generation due to the presence of essential fermentation microorganisms and a rich composition of biodegradable elements such as carbohydrates and lipids [92]. Throughout the process, the interaction between resultant byproducts like NH_3 and VFAs plays a crucial biochemical role, ensuring stable digestions while potentially decreasing methane output [93]. An estimation for the electrical power setup in a biogas plant primarily reliant on CD involves multiplying the volume of daily dung by 2.4 kW_{el} d/m^3. For instance, a farm housing 200 cows might produce approximately 10 m^3/d dung with a 10% dry matter content [84].

The limited CH_4 output observed in the mono-digestion of CD can be attributed to the dung reaching the residue phase post-internal digestion. This phase absorbs a portion of the nutrients, resulting in reduced methane production. However, the residual

bacteria present in the residue continue to contribute to the biodegradation of organic materials throughout the anaerobic digestion AD processes. Its high lignin and N_2 concentrations may have a detrimental impact on biogas generation processes [94]. Furthermore, its poor methane output as a single substrate includes its high-water content and high fiber percentage [95].

Under mesophilic conditions, the mono-digestion of diverse raw materials from various biomasses resulted in differing CH_4 outputs. Among these, maize grains displayed the highest CH_4 production, generating 393 m^3 Mg^{-1} VS within 40 days, whereas cow dung exhibited the lowest yield at 67 m^3 Mg^{-1} VS in 24 days. Conversely, when subjected to thermophilic conditions, food waste showcased the highest CH_4 yield of 435 m^3 Mg^{-1} VS within 28 days, while municipal sewage sludge yielded the least at 28 m^3 Mg^{-1} VS over 30 days (refer to Table 2-3) [94].

Table 2-3 Methane yields from Mono-digestion of various raw materials [94]

Material		Methane yield m^3 Mg^{-1} VS	Condition(s)	Interval (day)	Reference
CM		67	36±1°C Wet digestion pH 7. 25-7. 02	24	Achinas et al. 2018
		204±16	35±1°C WD (CSTR)	20	Cropgen 2006
Maize	Grains	393	40°C WD	40	Simona et al. 2015
	Stalks	234	40°C Dry digestion	40	
	Cobs	207	40°C DD	40	
Grass	Ley	290±7 - 340±4	37.5°C DD	30	Prade et al. 2019
Straw	Rice	333 (theoretical)	37±1°C DD pH 6.8-8.0	23	Yuan 2013
		178 (experimental)	37±1°C DD pH 6.8-8.0	23	
	Sugar beet top	181±9	35±1°C WD	20	Cropgen 2006
	Oat straw	138±17	35±1°C WD	20	
Food waste		353	35±1°C Semi-dry digestion pH 7.10	30	El-Mashad and Zhang 2010
		435	50±2°C DD pH 7.57(±0.13)	28	Zhang et al. 2006
Sewage sludge		255	35°C WD	30	Montañés et al. 2014
		28	55°C WD	35	

Figure 2-2 is derived from the mono-digestion outcomes provided in Table 2-3.

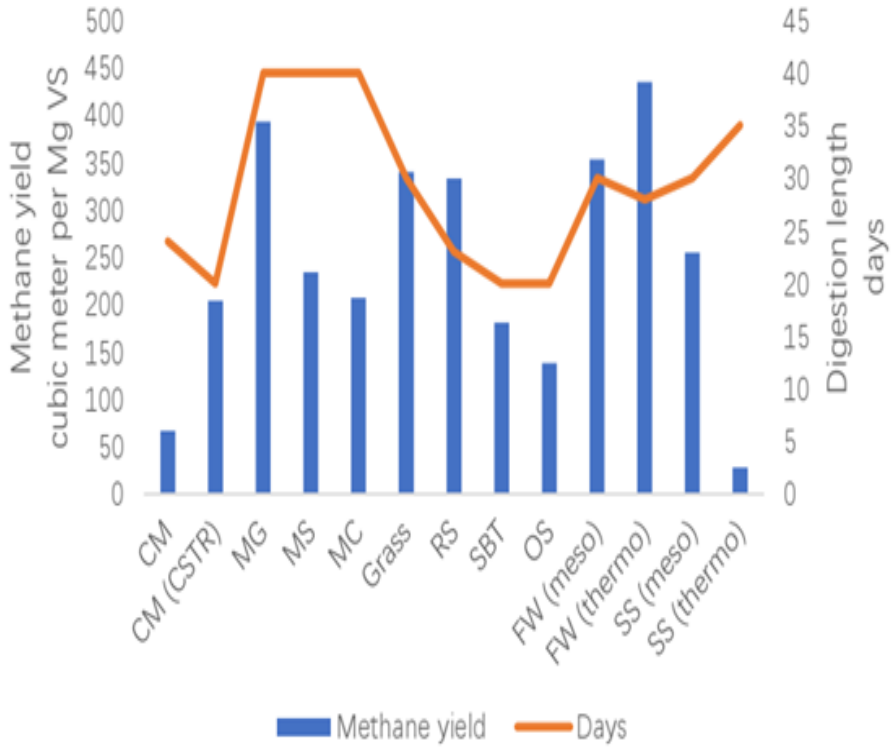

Figure 2-2 CH_4 yield obtained from mono-digestion of various raw materials [94]

2.4 Co-digestion between Cow Dung with Some Common Biowaste

Today, the co-digestion of different substrates stands as the prevailing process type in biogas plants within farming communities, and it has become a standard technology in most European nations, as well as in Asia and the United States [96]. Co-digestion boosts biogas generation by creating positive synergy in the medium and replenishing deficient nutrients with co-substrates. Moreover, co-digestion also aids in the establishment of ideal moisture levels of raw materials supplied into the digester. Furthermore, Huang et al. noted co-digestion offers improved fertilizer stability compared to mono-digestion, thereby proving to be an effective method for improving the degradation of biowastes [94].

The utilization of animal dung in co-digestion presents three primary advantages. Initially, it supplies essential nutrients like trace metals and vitamins crucial for microbial growth. Secondly, it contributes to lowering the pH. Thirdly, its high moisture content assists in diluting concentrated organic wastes, mitigating potential inhibitions and difficulties in managing these wastes individually [95]. Furthermore, as compared to mono-digestion of cow dung, it improves microbial biodegradability and yields a 25-32% increase in specific CH_4 production [97].

All of the information gathered for the co-digestion was regarding the mesophilic process. Cow dung is an excellent "carrier" substrate during the mixed digestion of different wastes like food waste, organic industrial waste, and sewage sludge because it can optimize biogas production. The CD combination with different biowaste categories showcased a wide spectrum of yields (depicted in Figure 2-3, derived from Table 2-4). The methane yields ranged from 416 m^3 Mg^{-1} VS, obtained from a 1:2 combination of CD and oat straw within a 50-day period, to 121 m^3 Mg^{-1} VS, derived from a 1:1 blend of CD and kitchen waste over 45 days. [94].

Table 2-4 Methane yields from various combinations of CD with and another biowaste categories [94]

Material	Mixing ratio (CM:other)	Methane yield (m^3 Mg^{-1} VS)	Condition(s)	Interval (day)	Note	Reference
Maize straw (Central China)	10:3	175	37±0.5°C WD	30		Wang et al. 2016
		378	37±0.5°C WD	30	Alpha-amylase enzyme.	
	10:1	165	38±0.5°C WD	32	CSTR	Wang et al. 2017
Maize straw, fruit & vegetable waste (Central China)	CM:MS 10:1, 1% FVW	175	38±0.5°C WD	32	CSTR.	
	CM:MS 10:1, 5% FVW	202	38±0.5°C WD	32	CSTR	
Food waste (San Francisco, USA)	6.8:3.2	282	35±1°C WD	30		El-Mashad and Zhang 2010
	5.2:4.8	311	35±1°C WD	30		
Kitchen waste (Northwest China)	1:1	121	35°C SDD Initial pH 6.5	45		Zhai et al. 2015
		180	35°C SDD Initial pH 7.5	45		
Oat straw (Northern China)	4:1	158	37±2°C WD pH 6.63-8.4	50		Zhao et al. 2018
(CM from Central China)	1:2	416	37±2°C WD pH 6.63-8.4	50		
Sugar beet top (Central Finland)	9.5:0.5	149±12	35±1°C WD	28	CSTR	Cropgen 2006
	8.5:1.5	229±54	35±1°C WD	59	CSTR	
Paper and pulp sludge (Indonesia)	57%:36% Rest is water	269	29.0–32.5°C WD pH 6.2–7.3	40		Priadi et al. 2013

Figure 2-3 is derived from the co-digestion outcomes provided in Table 2-4.

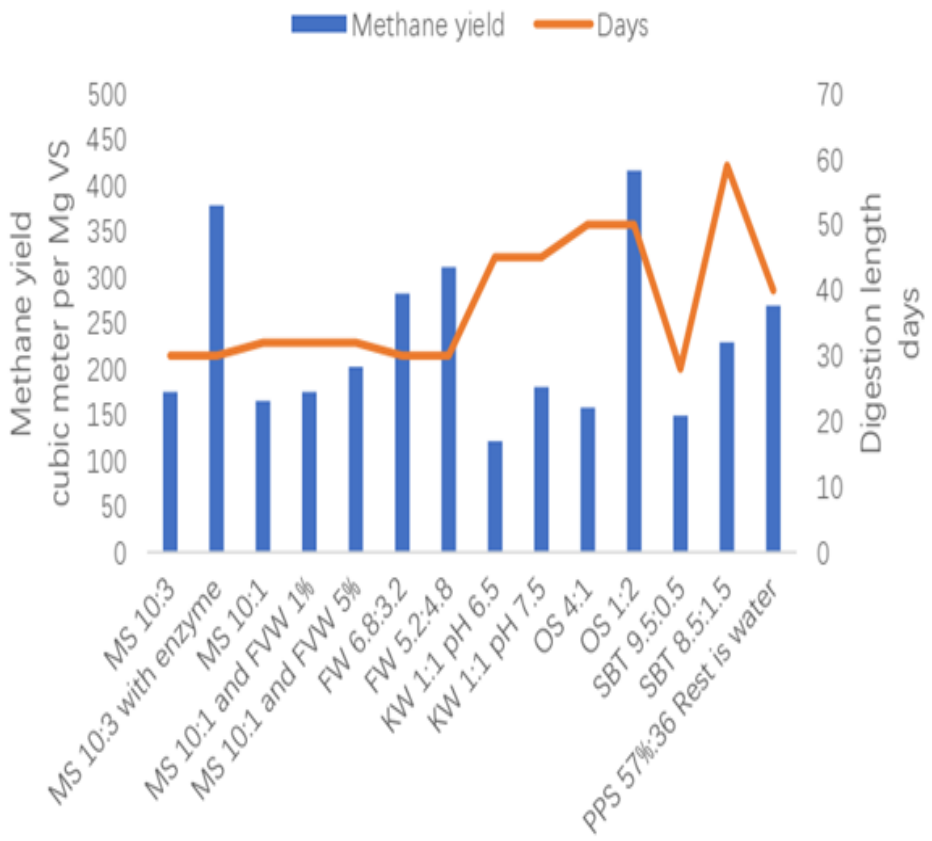

Figure 2-3 Methane yield from various combinations of CD with and another biowaste categories [94].

2.4.1 Mixed Food Waste

Food waste (FW) has high-energy potential as a feedstock for AD. The main factors are the contamination levels, the pre-treatment needs, and the necessity for pasteurization since it includes animal by-products (ABP) in the form of meat, dairy products, shellfish, aquatic animals, or invertebrates. Additionally, intricate organic compounds present in FW, including lipids sourced from animal fats, vegetable oils, and high-molecular-weight carbohydrates, pose challenges in biodegradation, thereby rendering hydrolysis a constraining phase in the anaerobic digestion of FW [98].

In general, dairy dung contains more macro- and micronutrients than FW. Combining cow dung with FW increases nutrient availability for the AD of FW [99]. This evidently demonstrates that co-digestion of FW alongside dung emerged as one of the more effective approaches for preserving reactor stability concerning pH maintenance, VS reduction, and CH_4 yield. Although dung has a lesser biodegradability than FW, it enhances TS concentration and methanogenic variety since dung is a source of methanogens [100].

Additionally, co-digesting a high C/N ratio substrate, like FW, alongside a low C/N ratio substrate, like dung, enhances methanogenic processes. This balance in nutrient and carbon requirements regarding VS and chemical oxygen demand (COD) prevents the VFA accumulation and enhances the system's buffering capacity [101]. For instance, mesophilic co-digestion FW + Dung yielded a 26% increase in CH_4 production versus the combined CH_4 yields from individual digestions of dung and FW [96].

3 Description of Biogas Production Setup

The experimental setup for this study comprised two 500-liter bioreactors termed digesters, along with a storage bag designated for biogas retention. Additionally, an upstream Biogas 5000 Geotech Analyzer was incorporated to analyze the biogas produced. To facilitate the bottles filling within biogas, a small refrigerator compressor (FN43GY model) was employed. The pressure within the bottles was regulated at 10 bars in the gaseous phase. Safety measures included incorporating two check valves and installing two pressure gauges, one upstream and one downstream of the compressor[102].

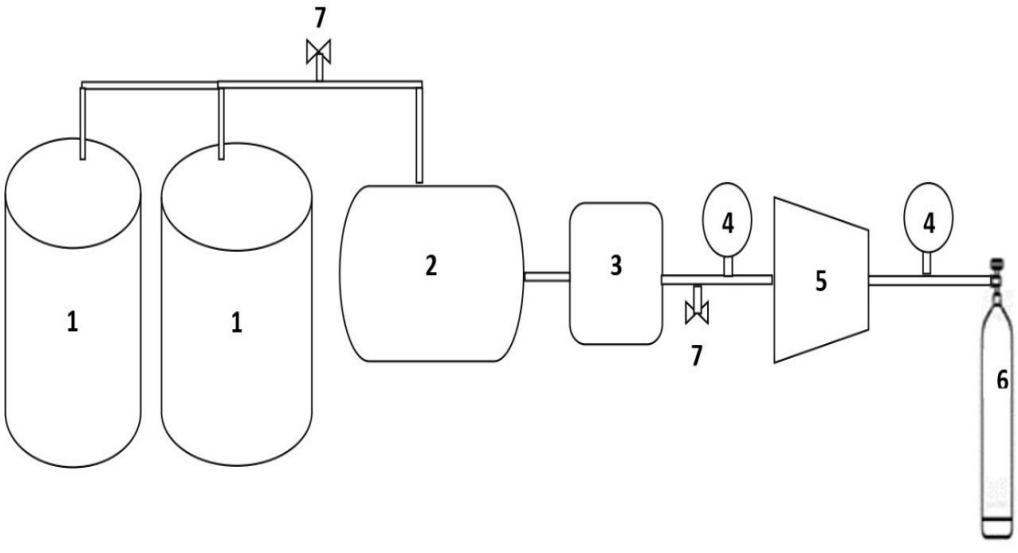

1- Digester 2- Bag 3- Analyzer 4- Manometers 5- Compressor 6- Bottles 7- Valves

Figure 2-4 Schematic Representation of the Experimental Biogas Setup [102].

Figure 2-4 illustrates the schematic representation of the experimental setup employed for production of biogas. This research took place within the Laboratory of Applied Energy Physics (LPEA) situated in the Department of Physics at Batna 1 University [102].

Several experiments on the quality of biogas composition from mono-digestion of dung and co-digestion of dung with FW were conducted. A thermometer, an electrical balance, and a laboratory oven were used to measure ambient chamber temperature, the mass of substrates, and the total solid (TS) concentration of substrates respectively. The digesters are equipped with additional valves to store and analyze the biogas produced for each digester separately.

3.1 Source of Substrates

3.1.1 Cow Dung

The studied farm is located in the Aïn Yagout region of Batna Province, Algeria. It contains approximately 130 dairy cows and produces 3,250 Liters of milk each day. The farmer has faced many problems, especially energy supply for his daily business, because of the disconnection from the grid.

Figure 2-5 The farm in Aïn Yagout, Batna Province, Algeria

Digesters were fed with fresh dung mixed in a proportion of 1:1 with water. The total cow dung used in the experiments is around 500 kg.

An electric stirrer was utilized within the digesters to ensure proper substrate homogenization during the experiments.

Figure 2-6 Preparation of the cow dung substrate

After feeding the digesters, it's crucial to seal them to establish the anaerobic conditions required for the anaerobic digestion process.

3.1.2 Food Waste

In this study, the substrate also used is FW, this substrate was gathered from the restaurant of Batna 1 University. This substrate is composed of easily biodegradable kitchen waste such as beets, carrots, salad, and cooked food, mainly rice and potatoes. The FW were fragmented into small pieces to guarantee substrate homogenization using a mixer.

Figure 2-7 Preparation of the food waste substrate

3.1.3 Substrate Characterizations

The dry matter is determined by the drying process in a laboratory oven maintained at 105°C until a consistent mass is achieved. The measurement method consists of placing 50 g of the substrate sample in the oven and keeping it there for 24 hours.

Figure 2-8 The oven laboratory used

The substrate sample is weighed after cooling by an electrical balance. The total solid concentration is expressed as a percentage relative to the weight of the sample.

Figure 2-9 The substrates weighing

We used this equation to calculate the total solid concentration:

$$TS = \frac{M2 * 100}{M1}$$

TS: Total Solid Concentration (%)

M1: The wet sample mass (g).

M2: The dry sample mass (g).

For CD substrate, we obtained TS = 7%. On the other hand, we obtained TS = 14% for FW.

3.2 Operational Conditions

The substrate digestion is heated to 35°C using an electric heater placed within an closed chamber to minimize heat loss. Monitoring the chamber's ambient temperature was facilitated by a thermometer.

Figure 2-10 The electric heater and the thermometer used

3.3 The Biogas Storage

We only stored the raw biogas generated from CD in the principal storage bag. At the same time, the biogas produced from co-digestion of CD and FW was stored separately

in another bag for analyzing and comparing the results between the quality of biogas obtained.

Figure 2-11 The biogas storage

3.4 The Biogas Analysis

The analysis of biogas, consistently saturated with moisture and displaying daily variations in composition, was conducted using the Biogas 5000 Geotech Analyzer. This analyzer gives us the tenor percentage of CH_4, CO_2, O_2 H_2S, and Bal. The balance is the sum of other gases like: N_2, H_2, CO and NH_3.

As standard, measures 4 gases: CH_4 & CO_2 (with measuring range 0 - 100% for both), O_2 (measuring range 0 - 25%), and H_2S (the order: 0-5000ppm)

Figure 2-12 The different results of biogas analysis

3.5 The Biogas Compression

Because there is no facility here in Algeria to compress biogas in bottles, we engaged in realizing our design of a biogas compressor by using a small refrigerator compressor FN43GY model. This compressor consists of various elements such as manometers, check valves, and tubes.

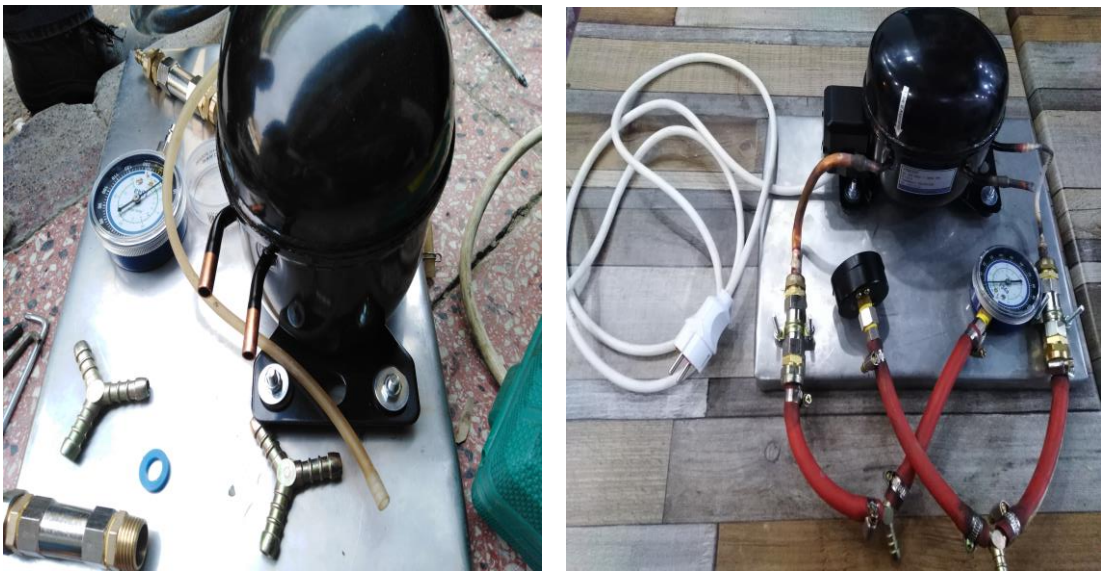

Figure 2-13 Compressor construction steps

3.6 Biogas Flammability

When the storage bags and bottles were filled with biogas, we tested the flammability and flame stability of this produced biogas. We used a lighter and a Bunsen burner for the ignition of this biogas produced.

Figure 2-14 Flame flammability tests

4 Conclusion

The chapter provides an overview of our experimental work concerning biogas production from varied substrates, specifically CD and FW. It delves into an in-depth explanation of the laboratory setup and the meticulous experimental protocol followed.

The next chapter will focus on the experimental analysis of the combustion of raw biogas using a SI engine test rig.

CHAPTER 3:

EXPERIMENTAL ENGINE TEST RIG SET-UP

CHAPTER 3

1 Introduction

This chapter is organized into four sections. The first part provides a theoretical overview of IC engine test rigs. The second part offers a description of the specific engine test rig used. The third part outlines the diagnostic and maintenance procedures for the setup. The final part details our experimental protocol and test procedures.

2 Theory of IC Engine Test Rig

An engine test rig comprises essential components such as an Internal Combustion (IC) engine, dynamometer, fuel metering system, air intake measuring equipment, and various other instruments. The primary aim purpose of an engine test rig is to either prepare the engine for testing, simulate operational conditions, or measure specific properties relevant to the testing objectives [103].

2.1 Operation of IC Engines

The reciprocating IC engine is engineered to transform the chemical energy accumulated in a fuel into mechanical energy. Among the most prevalent types of IC engines are the SI gasoline engine and the CI diesel engine. A relatively newer iteration is Homogeneous Charge Compression Ignition (HCCI) engine. These IC engines can function using either a four strokes cycle or a two strokes cycle.

2.1.1 SI Engine

SI engines are primarily utilized in auto vehicles like cars and motorcycles. However, due to challenges related to auto-ignition and flame propagation during combustion of premixed mixtures, these engines are not typically designed to be excessively large.

2.1.2 CI Engine

CI engines have a substantially broader range of applicability and are more suitable for commercial applications because they can function at substantially higher power outputs compared to SI engines. However, the combustion process in CI engines takes longer compared to SI engines. Consequently, CI engines typically aren’t capable of operating at the same speeds as SI engines.

2.1.3 HCCI Engine

Within the HCCI engine, combustion occurs through the compression of a homogeneous mixture formed in the combustion chamber, initiating ignition. HCCI combines elements of both engines. Similar to SI engines, HCCI requires a pre-mixed charge and, similar to CI engines, depends on auto-ignition to commence combustion. HCCI allows for higher compression ratios compared to SI engines, leading to enhanced efficiency similar to CI engines. Moreover, HCCI engines emit significantly less pollution compared to both SI and CI engines. Refer to Figure 3-1 for a general schematic depicting the operational principles of the engines [104].

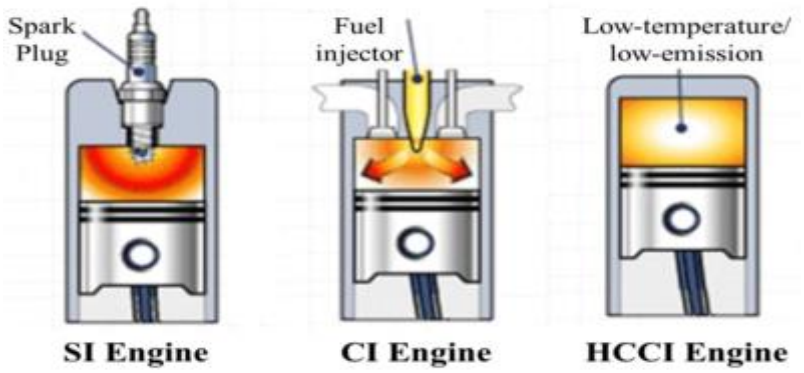

Figure 3-1 Different reciprocating engine types [104]

2.2 Engine Dynamometer

A dynamometer serves as a mechanical tool designed to measure the torque generated by a machine during its testing phase. In the context of engines, an engine dynamometer, connected to the engine's crankshaft, is a widely used type of dynamometer in various industries. This dynamometer applies resistance or load to the engine across different angular velocities. This load can be introduced through different types of brakes, such as water, electric, or friction brakes. Engine dynamometers are instrumental in evaluating the performance of an engine and are generally classified into two types: hydraulic and electric [105].

2.2.1 Hydraulic Dynamometer

Water brake dynamometers function based on the principle of using water flow that corresponds to the applied load, generating resistance for the engine. In this mechanism, each absorption section regulates the water flow, directing it through the input manifold towards the rotor’s center. Centrifugal force propels the water out of the dynamometer body, and as it moves outward, it enters pockets on the stationary stator plates. In these

pockets, the water undergoes deceleration, contributing to the applied load on the motor through the continuous acceleration and deceleration of water [105].

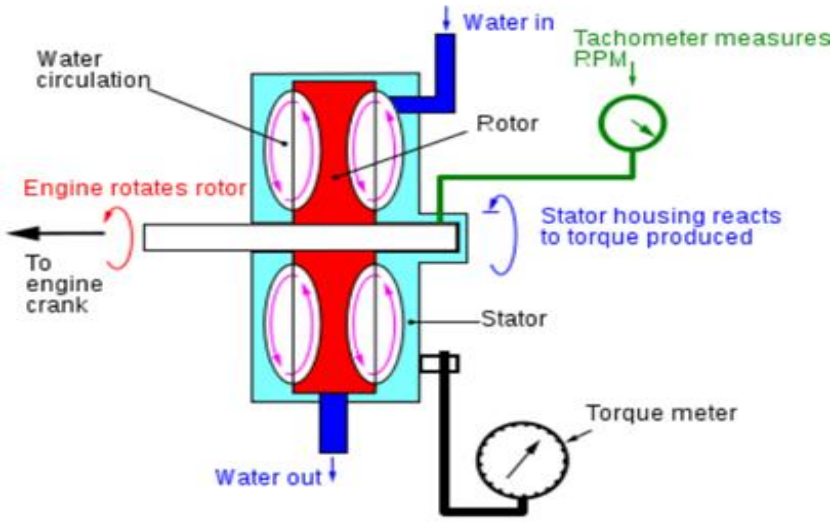

Figure 3-2 Schematics of a hydraulic dynamometer [105]

2.2.2 Electric Dynamometer

An electric dynamometer functions as a generator that loads the engine. The output from this generator requires measurement through electric instruments, and the value is adjusted to account for generator efficiency. It's important to note that generator efficiency can vary with factors such as loading, speed, and temperature, which can introduce some imprecision into the obtained values. However, torque imparted by the frame of the stator can be directly assessed by cradling the generator. This torque is produced by a magnetic connection between the armature or stator, resembling the engine's braking torque [105].

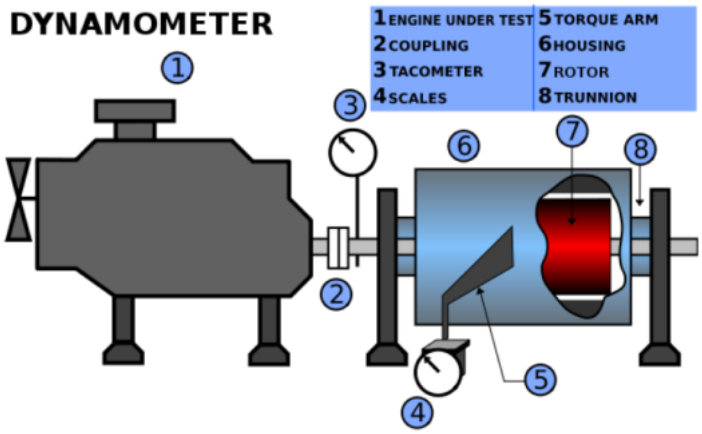

Figure 3-3 Schematics of an electric dynamometer [105]

2.3 Performance of Engine Test Rig

The IC engines performance can be evaluated on dynamometers, with various critical parameters are observed and analyzed. Among the key performance indicators are:

- Torque
- Brake Power
- Average effective brake pressure
- Fuel consumption
- Air/Fuel
- BSFC
- BTE

2.3.1 Torque

The most critical factor when choosing an engine. It denotes the torsional force the engine may provide from its main shaft to the vehicle's differential. So, we can say that the engine torque represents the capacity of the engine to produce work. It may be calculated using the following formula:

$$T = f \times d \quad \text{(N.m)} \tag{3-1}$$

Where f is the applied mass (Kg), and d is the distance between calibration weight and dynamometer shaft (m).

2.3.2 Brake Power

BP measures of the capacity of the engine's work in a given time. It indicates the ability to meet a certain amount of work produced in the unit. This is the real power that is transmitted to the output shafts in any case. The mechanical BP of an engine is calculated by multiplying the torque applied by the rotational speed. This formula gives it:

$$BP = \frac{2\pi \times N \times T}{60} \text{ (kW)} \tag{3-2}$$

In this equation, "N" stands for the speed measured in revolutions per minute (rpm), and "T" represents the torque measured in Newton-meters (N·m).

Ideally, all measurements should be calibrated to conform with standard atmospheric conditions.

$$BP_c = BP \times \frac{Ps}{P} \times \frac{T}{Ts} \text{ (kW)} \quad (3\text{-}3)$$

Where T & Ts represent the ambient & the standard temperatures, respectively (°C). P & Ps denote the ambient & the standard pressures (Pa).

2.3.3 Mean Effective Brake Pressure

MEP is a more relevant measure for comparing engine performance as it normalizes the work produced per cycle against the cylinder volume displaced per cycle. It represents the average pressure applied by the gas on the piston over a complete operating cycle. It can be calculated using the following formula:

$$PMEB = \frac{BP}{V_D} \text{ (kN/m}^2\text{)} \quad (3\text{-}4)$$

Where V_D is the engine displacement (cm^3).

2.3.4 Fuel Consumption

This parameter, determined experimentally, indicates the "speed of consumption" of an engine. It is calculated by measuring the time the engine takes to consume a specified volume of test fuel. This parameter is given by the following formula:

$$\dot{m}_f = \rho_f \times V_f \text{ (Kg/s)} \quad (3\text{-}5)$$

Where ρ_f is the fuel density (Kg/m^3), and V_f is the fuel consumed volume rate (m^3/s)

2.3.5 Air/Fuel

It is expressed as the ratio of air consumed in combustion to the amount of fuel burnt. When neither CO nor O_2 is present in the products, combustion is complete, and the air fuel ratio is termed theoretical or stoichiometric. This formula gives it:

$$A/F = \frac{\dot{m}_a}{\dot{m}_f} \quad (3\text{-}6)$$

In this equation, $\dot{m}_a$ represents the rate of air consumption (Kg/s), and $\dot{m}_f$ denotes the rate of fuel consumption (Kg/s), respectively.

2.3.6 Brake-Specific Fuel Consumption

The BSFC is a comparative factor that illustrates the efficiency with which an engine converts delivered fuel to useful power. It provides insight into the fuel amount consumed by the engine for the work it produces and can be determined by the following relation:

$$BSFC = \frac{\dot{m}_f}{BP} \tag{3-7}$$

2.3.7 Brake Thermal Efficiency

The BTE is the proportion between the power produced at the crankshaft and the energy content within the fuel needed to generate this power.

$$B_{th} = \frac{BP \times 3600}{\dot{m}_f \times LCV} \times 100 \tag{3-8}$$

Where LCV represents the lower calorific value of the fuel (kJ/Kg)

The LCV of gasoline is 44000 kJ/Kg, and the LCV of our raw biogas is 20283.09 kJ/Kg

3 Description of Engine Test Rig Set-up:

In the execution of this project, a hydraulic dynamometric bench housed in the Motor Laboratory at the Batna 2 University, was used.

In Figure 3-4, the schematic representation of the experimental engine test rig used is presented. The basic engine test rig consists of the instrumentation unit TD114, the hydraulic dynamometer TD115 and the engine GX140, as shown in Figures 3-4.

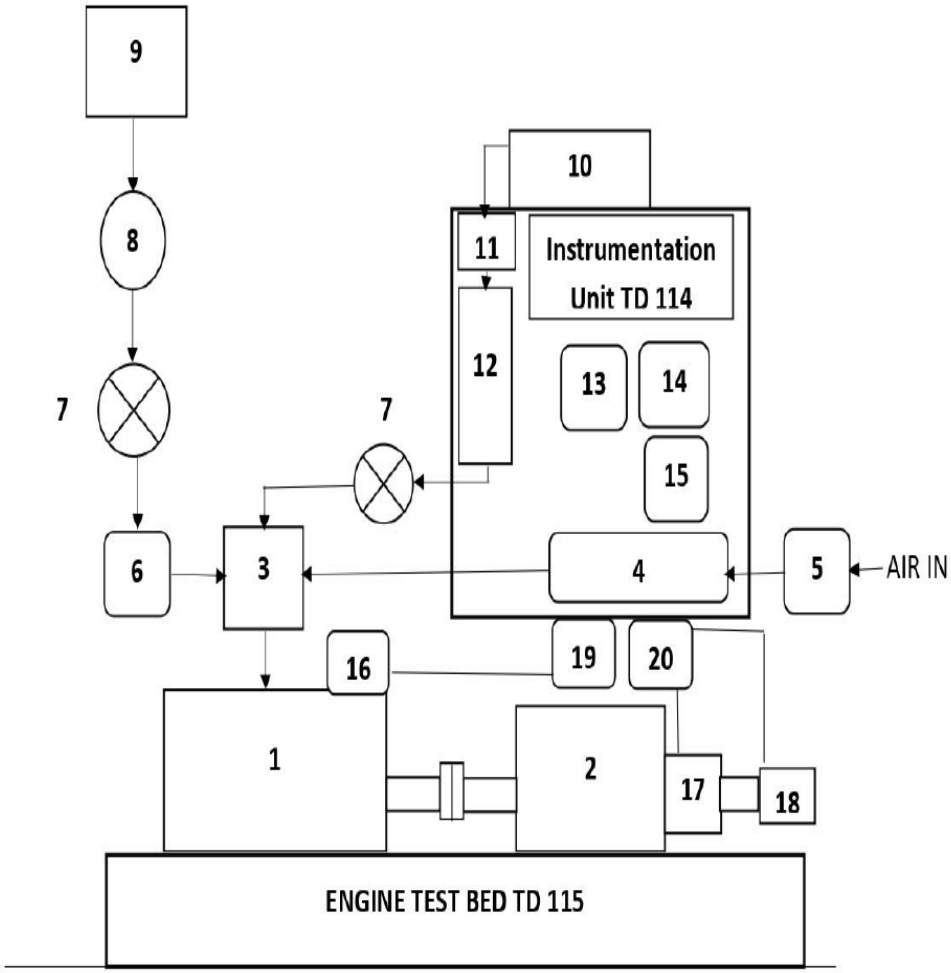

1- Engine, **2-** Hydraulic dynamometer, **3-** Carburetor, **4-** Inclined tube manometer, **5-** Airbox/viscous flowmeter, **6-** Gas meter, **7-** Control valve, **8-** Biogas flow manometer, **9-** Biogas bottle, **10-** Gasoline tank, **11-**Gasoline tank level, **12-** Graduated flow pipette, **13-** Tachometer, **14-** Torque meter, **15-** Exhaust temperature meter, **16-** C/A Thermocouple, **17-** Rotary potentiometer, **18-** Pulse counting system, **19-** Thermocouple sockets, **20-** 4/5 Pin canon (tachometer/torque transducer).

Figure 3-4 Schematic experimental engine test rig representation [102]

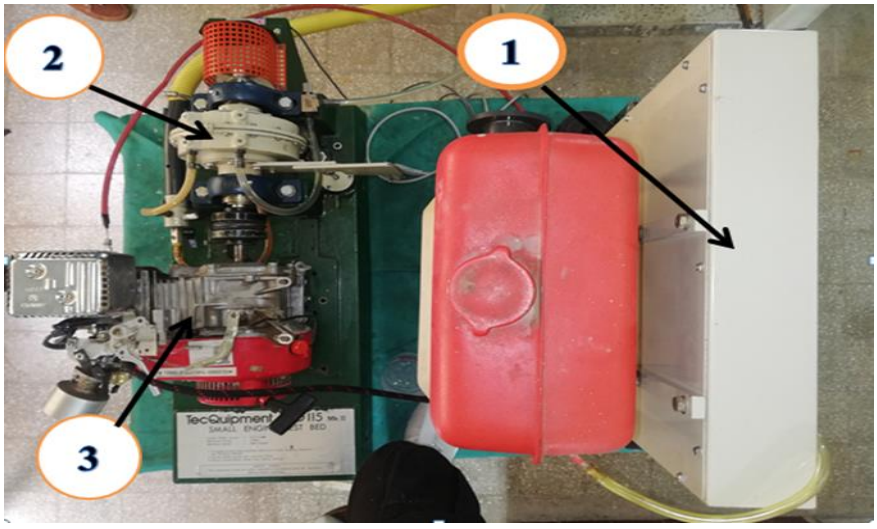

Figure 3-5 The engine test rig

3.1 Honda GX140 Engine

The Honda GX140 is a compact, air-cooled, single-cylinder 4-stroke gasoline engine manufactured by Honda Motor Company since 1983. This versatile engine is tailored for a range of general applications, such as:

- Pressure washers
- Commercial lawn and garden equipment
- Tillers and cultivators
- Generators
- Construction and industrial equipment
- Agricultural equipment
- Small vehicles
- Water pumps

Figure 3-6 Honda GX-140

The Honda GX140 engine is characterized by a single-cylinder setup, inclined at a 25° angle, and utilizes an overhead-valve configuration. It is capable of producing 3.6 kW of power at 4000 rpm. Additional specifications and details can be found in Table 3-1.

Table 3-1 Honda GX140 Specifications [106]

Model	GX140
Type	4-Stroke, OHV, Single cylinder, Inclined by 25°
Displacement	144 cm^3
Max. horsepower	5.0 HP (3.6 kW) at 4000 rpm
Max. torque (crank PTO)	9.8 N.m at 2800 rpm
Carburetor	Horizontal type, Butterfly valve
Cooling system	Forced-air
Ignition system	Transistorized magneto ignition
Lubricating system	Splash
Starting system	Recoil starter
Stopping system	Ignition primary circuit ground
Fuel used	Unleaded gasoline (octane number 86 or higher)
Fuel tank capacity	3.6 L
Fuel consumption	230 g/HPh
PTO shaft rotation	Counterclockwise (from PTO shaft side)

3.2 Hydraulic Dynamometer TD115

In this experiment, the TecQuipment TD115 hydraulic dynamometer is utilized to measure the engine torque. It also transmitted it to a torquemeter located on the instrumentation unit TD114.

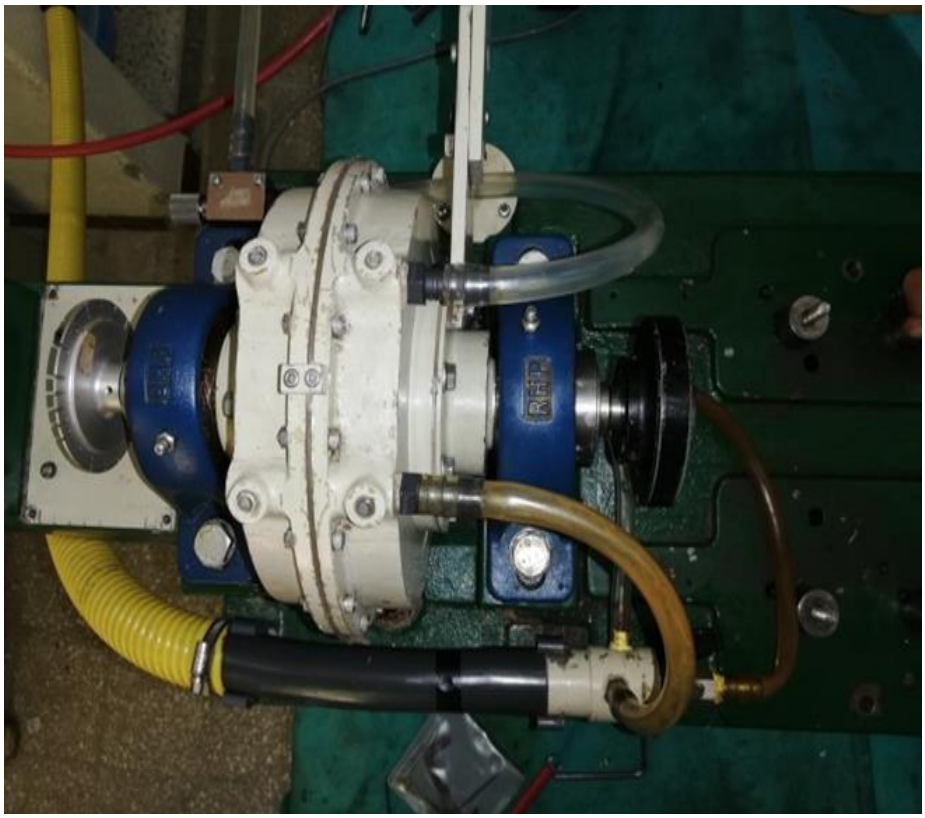

Figure 3-7 TD115 hydraulic dynamometer

The specifics of the TD115 hydraulic dynamometer are outlined comprehensively in Table 3-2.

Table 3-2 Specification characteristics of TD115

Type	Hydraulic
Water pressure	60 KPa
Interval	0-14 N.m
Water flow	4 L/min

Figure 3-8 illustrates the principles and arrangement of the dynamometer. The water flow is regulated using a needle valve (A) located on the bed. Water enters the upper section of the dynamometer casing (B) and exits from the lower part, eventually draining into a sump or drain through a tap (C). An air vent is also included with the dynamometer. The amount of water inside the dynamometer, and consequently the power taken up by the engine, is controlled by adjusting the needle valve (A) and tap (C). It is recommended to keep the drain line as short as possible, directing it to an open drain or collecting tank, with the outlet of the drain pipe kept from submersion [107].

The engine shaft turns a paddle (D) situated inside the vaned casing (B), stirring the water in the dynamometer. If there were no restrictions, the casing would spin at a speed close to that of the paddle. To control this, a spring-loaded nylon cable (E) is wrapped around the casing (B) and fastened to the casing top. As the dynamometer casing rotates, the two springs (F) consistently tighten. Additionally, there is a lubricating oil-filled damper (G) connected to the casing. Before commencing any experiments, it is advisable to verify the oil level [107].

The casing's (B) angular position is affected by both the torque T and the stiffness of the two springs (F). A rotary potentiometer (H) gauges the casing peripheral displacement, which correlates directly with the torque T. This information transmitted to the input of the TD114 torquemeter. It is worth noting that the dynamometer shaft has a height of 50 mm from the mounting pads of the base casting [107].

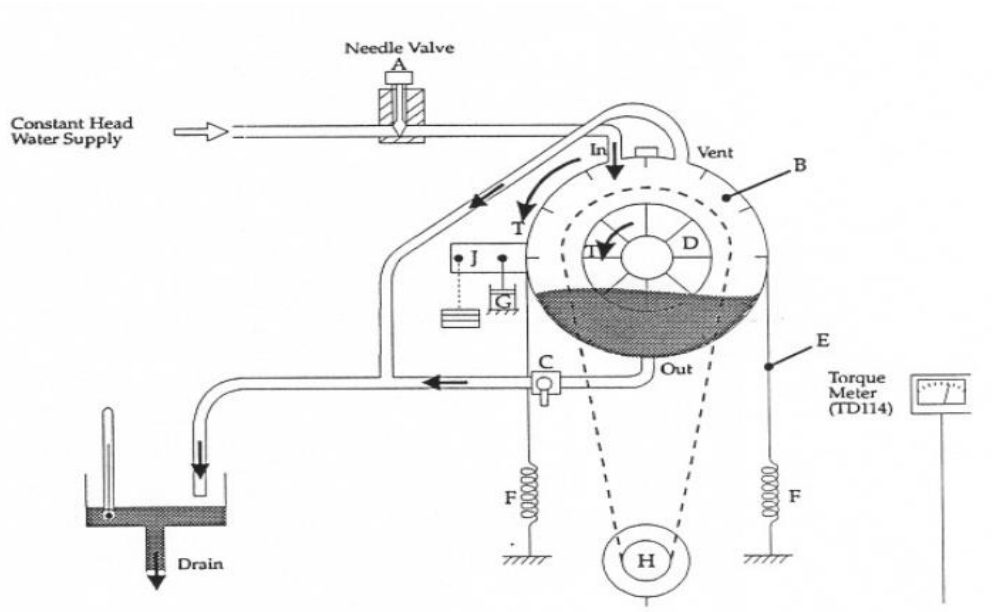

Figure 3-8 Schematic diagram of the hydraulic dynamometer [107].

3.3 Instrumentation Unit TD114

The experiment's instrumentation unit, the TecQuipment TD114, positioned in close proximity to the engine under examination. This unit not only houses the measurement equipment but also incorporates the fuel tank and its delivery systems. Additionally, it includes an airbox/viscous flow meter, utilized for attenuating the intake air before it enters the engine and for quantifying air consumption. Figure 3-9 provides both front and back views of the unit.

Figure 3-9 TD114 instrumentation unit

The unit indicators consist:

- Engine speed display (RPM).
- Torque display.
- Exhaust temperature display.
- Specific fuel consumption measuring instrument.
- Inclined manometer.
- Fuel tank.
- Air flow meter (venturi).
- Air-box.

A stop-watch, thermometer, and barometer are also required but not supplied with the engine test rig setup.

3.3.1 Engine Speed Measurement

An electronic method utilizing pulse counting gauges the engine speed. An optical head, containing an infrared transmitter and receiver, is mounted on the dynamometer chassis for this purpose. An oscillating disk, featuring radial slots, sits between the optical source and sensor, intermittently interrupting the beam as the engine revolves. The ensuing pulse train is electronically analyzed to produce a speed reading. The electronic tachometer is initially calibrated at the factory using a signal generator and usually doesn't require further adjustments. The linkage between the tachometer's optical head and the instrumentation unit is enabled by a 5-pin Cannon plug/socket connection.

Figure 3-10 Tachometer

3.3.2 Torque Measurement

The angular displacement recorded by the rotary potentiometer is input into a linear electronic circuit to produce the torque meter reading. Before each engine test, the torquemeter must be zeroed and calibrated. A 4-pin Cannon plug/socket connects to the torque transducer on the dynamometer.

Figure 3-11 Rotary potentiometer

3.3.3 Exhaust Temperature Measurement

A BS1827-compliant Chrome/Alumel thermocouple measures the temperature of the exhaust gas. The thermocouple is situated within a 1/8" BSP union that is brazed into the exhaust pipe near the engine's cylinder block. The leads of the thermocouple, marked with specific colors, are attached to terminals beneath TD114 Instrumentation Unit. A direct reading meter, featuring a scale ranging from 0 to 1000°C, is employed to measure the temperature.

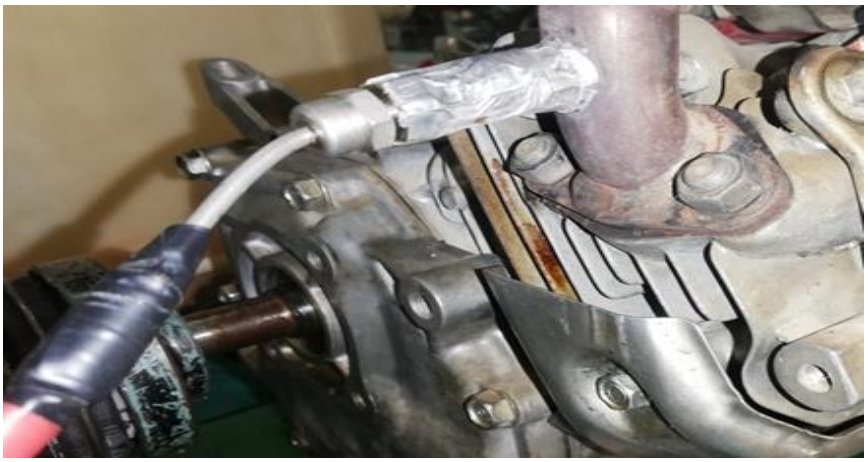

Figure 3-12 Chrome/Alumel thermocouple

3.3.4 Fuel Consumption System

The diagram in Figure 3-13 showcases the unit's fuel flow meter, which consists of a swift flow pipette and the scale indicating its capacity. A vane establishes a connection between the pipette and the fuel tank situated at the unit's rear from the bottom. The rate of fuel consumption is manually monitored. As the engine operates at the specified speed, the vane regulating the fuel flow from the tank to the pipette closes, enabling the engine to function on the existing fuel in the pipette. During this period, the scale displays the amount of fuel supplied to the engine, and a chronometer is utilized to determine the time required to consume a designated quantity of gasoline, such as 8ml, 16ml, or 32ml [107].

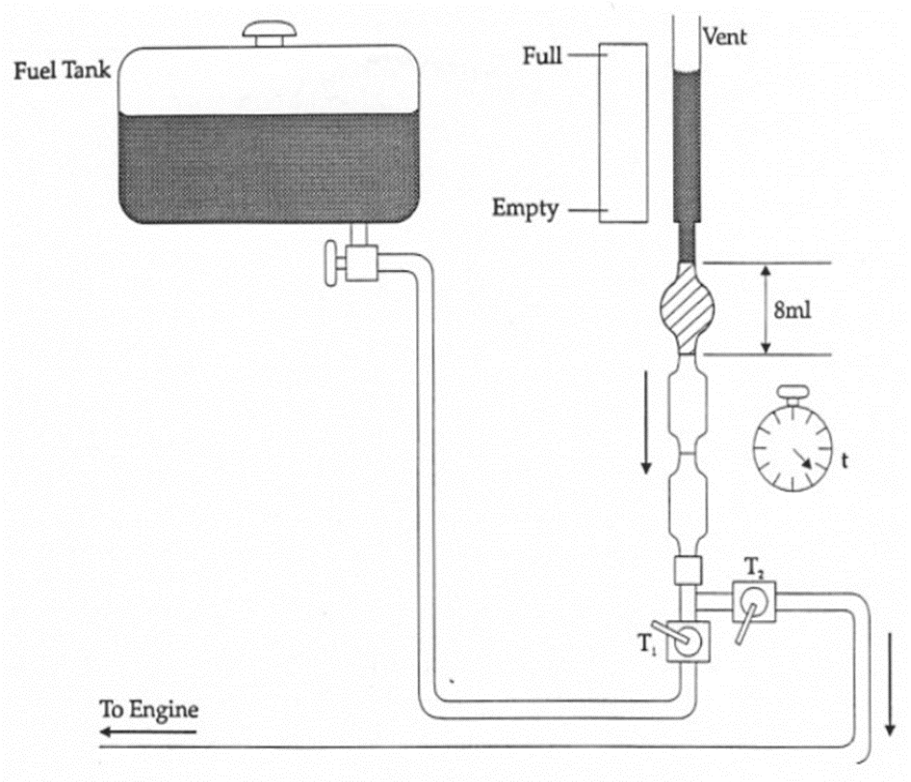

Figure 3-13 The fuel system [107]

3.3.5 Air Consumption Measurement

The air box/viscous flow meter is used to introduce moisture into the intake air before it enters the engine, allowing for the measurement of air consumption. The air box acts as a flow damper before the air reaches the engine carburetor and concurrently restricts intake pressure fluctuations. The incoming air is pulled in through an inlet and directed through an element made up of multiple small-bore tubes, after which it enters the damping volume [107].

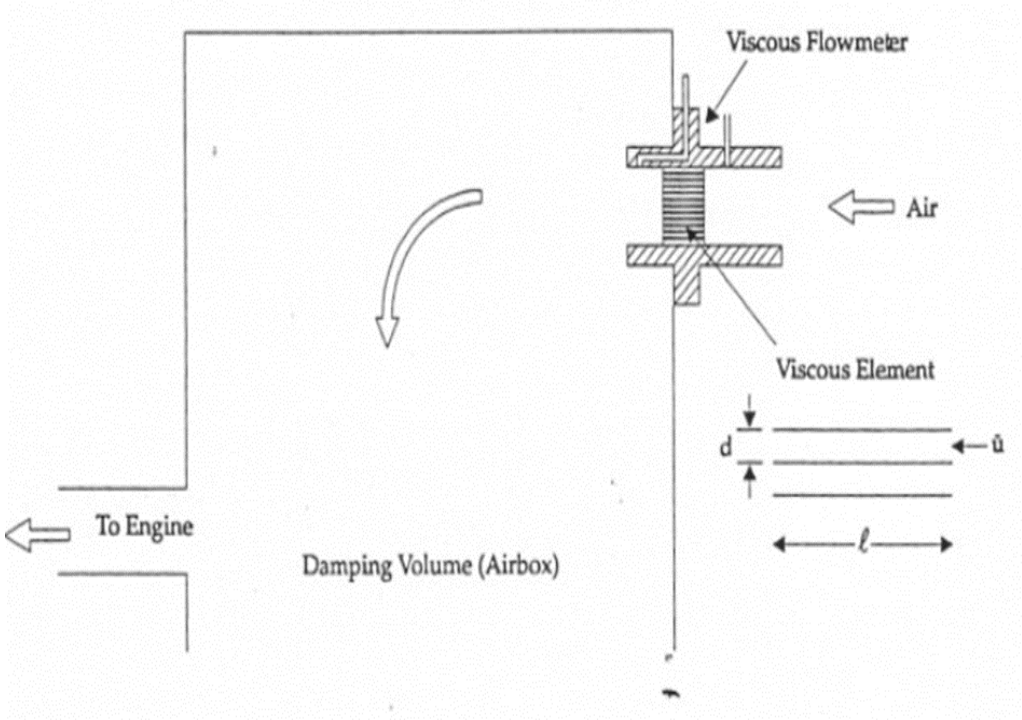

Figure 3-14 Design of an airbox [107].

The air's mass flow rate correlates directly with the average velocity considering a constant air density. Consequently, the pressure drops over the viscous element correlates with the flow rate. To measure the pressure decrease, an inclined tube manometer calibrated in millimeters of water is utilized. It is essential to zero this manometer before initiating the engine.

Figure 3-15 Inclined manometer for reading the pressure difference

4 Diagnostic & Maintenance of the Engine Test Rig Set-up:

The engine test rig set-up used in this experiment was broken and out of service 30 years ago. For this purpose, we did a general diagnostic and fixed it component by component.

4.1 Honda GX140 Engine

The first part we started with is the engine because it is the heart of the test rig set-up.

4.1.1 Air Filter and Air Filter Holder

We found the air filter was dusty, so we cleaned it with a compressor and a cloth.

Figure 3-16 Air filter and air filter holder cleaning

4.1.2 Engine Lubricating Oil

We changed the old lubricating oil by SAE 10w-40 oil type. The capacity of the engine oil is 0.6 L.

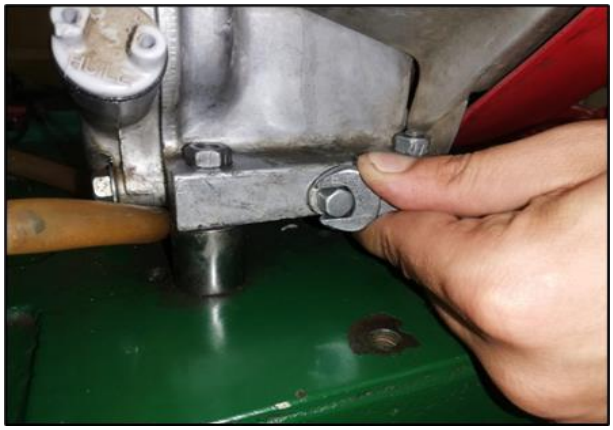

Figure 3-17 Lubricating oil changing

4.1.3 Fuel Tank

We cleaned the fuel tank with an acidic product because we found it in a bad situation with corrosion and impurities. We also changed the old tank for another new one.

Figure 3-18 Fuel tank repairing

4.1.4 Spark Plug

After that, we replaced the old spark plug with another new one to insure a good ignition. We turned on the engine switch and pulled the starter handle to check if the spark crossed the gap between the electrodes. As a result, the electrical circuit is suitable.

Figure 3-19 Spark plug changing

4.1.5 Carburetor

We changed the carburetor to another new one to better mix the air and the fuel.

Figure 3-20 Carburetor changing

As a result of all these configurations and maintenance, the engine started.

4.2 Hydraulic Dynamometer TD115

After the engine was fixed, we passed to tackle the hydraulic dynamometer TD115.

4.2.1 Dynamometer Opening

In the first step, we opened the dynamometer to see the situation of its internal components.

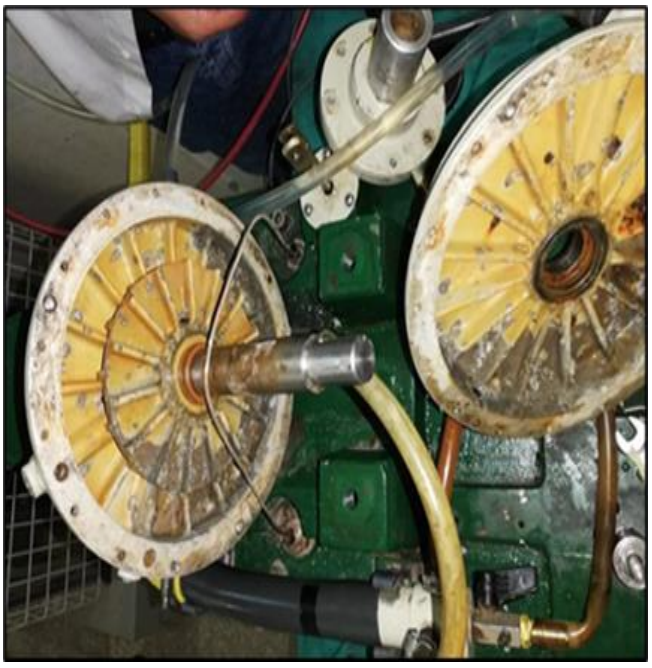

Figure 3-21 Dynamometer opening

4.2.2 Oil Seals and Bearing

In the second step, we removed the broken oil seals and bearings on both sides.

Figure 3-22 The broken oil seals and bearings

Then, we cleaned the rotor shaft and the stator of the dynamometer.

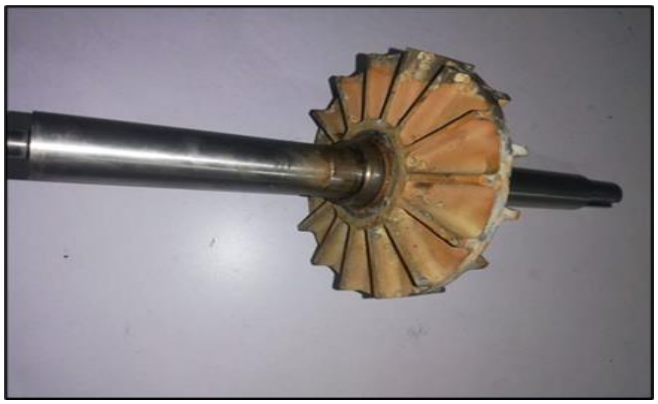

Figure 3-23 The stator and rotor of the dynamometer cleaning.

We mounted new bearings and new oil seals. The bearing reference is “25-47-12”, and the oil seal reference is “32-45-7”.

Figure 3-24 the bearing and oil seals changing.

4.2.3 Dynamometer Assembly

In the third step, we assembled the dynamometer in the bed of the test rig.

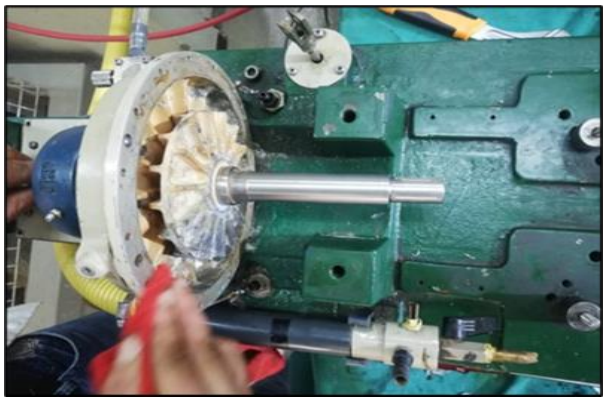

Figure 3-25 Dynamometer assembly

We checked oil damper tank's level and added to it.

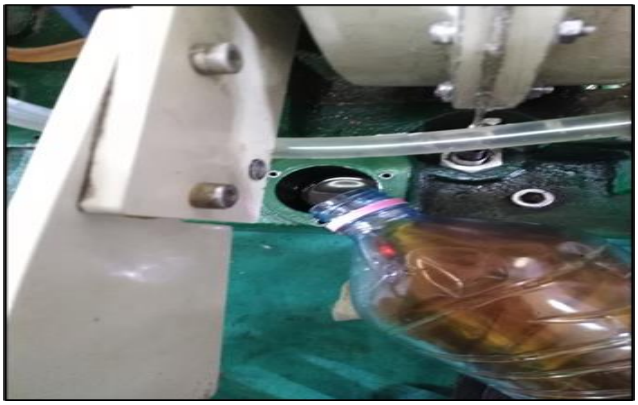

Figure 3-26 Oil damper tank adding

After that, we adjusted the position of the tachometer disc. We mounted the tachometer cover and ensured the lubrication of the bearings.

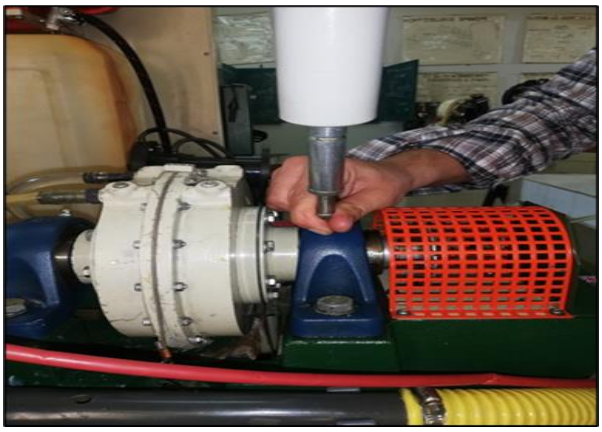

Figure 3-27 Lubricating of bearings

4.2.4 Water System Supply

Next, we passed to the water system supply by identifying the water leakages in pipes, orifices and valves for fixing them.

Figure 3-28 Water system components

Finally, we mounted the water system supply in the bed test rig.

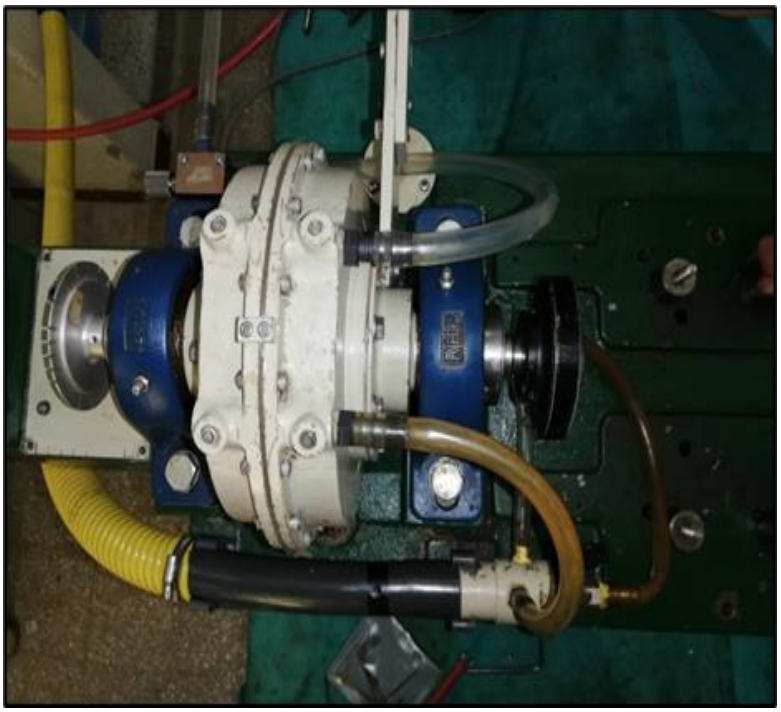

Figure 3-29 Dynamometer after repairing

4.3 Instrumentation Unit TD114

After repairing the engine and the dynamometer, we moved to test the TD114 measuring unit.

4.3.1 Air Flow Meter

We cleaned and tested the air circulation in the venturi (inlet and outlet) and the two orifices towards the inclined flowmeter.

Figure 3-30 The venturi tubes and the air box cleaning

We eliminated the air leakages on the inclined flowmeter and cleaned the tube and the fluid reservoir.

Figure 3-31 An inclined flow meter

Unfortunately, we cannot find the correct hydraulic oil (paraffin) in the cylinder. Its density at 20°C is 0.784 $g.cm^{-3}$.

Figure 3-32 The paraffin density

4.3.2 Thermocouple

We changed the thermocouple with another good condition. We also checked the temperature displayed panel. Furthermore, we changed the two wires in the terminals under the measuring unit (Blue and brown).

Figure 3-33 Thermocouple

5 Experiments

The goal of these experiments is to analyze changes in engine performance metrics such as exhaust gas temperature, fuel mass flow rate, brake-specific fuel consumption, and brake thermal efficiency[102].

5.1 Experimental Protocol

The experiments were carried out for both fuels, namely raw biogas and gasoline, using a hydraulic dynamometer connected to a single cylinder gasoline engine. This was done under varying loads (0 and 3.5 N.m) and across four different speed settings: 2000, 2500, 3000, and 3500 rpm [102].

For each engine speed, essential data including torque, fuel flowrate, and exhaust temperature will be measured to determine the characteristics of engine's performance[102].

Gasoline consumption is gauged by timing the engine's consumption of 8 ml from the graduated flow pipette[102].

Similarly, raw biogas consumption is assessed by timing the engine's utilization of $0.01m^3$ of biogas with the assistance of an (AC-5M) gas meter model.

5.2 Biogas adaptation

The regular gasoline carburetor was replaced by a specialized dual-fuel carburetor for LPG/CNG gasoline. This modified carburetor mixes air and raw biogas in appropriate ratios before entering the engine cylinder. The engine’s fueling system was modified to adapt the biogas as a fuel for this given engine [102].

Figure 3-34 LPG/CNG gasoline dual fuel carburetor [108]

Figure 3-35 The test rig set-up runs on biogas[102]

6 Conclusion

This chapter thoroughly presents the experimental work conducted on the engine test rig. The subsequent chapter will delve into a comprehensive discussion of the results obtained concerning biogas production and engine performance when utilizing biogas as a fuel.

CHAPTER 4:

RESULTS & DISCUSSION

CHAPTER 4

1 Introduction

This chapter describes the experimental results in two parts, each addressing distinct aspects. The initial part focuses on the effects of mono-digestion of CD and co-digestion of (CD + FW) on the biogas produced composition. The second part delves into the performance characteristics of the engine, including exhaust temperature, fuel mass flow rate, brake-specific fuel consumption, and brake thermal efficiency. These experiments were systematically conducted using two distinct fuels: raw biogas and gasoline.

2 Biogas Production Results

The BIOGAS 5000, Geotech's portable gas analyzer, serves as a valuable tool for monitoring gases in biogas applications. This unit ensures the accuracy and reliability of data collection in gas analysis. Specifically designed for raw biogas streams, the analyzer measures the composition in terms of percentage of CH_4, CO_2, and O_2. Additionally, it includes the measurement of H_2S within the range of 0-5,000 parts per million (ppm).

After a 15-day period from the filling of substrates consisting of CD and FW into the digesters, we obtained these results:

2.1 Mono-Digestion

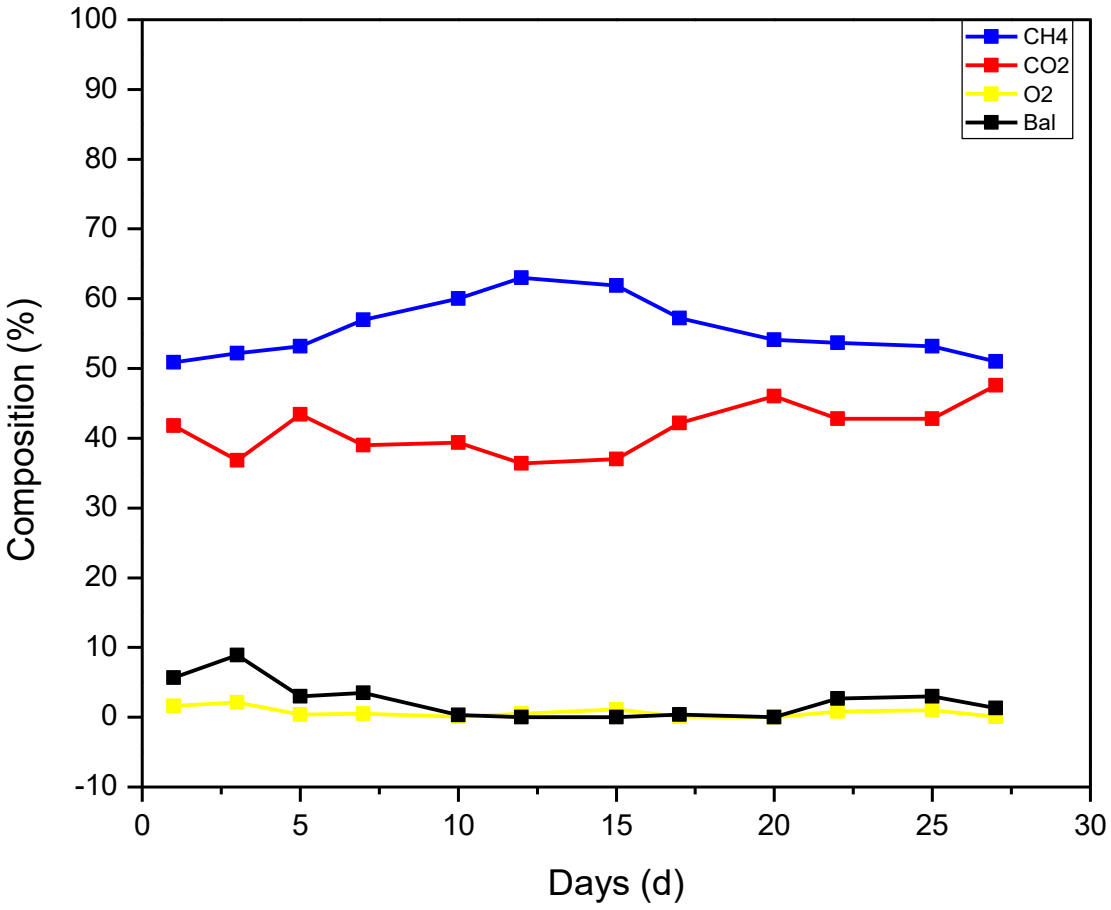

Figure 4-1 The daily biogas composition for CD mono digestion process

Figure 4-1 illustrates the daily biogas composition during the digestion of cow dung.

The findings indicate that the highest CH_4 concentration in the produced biogas was 63%, observed on day 12 from the beginning of the analysis (highlighted in blue color). Before this day, there was a noticeable rise in methane concentration, followed by a slight decrease. This decrease is logical, because this study used in batch digesters. It is noteworthy that methane yield in batch systems is predominantly influenced by the properties of the utilized feedstock.

On other hand, the highest concentration of carbon dioxide (CO_2) reached 47.6%, recorded on day 27 (highlighted in red color). The average CO_2 concentration remained relatively constant, with minor fluctuations. These fluctuations can be attributed to challenges associated with operational conditions, such as variations in ambient temperature and insufficient mixing within the digesters.

The concentration of oxygen (O_2), highlighted in yellow color, is a crucial parameter due to its potential. An increase in O_2 concentration could signify air leakage into the system. The highest O_2 value, recorded on day 3, reached 2.1%. Additionally, on the same day, the highest balance concentration value of 8.9% was noted (highlighted in black).

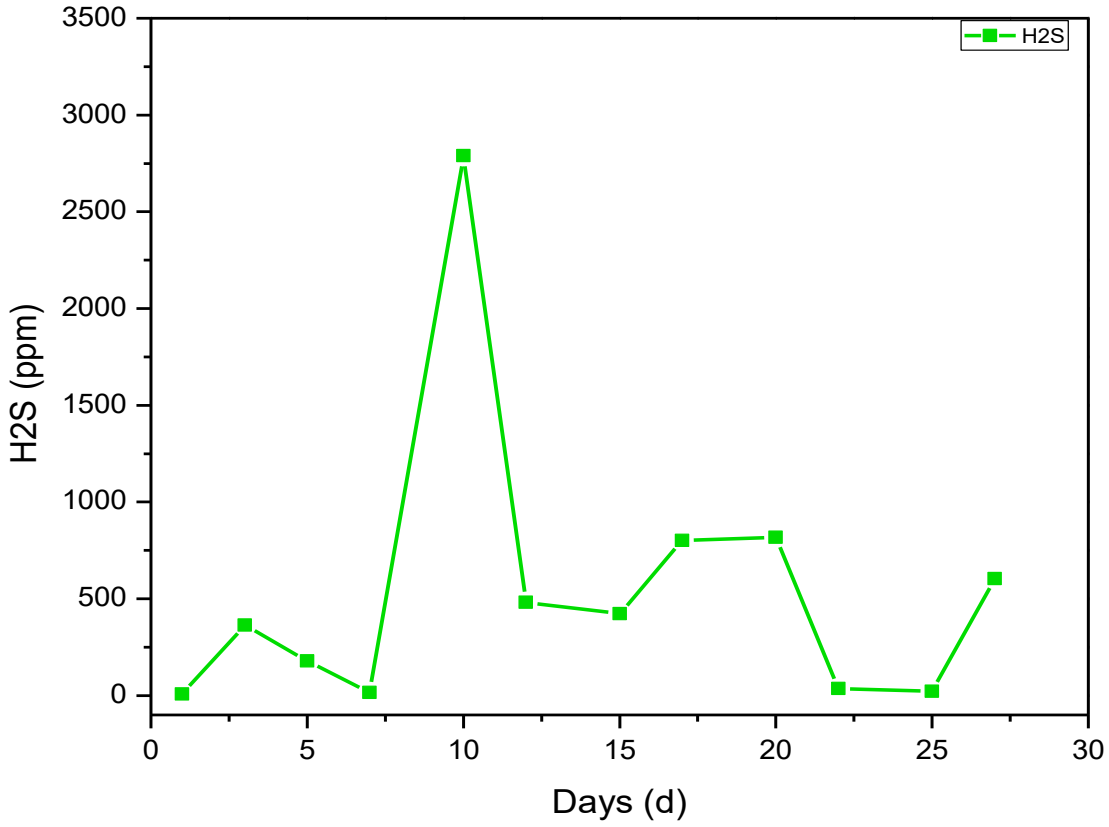

Figure 4-2 The daily H_2S concentration for mono-digestion of cow dung

The peak concentration of hydrogen sulfide (H_2S), reaching 2789 ppm, was observed on day 10. Subsequently, H_2S values demonstrated stability, consistently remaining below 1000 ppm on the other days. Monitoring H_2S levels is essential to prevent engine damage. The presence of H_2S in biogas is predominantly influenced by the characteristics of the feedstock. Biogas plants accepting mixed or variable feedstocks face considerable challenges in monitoring and managing H_2S levels.

To provide a quantitative example, Achinas et al. conducted research on a wet mono-digestion using a CD containing 12.13% TS. In their study, they generated 104 m^3 Mg^{-1} VS of biogas, with 64% of CH_4, under constant mesophilic conditions (36 ±1°C) over a 24-day period, maintaining a pH level of 7.25 [92].

2.2 Co-Digestion

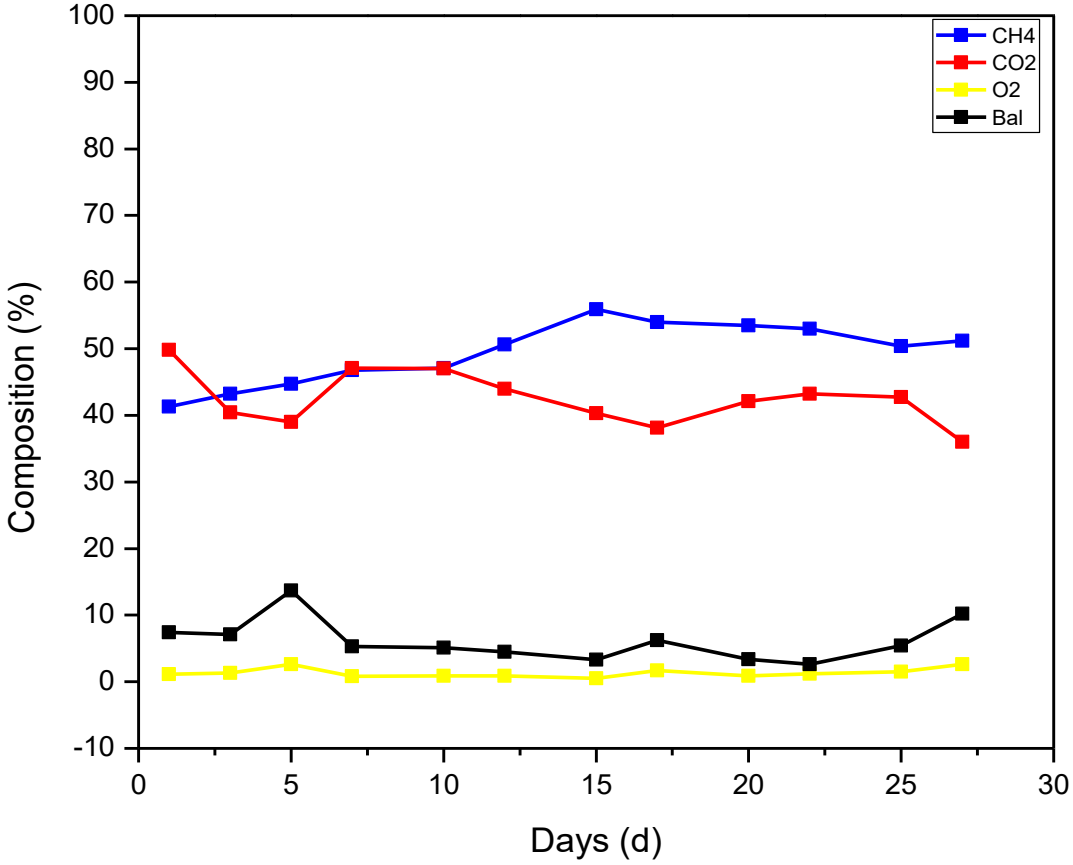

Figure 4-3 The daily biogas composition for CD + FW Co-digestion

Figure 4-3 illustrates the graph depicting the daily composition of biogas during the co-digestion of CD and FW.

The peak CH_4 concentration into biogas produced during co-digestion reached 55.9%, observed on day 15 (highlighted in blue color). This value is comparatively lower than the dung mono-digestion, as a result of dung generally having higher concentrations of nutrients than food waste.

On other hand, the highest CO_2 concentration reached 49.8% on the first day of the analysis (highlighted in red color), exceeding the value observed in mono-digestion. Additionally, fluctuations in CO_2 values were noted throughout the analysis period.

Concerning O_2 concentration, highlighted in yellow color, the highest values were recorded on two days: day 5 and day 27, both reaching 2.6%. On these days, corresponding balance values of 13.7% and 10.2%, respectively, were also obtained (highlighted in black color). The correlation between an increase in O_2 concentration and an increase in the balance concentration is from N_2 presence in the balance.

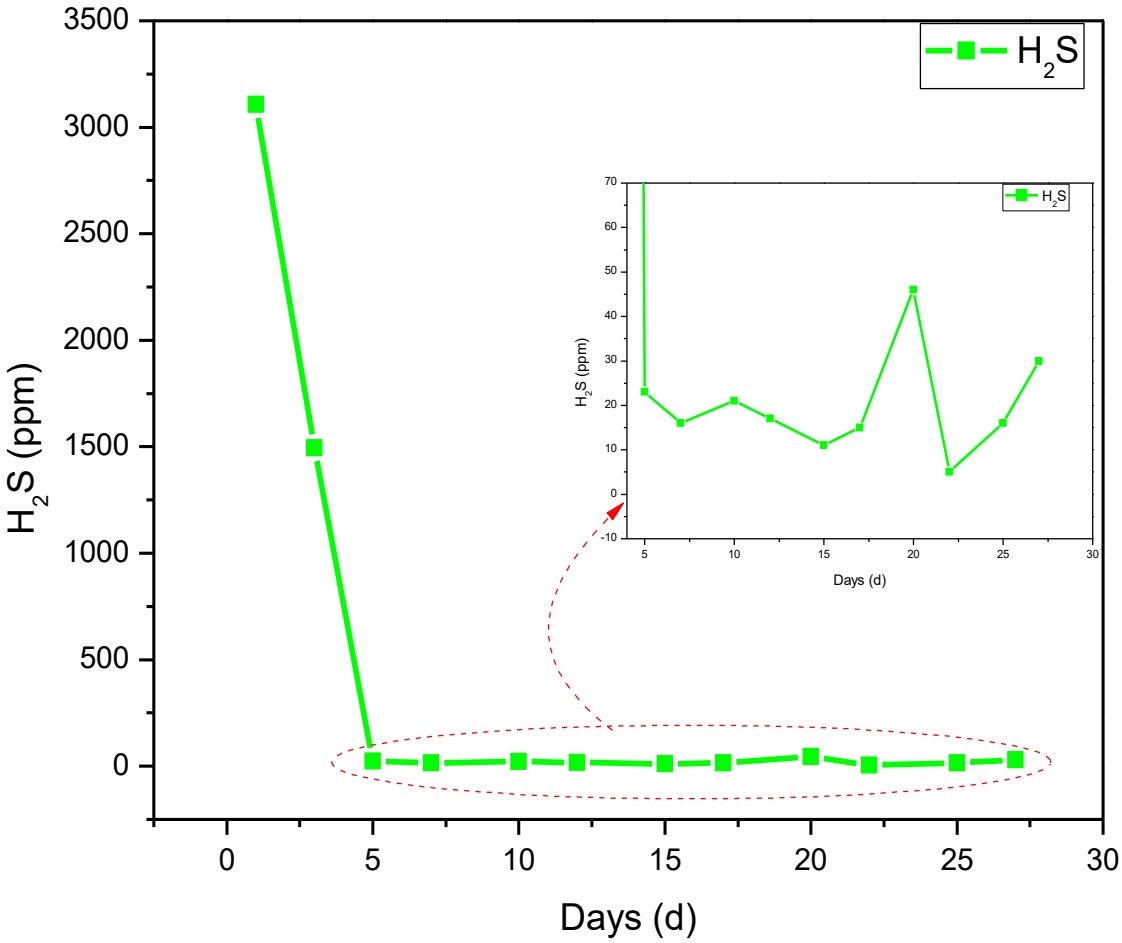

Figure 4-4 The daily H_2S concentration for CD + FW Co-digestion

The highest concentration of H_2S, peaking at 3108 ppm, was also obtained on the first day of the analysis. Subsequently, there was notable stabilization in its values throughout the analysis period.

Makhura et al., explored the impact of co-digestion involving CD and FW, including an inoculum small fraction, on total biogas yield under mesophilic conditions (37°C). Their findings indicated that in co-digestion scenarios where food waste predominates over cow dung, more biogas is produced [108].

3 SI Engine Performance Results

The investigation focused on engine performance using gasoline and raw biogas across different speeds and load conditions. The following are the findings regarding the performance parameters:

3.1 Exhaust Gas Temperature

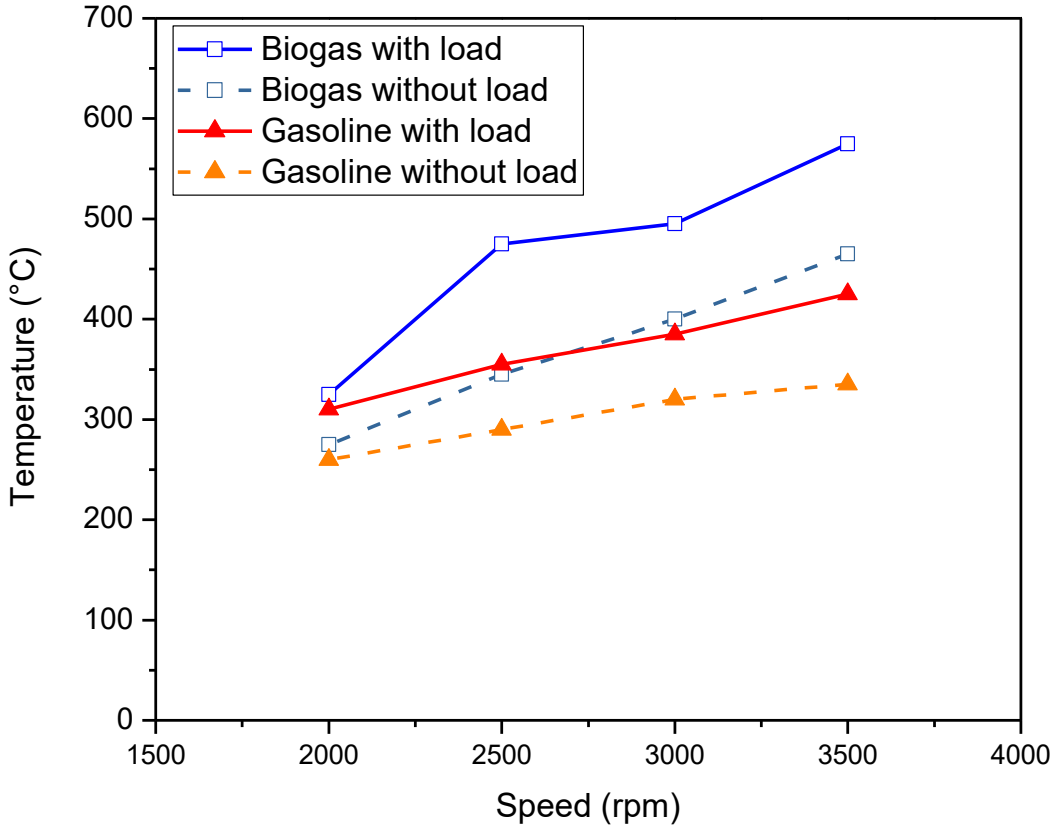

Figure 4-5 EGT versus speed with load and no-load.

The graph in Figure 4-5 illustrates the variations in exhaust gas temperature across different engine speeds under load and no-load conditions for both raw biogas and gasoline scenarios.

The findings indicate a gradual increase in EGT with the rise in speed across all options. Notably, the "load" condition consistently resulted in higher temperatures compared to the "without load" scenario. This outcome can be traced back to the rise in both in-cylinder temperature and pressure. In the raw biogas case, the temperature reached a maximum value of 575°C at 3500 rpm with a load, contrasting with 465°C in the case no-load. For gasoline, the temperatures reached 425°C at 3500 rpm with a load, contrasting with 335°C without load [102].

The elevated EGT in the raw biogas case is primarily attributed to the air/biogas mixing carburetor used, leading to a high likelihood that the engine operates close to stoichiometry. Mariani et al., suggested a potential remedy by implementing Exhaust Gas Recirculation (EGR), a process that recycles uncooled exhaust gas and mixes it with the fresh charge, comprising an air-biogas mixture. This approach helps in

controlling in-cylinder gas temperature. According to the adopted EGR quantity, the intake charge temperature rises proportionally [109].

3.2 Fuel Mass Flowrate

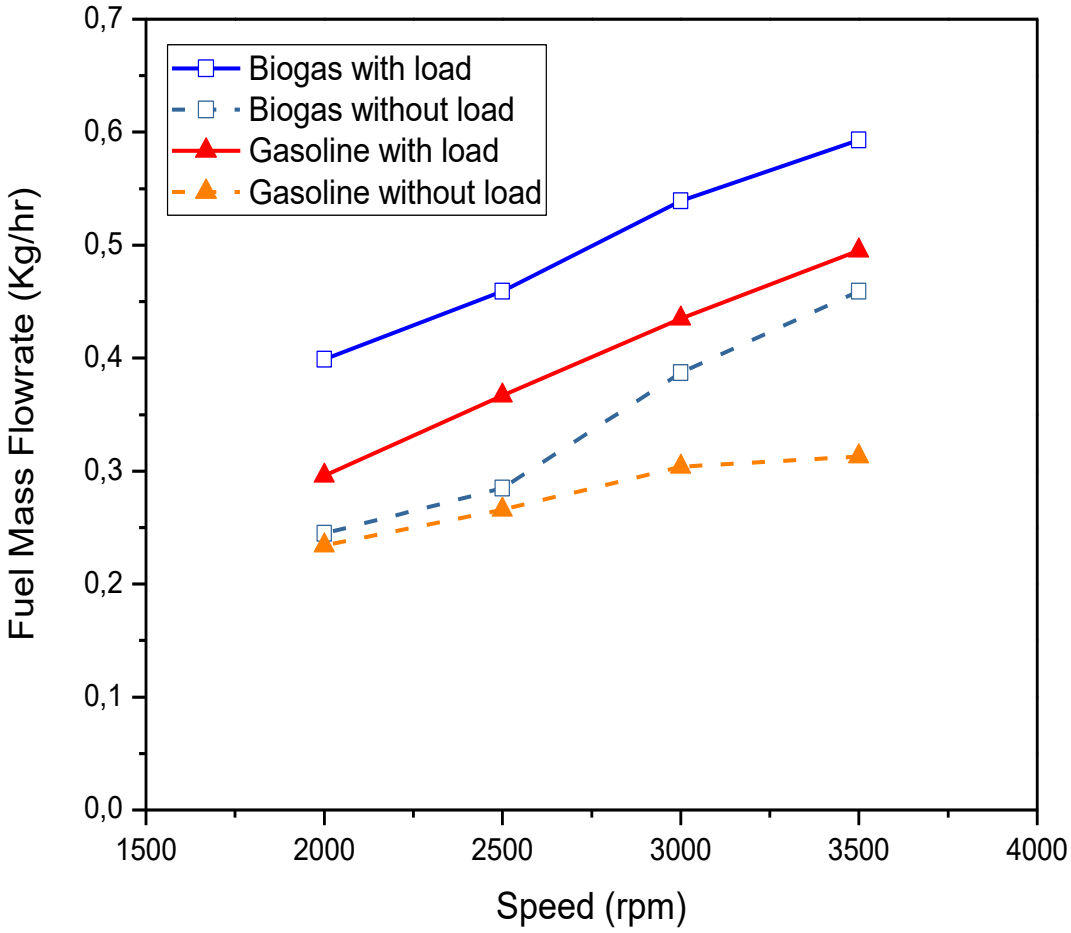

Figure 4-6 Fuel mass flow-rate versus speed with load and no-load.

Figure 4-6 displays the variations in fuel mass flow rate for both scenarios (with and without load) across different speeds using raw biogas and gasoline.

As anticipated, the findings demonstrate a corresponding increase in fuel mass flow rate with the rising engine speed across all test cases. Across both fuel types, the correlation between fuel mass flow rate and load exhibited an almost linear trend, consistently indicating higher values under loaded conditions compared to those no-load. At a speed of 3500 rpm, the fuel mass flow rates for raw biogas were 0.593 Kg/h under load and 0.459 Kg/h without load. Comparatively, for the case of gasoline at the same speed, the rates were 0.495 Kg/h with load and 0.313 Kg/h without load [102].

A higher fuel mass flowrate was required when using raw biogas to produce adequate heat input to sustain the applied load. This adjustment accounts for the inert elements present in raw biogas, like CO_2 and N_2, which significantly influence the overall engine performance. Moreover, owing to its lower density in contrast to gasoline, biogas exhibits smoother flow characteristics [77].

3.3 Brake-Specific Fuel Consumption

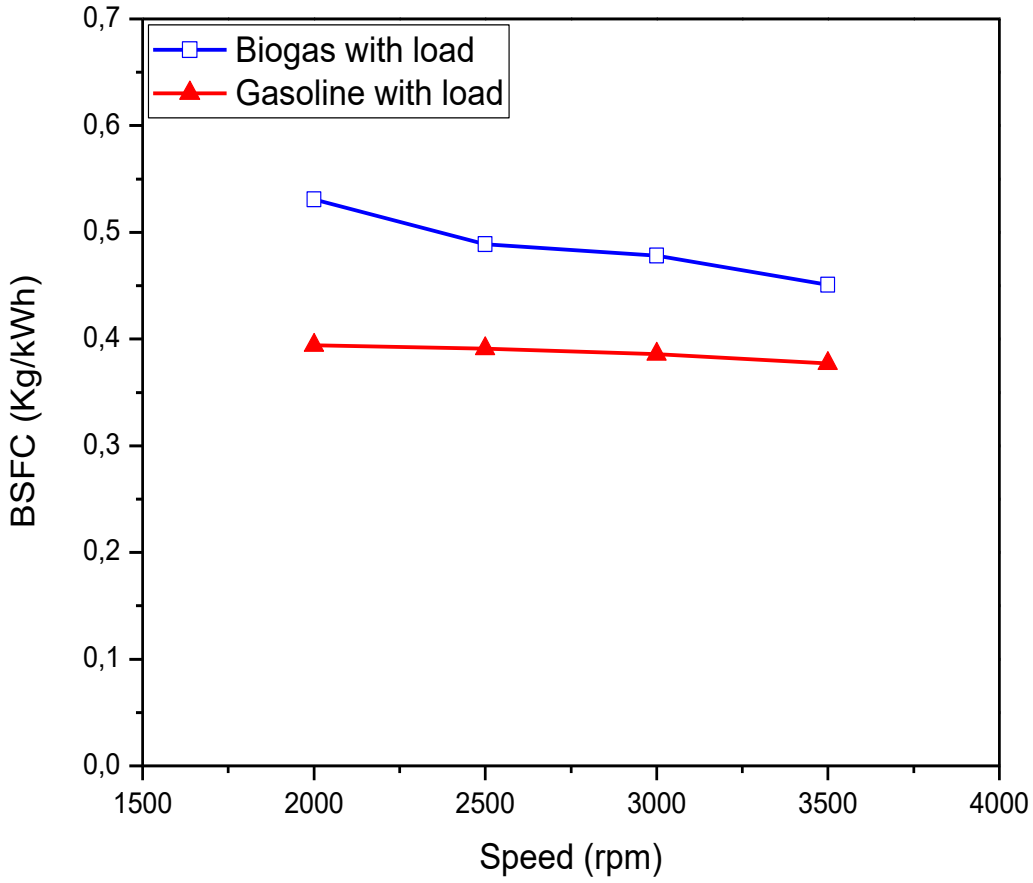

Figure 4-7 Brake-specific fuel consumption versus speed.

From Figure 4-7, it is evident that BSFC experiences a slight decrease with the increase in speed at an equal load. For gasoline, the BSFC remains consistently lower compared to raw biogas across varying speeds, with marginal fluctuations at higher speeds, showcasing a slight decrease. In the case of raw biogas, the BSFC demonstrates a reduction from 0.531 Kg/kWh to 0.451 Kg/kWh across the speed range of 2000 to 3500 rpm. In contrast, for gasoline, the BSFC drops from 0.394 Kg/kWh to 0.377 Kg/kWh within the same speed range [102].

The higher BSFC observed in biogas compared to gasoline is attributed to the lower heating value of biogas. This lower value results in reduced combustion and flame propagation speeds, requiring a higher volume of fuel to generate the same level of power. Additionally, the notable CO_2 content in raw biogas contributes significantly to higher values of BSFC. Utilizing raw biogas with a reduced CO_2 concentration has the potential to elevate peak in-cylinder pressure while concurrently lowering BSFC [102].

The observed decline in BSFC at higher speeds with biogas compared to gasoline indicates that as the engine nears its optimal operational speed, characterized by its peak efficiency, biogas becomes comparatively more efficient in terms of BSFC. This contributes yet another favorable aspect to the benefits of biogas utilization. Simsek et al. observed an increase in BSFC with the biogas use [75]. Hence, to produce an equivalent power output within a specific timeframe, the engine requires a notably larger volume of raw biogas compared to gasoline, solely considering the flow rate.

3.4 Brake Thermal Efficiency

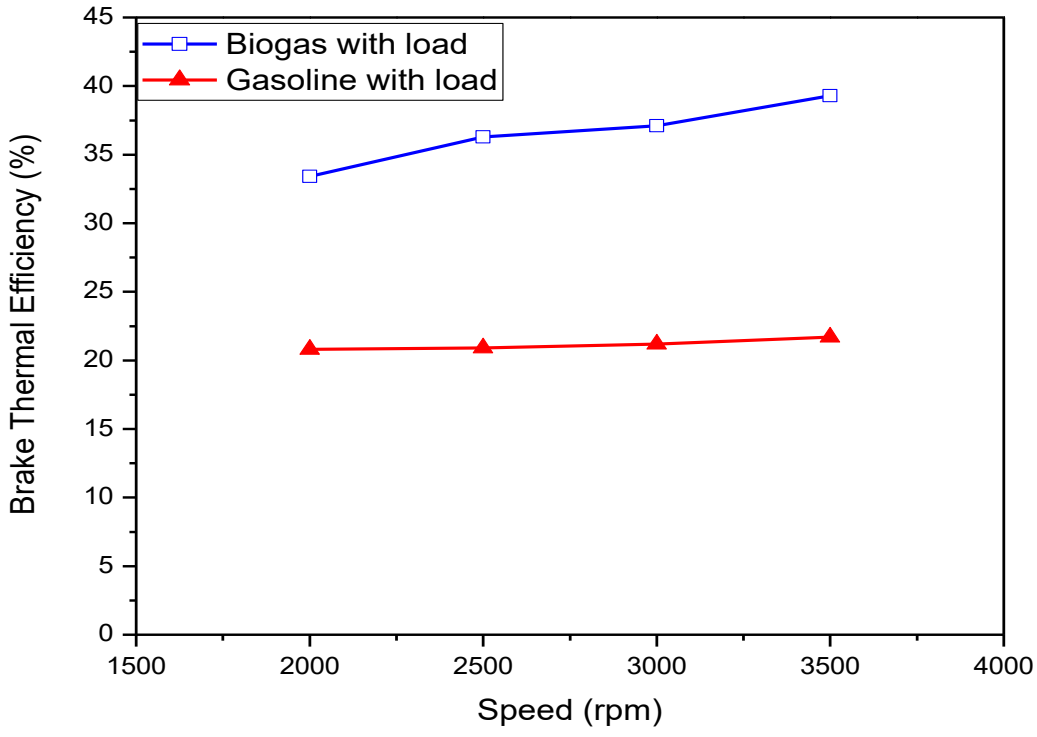

Figure 4-8 Brake thermal efficiency versus speed.

Figure 4-8 highlights two advantages of using biogas as a fuel. Firstly, its BTE surpasses that of gasoline, nearly doubling at the maximum speed of 3500 rpm. Muhajir et al., have also highlighted that biogas exhibits a higher BTE compared to gasoline

[110]. Secondly, the BTE for biogas escalates with increasing engine speed, while maintaining near-constant levels for gasoline. Aguiar et al., noted that the engine tends to function with lower efficiency, especially under lighter loads when using gasoline [111]. Comparatively, when employing raw biogas, the BTE increases from 33.4% to 39.3% while increasing the speed from 2000 to 3500 rpm with a torque of 3.5 N.m. In contrast, for gasoline, the BTE increases from 20.8% to 21.7% with the speed increasing from the same range of speed at 3.5 N.m [102].

Raw biogas exhibits superior mixing capabilities with air, thereby enhancing the process of combustion. Additionally, the potential presence of hydrogen (H_2) within raw biogas can augment the volumetric burning velocity of fuel, positively influencing combustion stability. Zhang et al. found that elevating the H_2/CH_4 within biogas composition leads to an increase in the power output, especially in ultra-lean conditions [112]. Furthermore, the inherent resistance to engine knock in raw biogas allows engines to operate at high compression ratios, contributing to high thermal efficiency.

4 Conclusion

This chapter provides a summary of our experimental results from the two setups:

- In summary, the highest CH_4 concentration achieved was 63% for mono-digestion of dung, whereas it was slightly lower at 55.9% in the dung + food waste co-digestion. Conversely, the highest CO_2 concentration reached 49.8% in the co-digestion, surpassing the 47.6% observed in mono-digestion. Additionally, the peak H_2S concentration was higher in co-digestion at 3108 ppm compared to 2789 ppm in mono-digestion.

- At 3500 rpm, the raw biogas, when used as fuel under load conditions, reached the highest exhaust temperature of 575°C. Conversely, gasoline under no load conditions recorded a minimum exhaust temperature of 335°C. This disparity was also reflected in fuel consumption, with the engine consuming 0.593 Kg/h of raw biogas compared to 0.495 Kg/h of gasoline.

- At a torque of 3.5 N.m, the Brake Specific Fuel Consumption (BSFC) for gasoline is lower compared to raw biogas. Specifically, the BSFC for gasoline decreases by approximately 5% between 2000 rpm and 3500 rpm. In contrast, for raw biogas, there

is a more significant decrease in BSFC of around 15% over the same speed range between 2000 rpm and 3500 rpm.

- Under a torque of 3.5 N.m, the Brake Thermal Efficiency (BTE) for raw biogas is significantly higher than that for gasoline. Specifically, for raw biogas, there is a substantial increase in BTE of around 18% between 2000 rpm and 3500 rpm. In contrast, for gasoline, there is a comparatively smaller increase in BTE of around 5% over the same speed range between 2000 rpm and 3500 rpm.

GENERAL CONCLUSION

General Conclusion

Within the context of this thesis, an examination is carried out on the operational characteristics of the Honda GX140 engine using raw biogas as fuel. The parameters under investigation include exhaust temperature, the mass flow rate of fuel, brake-specific fuel consumption (BSFC), and brake thermal efficiency (BTE).

In the first experimental setup, an in-depth investigation was conducted into the composition of raw biogas derived from both cow dung mono-digestion and the cow dung with food waste co-digestion. The primary key findings of the investigation can be summarized as follows:

- The results revealed that the quality of biogas production for the single-substrate (mono-digestion) of dung are better than the quality of biogas production for the co-digestion of cow dung and food waste.
- The highest CH_4 concentration in the biogas produced was 63% for mono-digestion of cow dung compared to 55,9% for co-digestion of cow dung and food waste.
- The highest CO_2 concentration in the biogas produced was 47,6% for mono-digestion of cow dung compared to 49.8% for co-digestion of dung and food waste.
- H_2S concentration of co-digestion of dung and food waste is more stable than mono-digestion of dung.

For the second experimental setup, we tested the Honda GX140 engine in the engine test rig TecQuipmentTD115 under load and without load, and compared the results of raw biogas combustion with those of gasoline. The primary conclusions drawn from this comparison are outlined below:

- The exhaust gas temperature demonstrates an upward trend with increasing speed and load. Notably, when employing raw biogas, the exhaust temperature surpasses that recorded for gasoline.
- A sharp increase in fuel mass flowrate is observed as the speed rises in all scenarios. Notably, the relationship between fuel mass flowrate and load is characterized by a nearly linear trend, and cases under load generally exceed those without load.

- The BSFC for gasoline is comparatively lower compared to raw biogas. Additionally, the BSFC tends to remain relatively constant as speed increases, exhibiting a marginal decrease at the maximum speed.
- The analysis of BTE highlights a significant performance improvement in the engine when using biogas compared to gasoline. This highlights biogas as a promising substitute for traditional fossil fuels like gasoline.

These preliminary investigations into the use of biogas as a fuel in a small SI engine strongly indicate its high potential. Not only does biogas emerge as a carbon-neutral option, but it also demonstrates enhanced efficiency and effectiveness. The outcomes strongly affirm that the engine operates at an enhanced level when utilizing biogas as its fuel source.

The outlined experiments offer an initial exploration into the biogas potential as an IC engine fuel. Subsequent research endeavors are underway to conduct more in-depth investigations into the effects of this fuel on engine dynamics, performance, and emissions.

REFERENCES

1. *Biogas in the Sustainable Society- the Nordic Way*. 2019: Biogas Research Center-Linköping University.
2. Nkoa, R., *Agricultural benefits and environmental risks of soil fertilization with anaerobic digestates: a review.* Agronomy for Sustainable Development, 2014. **34**(2): p. 473-492.
3. Schink, B., *Energetics of syntrophic cooperation in methanogenic degradation.* Microbiology and molecular biology reviews, 1997. **61**(2): p. 262-280.
4. Lozanovski, A., J.P. Lindner, and U. Bos, *Environmental evaluation and comparison of selected industrial scale biomethane production facilities across Europe.* The International Journal of Life Cycle Assessment, 2014. **19**(11): p. 1823-1832.
5. Sarker, S., et al., *A review of the role of critical parameters in the design and operation of biogas production plants.* Applied Sciences, 2019. **9**(9): p. 1915.
6. Atelge, M., et al., *A critical review of pretreatment technologies to enhance anaerobic digestion and energy recovery.* Fuel, 2020. **270**: p. 117494.
7. Rabii, A., et al., *A review on anaerobic co-digestion with a focus on the microbial populations and the effect of multi-stage digester configuration.* Energies, 2019. **12**(6): p. 1106.
8. Achinas, S. and G.J.W. Euverink, *Theoretical analysis of biogas potential prediction from agricultural waste.* Resource-Efficient Technologies, 2016. **2**(3): p. 143-147.
9. Li, Y., et al., *Biogas production from co-digestion of corn stover and chicken manure under anaerobic wet, hemi-solid, and solid state conditions.* Bioresource technology, 2013. **149**: p. 406-412.
10. Ertem, F.C., *Improving biogas production by anaerobic digestion of different substrates: calculation of potential energy outcomes*. 2011, Halmstad University.
11. Banks, C.J., et al., *Trace element requirements for stable food waste digestion at elevated ammonia concentrations.* Bioresource technology, 2012. **104**: p. 127-135.
12. Fathya, S., K. Assia, and M. Hamza, *Influence of inoculums/substrate ratios (ISRs) on the mesophilic anaerobic digestion of slaughterhouse waste in batch mode: Process stability and biogas production.* Energy Procedia, 2014. **50**: p. 57-63.
13. Carlsson, M., *When and why is pre-treatment of substrates for anaerobic digestion useful?* 2015, Luleå tekniska universitet.
14. Li, Y., et al., *Strategies to boost anaerobic digestion performance of cow manure: Laboratory achievements and their full-scale application potential.* Science of the Total Environment, 2021. **755**: p. 142940.
15. Ahmed, S., D. Einfalt, and M. Kazda, *Co-digestion of sugar beet silage increases biogas yield from fibrous substrates.* BioMed research international, 2016. **2016**.
16. Dioha, I., et al., *Effect of carbon to nitrogen ratio on biogas production.* International Research Journal of Natural Sciences, 2013. **1**(3): p. 1-10.
17. Langat, K., *Biogas production potential of different substrate combinations from Kaitui location, Kericho County, Kenya*. 2019, JKUAT-IEET. p. 62.
18. Feliu Jofre, Á. and X. Flotats Ripoll, *Renewable gases. An emerging energy vector*. 2020: Naturgy Foundation.
19. Singh, B., Z. Szamosi, and Z. Siménfalvi, *Impact of mixing intensity and duration on biogas production in an anaerobic digester: a review.* Critical reviews in biotechnology, 2020. **40**(4): p. 508-521.
20. Wang, B., et al., *Optimizing mixing mode and intensity to prevent sludge flotation in sulfidogenic anaerobic sludge bed reactors.* Water Research, 2017. **122**: p. 481-491.
21. Mao, C., et al., *Review on research achievements of biogas from anaerobic digestion.* Renewable and sustainable energy reviews, 2015. **45**: p. 540-555.
22. Drosg, B., *Process monitoring in biogas plants*. 2013: IEA Bioenergy.

23. Lettinga, G., S. Rebac, and G. Zeeman, *Challenge of psychrophilic anaerobic wastewater treatment.* TRENDS in Biotechnology, 2001. **19**(9): p. 363-370.
24. Westerholm, M., et al., *Microbial community adaptability to altered temperature conditions determines the potential for process optimisation in biogas production.* Applied energy, 2018. **226**: p. 838-848.
25. Wang, C., Y. Li, and Y. Sun, *Acclimation of Acid-Tolerant Methanogenic Culture for Bioaugmentation: Strategy Comparison and Microbiome Succession.* ACS omega, 2020. **5**(11): p. 6062-6068.
26. Lahav, O. and B. Morgan, *Titration methodologies for monitoring of anaerobic digestion in developing countries—a review.* Journal of Chemical Technology & Biotechnology: International Research in Process, Environmental & Clean Technology, 2004. **79**(12): p. 1331-1341.
27. Martín-González, L., X. Font, and T. Vicent, *Alkalinity ratios to identify process imbalances in anaerobic digesters treating source-sorted organic fraction of municipal wastes.* Biochemical Engineering Journal, 2013. **76**: p. 1-5.
28. Van, D.P., et al., *A review of anaerobic digestion systems for biodegradable waste: Configurations, operating parameters, and current trends.* Environmental Engineering Research, 2020. **25**(1): p. 1-17.
29. Theaker, H., et al., *Effect of a variable organic loading rate on process kinetics and volatile solids destruction in synthetic food waste-fed anaerobic digesters.* Waste Management, 2021. **134**: p. 149-158.
30. Khafipour, A., et al., *Response of microbial community to induced failure of anaerobic digesters through overloading with propionic acid followed by process recovery.* Frontiers in Bioengineering and Biotechnology, 2020: p. 1434.
31. Sahu, N., et al., *Optimization of hydrolysis conditions for minimizing ammonia accumulation in two-stage biogas production process using kitchen waste for sustainable process development.* Journal of environmental chemical engineering, 2017. **5**(3): p. 2378-2387.
32. Isaksson, S., *Biogas production at high ammonia levels: The importance of temperature and trace element supplementation on microbial communities*. 2018.
33. Krakat, N., et al., *Methods of ammonia removal in anaerobic digestion: a review.* Water Science and Technology, 2017. **76**(8): p. 1925-1938.
34. Labatut, R.A. and C.A. Gooch, *Monitoring of anaerobic digestion process to optimize performance and prevent system failure.* 2014.
35. Khan, M., et al., *Optimization of process parameters for production of volatile fatty acid, biohydrogen and methane from anaerobic digestion.* Bioresource technology, 2016. **219**: p. 738-748.
36. Kavuma, C., *Variation of methane and carbon dioxide yield in a biogas plant*. 2013: Royal Institute of Technology. p. 30.
37. Ciambellotti, A., et al., *Absorption Chillers to Improve the Performance of Small-Scale Biomethane Liquefaction Plants.* Energies, 2021. **15**(1): p. 92.
38. Spyridonidis, A., et al., *Performance of a full-scale biogas plant operation in greece and its impact on the circular economy.* Water, 2020. **12**(11): p. 3074.
39. Wang, H., R. Larson, and T. Runge, *Impacts to hydrogen sulfide concentrations in biogas when poplar wood chips, steam treated wood chips, and biochar are added to manure-based anaerobic digestion systems.* Bioresource Technology Reports, 2019. **7**: p. 100232.
40. Dumont, E., *H2S removal from biogas using bioreactors: a review.* International Journal of Energy and Environnement, 2015. **6**(5): p. 479-498.

41. García, M., D. Prats, and A. Trapote, *Presence of siloxanes in the biogas of a wastewater treatment plant separation in condensates and influence of the dose of iron chloride on its elimination.* 2016.
42. *DuoSphere Double Membrane Gas Holder Overview*. Available from: https://www.westech-inc.com/products/anaerobic-digestion-biogas-storage-double-membrane-gas-holder-duosphere.
43. Berger, B., *THE GASHOLDER–SHAPED BY ITS FUNCTION. THE ITALIAN EXAMPLE.* 2015.
44. Barragán-Escandón, A., et al., *Assessment of power generation using biogas from landfills in an equatorial tropical context.* Sustainability, 2020. **12**(7): p. 2669.
45. *AN OVERVIEW OF RENEWABLE NATURAL GAS BIOGAS*. 2020. p. 46.
46. Adnan, A.I., et al., *Technologies for biogas upgrading to biomethane: A review.* Bioengineering, 2019. **6**(4): p. 92.
47. Abderezzak, B., *An innovative simulation tool for waste to energy generation opportunities.* Med. J. Model. Simul, 2017. **7**(038): p. 048.
48. Herrera, A., et al., *Environmental Performance in the Production and Use of Recovered Fertilizers from Organic Wastes Treated by Anaerobic Digestion vs Synthetic Mineral Fertilizers.* ACS Sustainable Chemistry & Engineering, 2022.
49. Na, R., et al., *Stabilization of Anaerobic Co-Digestion Process via Constant the Digestate Solids Content.* Processes, 2021. **9**(2): p. 197.
50. Plana, P.V. and B. Noche, *A review of the current digestate distribution models: storage and transport.* WIT Trans. Ecol. Environ, 2016. **202**: p. 345-357.
51. Ganesan, V., *Internal combustion engines*. 2012: McGraw Hill Education (India) Pvt Ltd.
52. Pulkrabek, W.W., *Engineering fundamentals of the internal combustion engine*. 2004.
53. Surata, I.W., et al., *Simple conversion method from gasoline to biogas fueled small engine to powered electric generator.* Energy Procedia, 2014. **52**: p. 626-632.
54. Kukoyi, T., et al. *Biogas use as fuel in spark ignition engines*. in *2016 IEEE International Conference on Industrial Engineering and Engineering Management (IEEM)*. 2016. IEEE.
55. Kriaučiūnas, D., S. Pukalskas, and A. Rimkus. *Simulation of spark ignition engine performance working on biogas hydrogen mixture*. in *MATEC Web of Conferences*. 2018. EDP Sciences.
56. Barik, D. and S. Murugan, *Production and application of biogas as a gaseous fuel for internal combustion engines.* International Journal of Engineering Research & Technology (IJERT), 2012. **1**(7): p. 2278-0181.
57. Taamallah, S., et al., *Fuel flexibility, stability and emissions in premixed hydrogen-rich gas turbine combustion: Technology, fundamentals, and numerical simulations.* Applied energy, 2015. **154**: p. 1020-1047.
58. Hotta, S.K., N. Sahoo, and K. Mohanty, *Comparative assessment of a spark ignition engine fueled with gasoline and raw biogas.* Renewable Energy, 2019. **134**: p. 1307-1319.
59. Porpatham, E., A. Ramesh, and B. Nagalingam, *Effect of compression ratio on the performance and combustion of a biogas fuelled spark ignition engine.* Fuel, 2012. **95**: p. 247-256.
60. Simsek, S. and S. Uslu, *Investigation of the impacts of gasoline, biogas and LPG fuels on engine performance and exhaust emissions in different throttle positions on SI engine.* Fuel, 2020. **279**: p. 118528.
61. Sudarsono, A.A.P.S., et al., *The Effect of Compression Ratio on Performance of Generator Set Fuelled with Raw Biogas.* Journal of Advanced Research in Fluid Mechanics and Thermal Sciences, 2022. **89**(1): p. 185-195.

62. Samanta, A., S. Das, and P. Roy, *Performance analysis of a biogas engine.* International Journal of Research in Engineering and Technology, 2016. **05**(01): p. 67-71.
63. Rossetto, C., et al., *Performance of an Otto cycle engine using biogas as fuel.* African Journal of Agricultural Research, 2013. **8**(45): p. 5607-5610.
64. Sendzikiene, E., et al., *Impact of biomethane gas on energy and emission characteristics of a spark ignition engine fuelled with a stoichiometric mixture at various ignition advance angles.* Fuel, 2015. **162**: p. 194-201.
65. Chandra, R., et al., *Performance evaluation of a constant speed IC engine on CNG, methane enriched biogas and biogas.* Applied energy, 2011. **88**(11): p. 3969-3977.
66. Kim, Y., et al., *Combustion characteristics and NOX emissions of biogas fuels with various CO2 contents in a micro co-generation spark-ignition engine.* Applied energy, 2016. **182**: p. 539-547.
67. Huang, J. and R. Crookes, *Assessment of simulated biogas as a fuel for the spark ignition engine.* Fuel, 1998. **77**(15): p. 1793-1801.
68. Joshi, A., et al., *Using biogas in SI engine by changing ignition parameter and compression ratio: A reveiw.* International journal for scientific research and development, 2015. **3**: p. 751-756.
69. Porpatham, E., A. Ramesh, and B. Nagalingam, *Investigation on the effect of concentration of methane in biogas when used as a fuel for a spark ignition engine.* fuel, 2008. **87**(8-9): p. 1651-1659.
70. Kriaučiūnas, D., et al., *Analysis of the influence of CO2 concentration on a spark ignition engine fueled with biogas.* Applied Sciences, 2021. **11**(14): p. 6379.
71. Karagöz, M., et al., *The effect of the CO2 ratio in biogas on the vibration and performance of a spark ignited engine.* Fuel, 2018. **214**: p. 634-639.
72. Mokrane, C., B. Adouane, and A. Benzaoui, *Composition and stoichiometry effects of biogas as fuel in spark ignition engine.* International Journal of Automotive and Mechanical Engineering, 2018. **15**: p. 5036-5052.
73. Prakash, J., et al., *Performance study of four stroke S.I. engine using upgraded biogas fuel.* Carbon – Sci. Tech., 2016. **8**(3): p. 74-85.
74. Putrasari, Y., et al., *Evaluation of performance and emission of SI engine fuelled with CNG at low and high load condition.* Energy Procedia, 2015. **68**: p. 147-156.
75. Simsek, S., S. Uslu, and H. Simsek, *Experimental study on the ability of different biogas level dual fuel spark ignition engine: Emission mitigation, performance, and combustion analysis.* Oil & Gas Science and Technology–Revue d'IFP Energies nouvelles, 2021. **76**: p. 74.
76. Arul Peter, A., et al., *Experimental investigation of a spark ignition engine using blends of biogas.* International Journal of Ambient Energy, 2020. **41**(4): p. 462-465.
77. Awogbemi, O. and S.B. Adeyemo, *Development And Testing Of Biogas-Petrol Blend as an alternative fuel for spark ignition engine.* Int. J. Sci. Technol. Res., 2015. **4**(9): p. 179-186.
78. Mathai, R., et al., *Comparative evaluation of performance, emission, lubricant and deposit characteristics of spark ignition engine fueled with CNG and 18% hydrogen-CNG.* International journal of hydrogen energy, 2012. **37**(8): p. 6893-6900.
79. Chen, L., S. Shiga, and M. Araki, *Combustion characteristics of an SI engine fueled with H2–CO blended fuel and diluted by CO2.* International journal of hydrogen energy, 2012. **37**(19): p. 14632-14639.
80. Park, C., et al., *Performance and emission characteristics of a SI engine fueled by low calorific biogas blended with hydrogen.* International Journal of hydrogen energy, 2011. **36**(16): p. 10080-10088.
81. Babu, M.G. and K. Subramanian, *Alternative transportation fuels: utilisation in combustion engines*. 2013: CRC Press.

82. Kukoyi, T., E. Muzenda, and A. Mashamba. *Biomethane and Bioethanol as alternative transport fuels*. in *presented at the IEC 2014*. 2014.
83. Kukoyi, T., et al. *Biomethane and hydrogen as alternative vehicle fuels: An overview*. in *International Engineering Conference, Nigeria*. 2015.
84. Al Seadi, T., *BioGas Handbook, Esbjerg, University of Southern Denmark Esbjerg.* Available in: http://www. lemvigbiogas. com/BiogasHandbook. pdf, 2008.
85. Ounnar, A., L. Benhabyles, and S. Igoud, *Energetic valorization of biomethane produced from cow-dung.* Procedia Engineering, 2012. **33**: p. 330-334.
86. Yamulki, S., *Effect of straw addition on nitrous oxide and methane emissions from stored farmyard manures.* Agriculture, Ecosystems & Environment, 2006. **112**(2-3): p. 140-145.
87. Yohaness, M.T., *Biogas potential from cow manure.* 2010.
88. Liu, G., *Potential of biogas production from livestock manure in China.* 2011.
89. Tauseef, S., et al., *Methane capture from livestock manure.* Journal of environmental management, 2013. **117**: p. 187-207.
90. Meskini, Z., et al., *Typology, productivity and socio-economic profile of dairy farms in Mostaganem province, Algeria.*
91. Manure, F.D., *Dairy Waste Anaerobic Digestion Handbook.* 2001.
92. Achinas, S., et al., *Influence of sheep manure addition on biogas potential and methanogenic communities during cow dung digestion under mesophilic conditions.* Sustainable Environment Research, 2018. **28**(5): p. 240-246.
93. Angelidaki, I. and B. Ahring, *Thermophilic anaerobic digestion of livestock waste: the effect of ammonia.* Applied microbiology and biotechnology, 1993. **38**(4): p. 560-564.
94. Zhao, C., *Cow manure and biowaste as a biogas substrate: a review.* 2020.
95. Angelidaki, I. and L. Ellegaard, *Codigestion of manure and organic wastes in centralized biogas plants.* Applied biochemistry and biotechnology, 2003. **109**(1): p. 95-105.
96. Zamanzadeh, M., et al., *Biogas production from food waste via co-digestion and digestion-effects on performance and microbial ecology.* Scientific reports, 2017. **7**(1): p. 1-12.
97. Chukwuma, E., et al., *Determination of optimum mixing ratio of cow dung and poultry droppings in biogas production under tropical condition.* African Journal of Agricultural Research, 2013. **8**(18): p. 1940-1948.
98. Ariunbaatar, J., et al., *Enhanced anaerobic digestion of food waste by thermal and ozonation pretreatment methods.* Journal of environmental management, 2014. **146**: p. 142-149.
99. Agyeman, F.O. and W. Tao, *Anaerobic co-digestion of food waste and dairy manure: Effects of food waste particle size and organic loading rate.* Journal of environmental management, 2014. **133**: p. 268-274.
100. Arelli, V., et al., *Dry anaerobic co-digestion of food waste and cattle manure: Impact of total solids, substrate ratio and thermal pre treatment on methane yield and quality of biomanure.* Bioresource technology, 2018. **253**: p. 273-280.
101. Zhang, Y., C.J. Banks, and S. Heaven, *Co-digestion of source segregated domestic food waste to improve process stability.* Bioresource technology, 2012. **114**: p. 168-178.
102. Ibrahim Rahmouni and B. Adouane, *An Experimental Investigation of Raw Biogas Combustion in aSmall Spark Ignition Engine using Cow Manure in Algeria.* Jordan Journal of Mechanical and Industrial Engineering, 2022. **16**(3): p. 353-359.
103. Williamsson, D., *Modularization of Test Rigs*. 2015.
104. Bendu, H. and S. Murugan, *Homogeneous charge compression ignition (HCCI) combustion: Mixture preparation and control strategies in diesel engines.* Renewable and Sustainable Energy Reviews, 2014. **38**: p. 732-746.

105. Winther, J., *Dynamometer Handbook of Basic Theory Applications*. 1975: Eaton Corporation.
106. Company, H.M. *HONDA GX140*. Available from: https://www.wersis.net/honda/gx140.html.
107. Limited, T., *TD 110-115 Mini Engine Test Rigs and Instrumentation*.
108. Makhura, E. Muzenda, and T. Lekgoba. *Effect of co-digestion of food waste and cow dung on biogas yield*. in *E3S Web of Conferences*. 2020. EDP Sciences.
109. Mariani, A., M. Minale, and A. Unich, *Use of biogas containing CH4, H2 and C02 in controlled auto-ignition engines to reduce NOx emissions.* Fuel, 2021. **301**: p. 120925.
110. Muhajir, K., I. Badrawada, and A. Susastriawan, *Utilization of biogas for generator set fuel: Performance and emission characteristics.* Biomass Conversion and Biorefinery, 2019. **9**(4): p. 695-698.
111. Aguiar, P.L.d., et al., *Performance evaluation of biogas fueled generator set.* Journal of the Brazilian Society of Mechanical Sciences and Engineering, 2021. **43**(9): p. 1-12.
112. Zhang, Y., et al., *Combustion and emission characteristics of simulated biogas from Two-Phase Anaerobic Digestion (T-PAD) in a spark ignition engine.* Applied Thermal Engineering, 2018. **129**: p. 927-933.

ANNEX

ANNEX 1: ENGINE TEST RIG SETUP MANUAL

TD110-TD115
Mini Engine Test Rigs and Instrumentation

The equipment described in this manual is manufactured and distributed by

TECQUIPMENT LIMITED

Suppliers of technological laboratory equipment designed for teaching.

BONSALL STREET, LONG EATON, NOTTINGHAM, NG10 2AN, ENGLAND.

Tel: +44 (0)115 9722611 : Fax: +44 (0)115 9731520

E-Mail: General Enquiries: *CompuServe,* mhs:sales@tecquip : *Internet,* sales@tecquip.co.uk
E-Mail: Parts & Service: *CompuServe,* mhs:service@tecquip : *Internet,* service@tecquip.co.uk
Information is available on the Internet at: http://www.tecquip.co.uk

PE/ajp/0197

THE MINI-ENGINE TEST RIGS

The basic test rig for each engine consists of the Engine (TD110, TD111 or TD113), Hydraulic Dynamometer (TD115) and Instrumentation Unit (TD114), as shown in Figure 3.1. A stop-watch, thermometer and barometer are also required but not supplied.

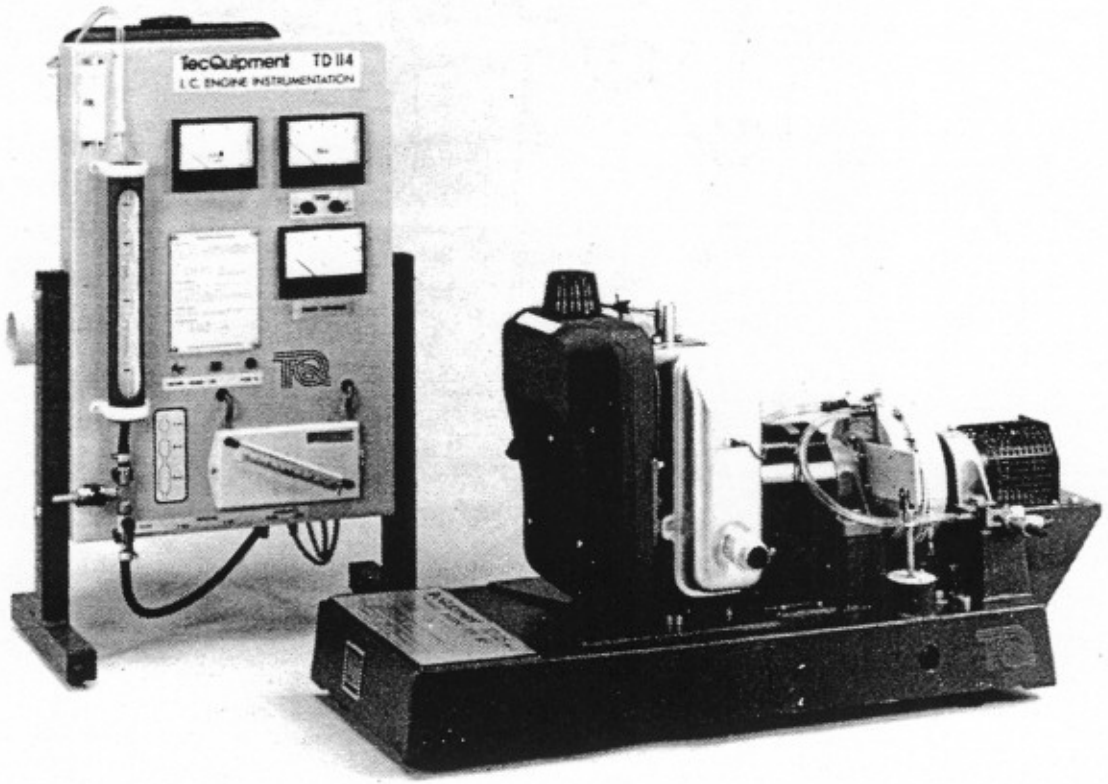

Figure 3.1. TD113 Engine complete with TD114 Instrumentation Unit and TD115 Hydraulic Dynamometer.

The information available from the engine can be extended by fitting the E32 MkII Engine Monitoring System to obtain pressure-volume and pressure-crank angle traces (not supplied).

Instrumentation Unit (TD114)

The Instrumentation Unit is designed to stand beside the engine under test. In addition to housing the instruments necessary for measuring the engine performance, it contains the fuel system and the airbox/viscous flow meter used to measure the consumption of air.

A front view of the Instrumentation Unit is shown in Figure 3.2.

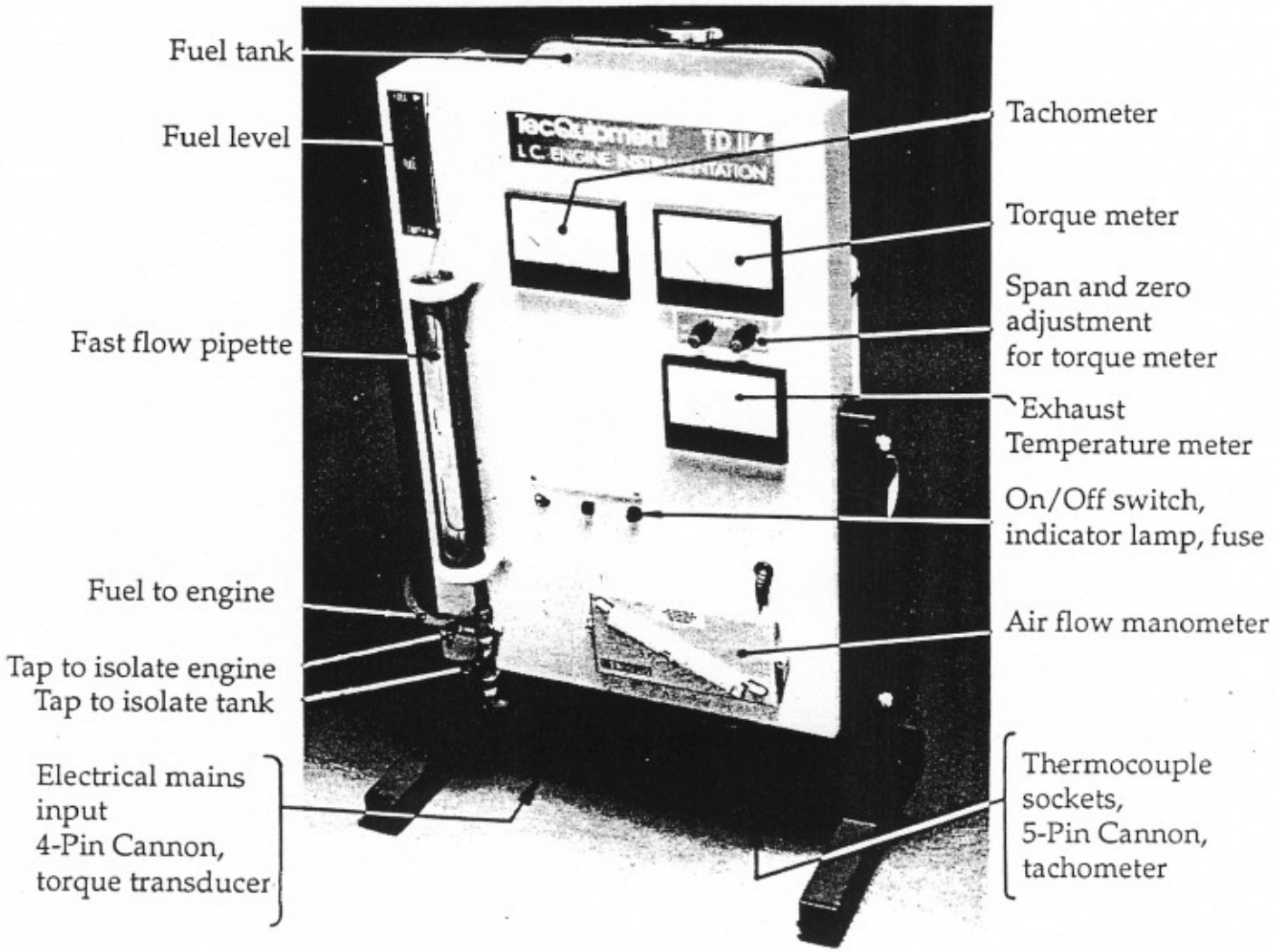

Figure 3.2. TD114 Instrumentation Unit

Measurement of Speed

Engine speed is measured electronically by a pulse counting system. An optical head mounted on the dynamometer chassis contains an infrared transmitter and receiver. A rotating disc with radial slots is situated between the optical source and sensor and, as the engine rotates, the beam is

interrupted. The resulting pulse train is electronically processed to provide a readout of engine speed.

The electronic tachometer is calibrated against a signal generator at the factory and should not need adjusting. However, it is good practice to occasionally check the accuracy of the system. This is readily done by using a hand-held tachometer on the shaft of the dynamometer, having first removed the safety guard.

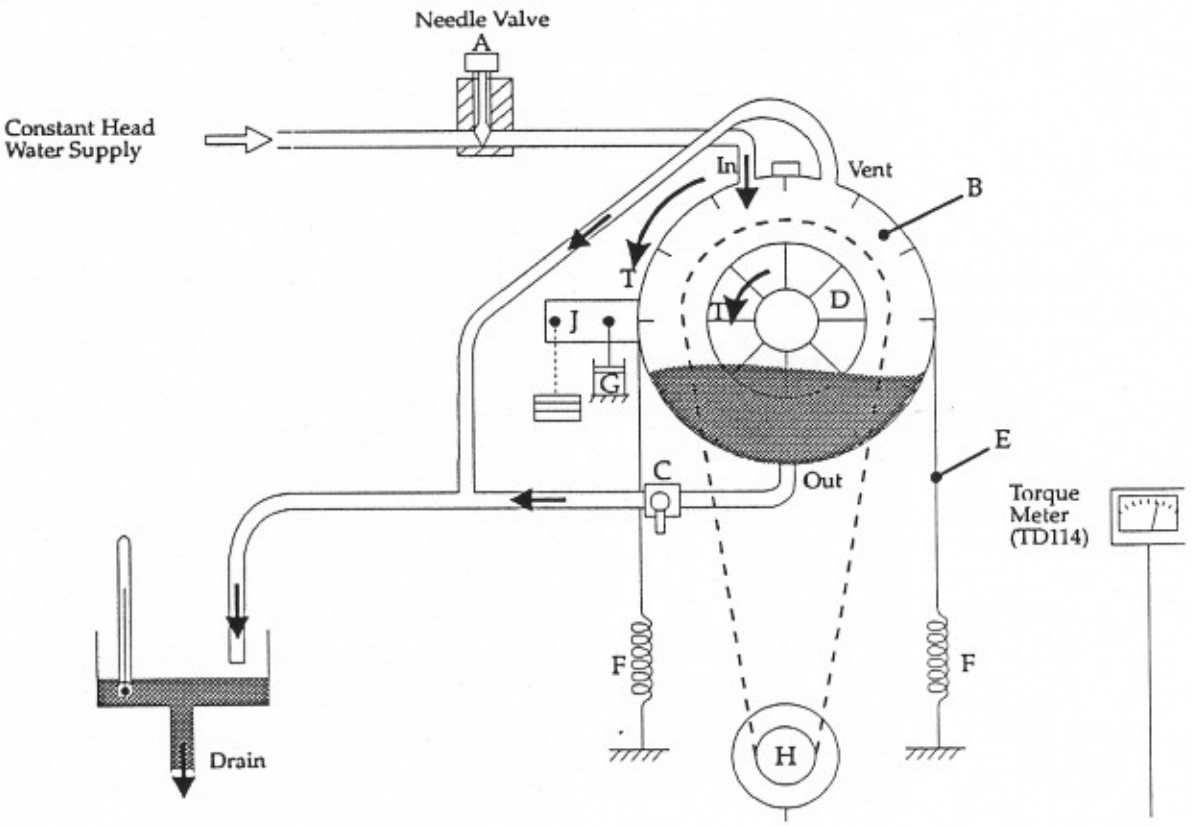

Figure 3.3. Schematic Drawing of Dynamometer and Torque Instrumentation

Hydraulic Dynamometer (TD115) Measurement of Torque

Engine torque is measured by the Hydraulic Dynamometer (TD115) and transmitted to a torquemeter located on the Instrumentation Unit (TD114).

Water Supply

A constant supply of clean water is required, which can be from a header tank, pressure regulated mains tap, or a pump/sump system. The delivery pressure is not too critical, as long as it is between 6 to 12m head (0.6 to 1.2 x 10^5 pa). The figure quoted is not an exact conversion. Typically, the flow rate is 4 litres/min at a head of 6m, using 10mm bore flexible plastic tubing.

TD115 Hydraulic Dynamometer

Figure 3.3 shows the principles and layout of the dynamometer. The flow of water is controlled by a needle valve (A) mounted on the engine bed. Water flows into the top of the dynamometer casing (B) and out through the bottom, discharging into a drain or sump through a tap (C). The dynamometer also has an air vent. The quantity of water in the dynamometer, and hence the power absorbed from the engine, depends on the settings of the needle valve (A) and tap (C).

The dynamometer drain pipe should be as short as possible and run downwards into an open drain or collection tank. The end of the drain pipe must not be submerged.

The engine shaft drives a paddle (D) inside the vaned casing (B) churning up the water inside the dynamometer. If not restrained, the casing would rotate at almost the same speed as the paddle. Restraint is provided by a spring loaded nylon cord (E) which passes round the casing (B) and is clamped to the top of the casing. The two springs (F) have equal stiffness, and are always in tension as the dynamometer casing rotates.

A damper(G) filled with lubricating oil is connected to the casing. The oil level should be checked before running any tests.

The angular position taken up by the casing (B) depends on the torque T and the stiffness of the two springs (F). The peripheral displacement of the casing

is proportional to the torque T and is measured by a rotary potentiometer (H), the output of which is fed into the input of the TD114 torquemeter.

The shaft of the dynamometer is at a centre height of 50mm from the mounting pads of the base casting.

Calibrating the TD114 Torquemeter

Before each engine test:

The torquemeter must be zeroed and calibrated before use. To do this:

1. Set the SPAN control to its maximum clockwise position.

2. Shake or rock the engine vigorously to overcome the stiction of the bearing seals. Vibration does this automatically when the engine is running.

3. Adjust the ZERO control until the torquemeter reads zero.

4. Check that the zero is accurate by shaking the engine again.

5. Hang a load of 3.5kg on the calibration arm (J) of TD115 (Figure 3.3).

6. Shake the engine until the torquemeter reading settles down to a constant value.

7. Adjust the SPAN control to give a torque reading of 8.6Nm.

8. Remove the calibration load and repeat steps 2 to 8 until satisfied that the zero and span settings are correct.

Linearity Calibration

The torque meter reading is obtained from the angular displacement detected by the rotary potentiometer fed into a linear electronic circuit. It is good practice to occasionally check the continuing overall linearity of the system by comparing the indicated torque obtained for a range of applied torques. This is also an exercise that may be given to the student to enhance his understanding of the method of measuring torque.

Follow the list given above, using loads of up to 4kg in increments of 0.5kg, instead of the single value of 3.5kg given in step 5. Record the indicated torquemeter reading for each load.

Calculate the applied torque from the relationship

$$T = mga \qquad \text{(Nm)} \qquad 3.1$$

where T is the applied torque (Nm), m is the applied mass (kg), and a is the distance between the calibration weight and dynamometer shaft (m).

The value of a is 0.25m for the TD115 Hydraulic Dynamometer. Figure 3.4 shows the result of a typical linearity check.

Measurement of Exhaust Temperature

Exhaust gas temperature is measured by a chrome/alumel thermocouple conforming to BS1827. The thermocouple is located in a 1/8" BSP union brazed into the exhaust pipe close to the cylinder block of the engine. Colour coded leads from the thermocouple are connected to terminals underneath the TD114 Instrumentation Unit. The temperature is indicated on a direct reading meter scaled from 0 to 1000°C.

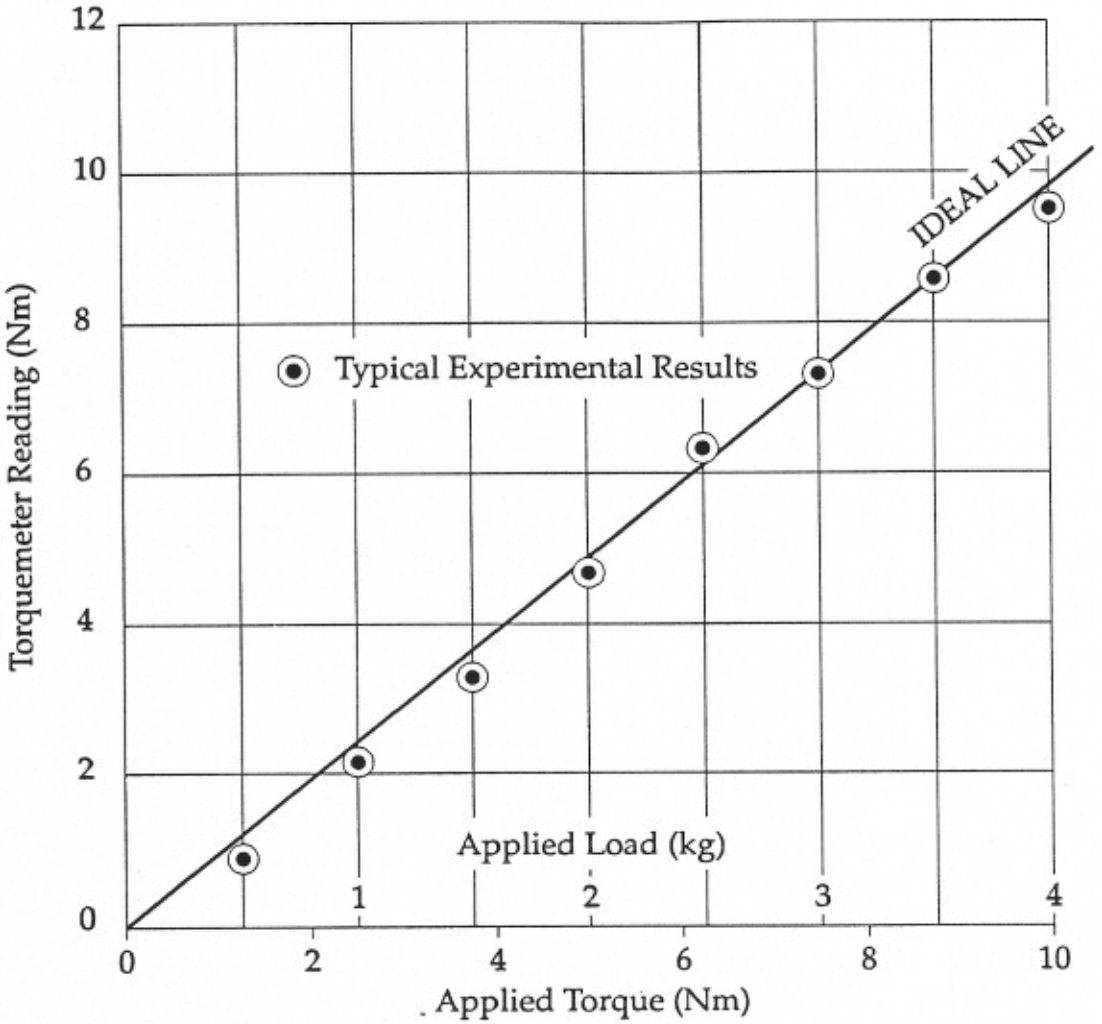

Figure 3.4 Torque Calibration

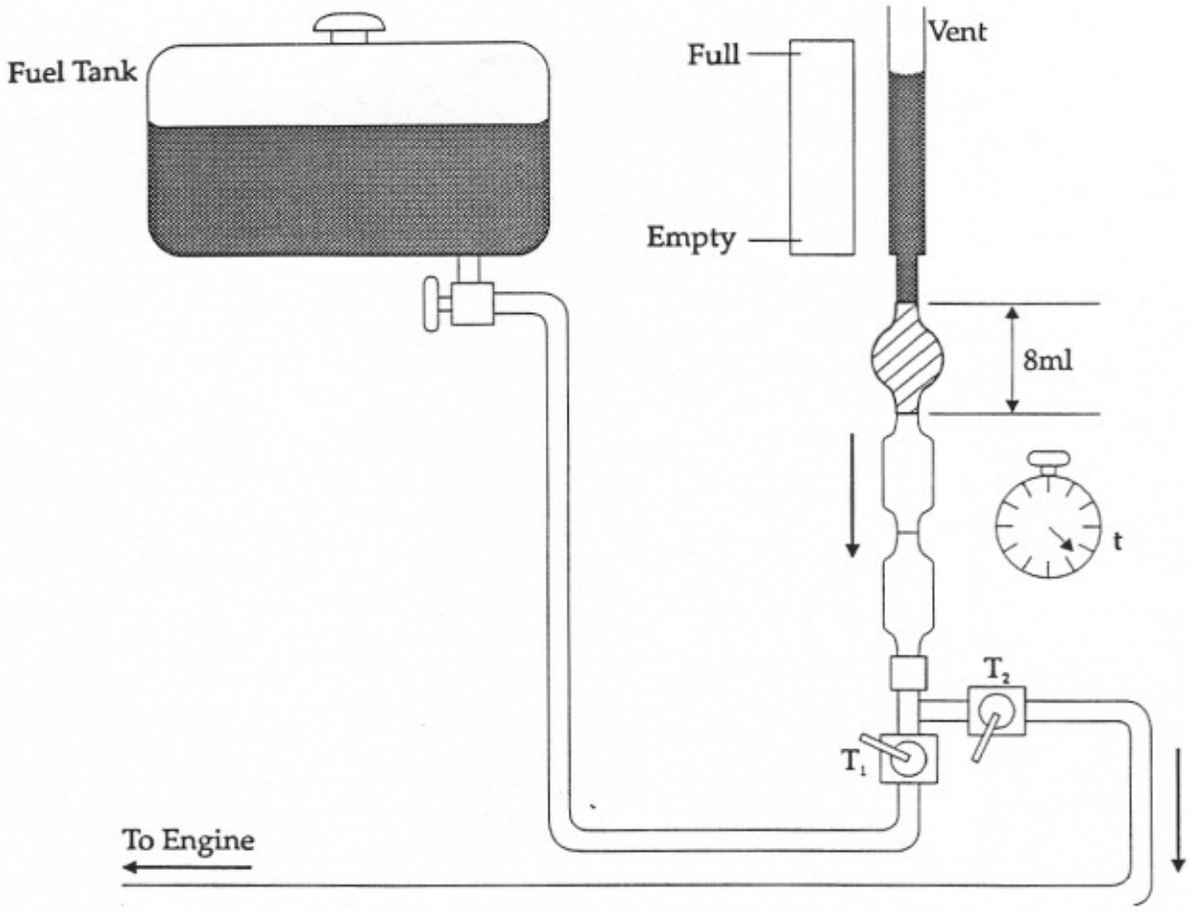

Figure 3.5 The Fuel System.

Fuel System

The fuel system is fed from a 4.5 litre fuel tank mounted on top of the TD114 Instrumentation Unit. Being gravity fed, the engine carburettor must be below the level of the tank. Figure 3.5 shows the fuel system. The lowest mark on the TD114 pipette must be mounted higher than the engine carburettor to ensure that the 32ml reservoir empties completely before the engine cuts out.

The fuel flows into the bottom of a pipette graduated in volumes of 8, 16 and 32ml.

A length of clear plastic tubing connected to the top of the pipette gives an indication of the contents of the fuel tank.

The tap T1 isolates the tank from the engine, enabling fuel to be consumed from the pipette. The fuel consumption is determined by measuring the time (t) taken for the engine to consume a given volume of fuel, say 8ml.

The tap T2 isolates the engine from the fuel supply. This tap should only be closed when the apparatus is not in use.

Assuming a specific gravity for water of 1000 kg/m^3:

$$\dot{m}_f = \frac{sg_f \times 1000 \times (8) \times 10^{-6}}{t} \quad \text{(kg/s)} \qquad 3.2$$

$$\dot{m}_f = \frac{sg_f \times (8) \times 10^{-3}}{t} \quad \text{(kg/s)} \qquad 3.3$$

It is more convenient to express the fuel consumption in units of kg/hr, so that

$$\dot{m}_f = \frac{sg_f \times (8) \times 10^{-3}}{t} \times 3600 \quad \text{(kg/hr)} \qquad 3.4$$

Typical values of specific gravity are:

Petrol	0.74
Petroil (petrol + lubricating oil)	0.741
Diesel fuel	0.84

If the same fuel system is used with both diesel and petrol engines, it is necessary to completely drain and flush the system before filling with the alternative fuel. Put sufficient of the alternative fuel into the tank to fill the system to just above the empty level. Drain off and dispose of the contaminated fuel. Refill with fresh fuel. Before commencing a test, remove any air bubbles that may have collected in the system.

Measurement of Air Consumption

Single cylinder engines tend to induce a pulsating flow of air since the air is being drawn in during only one of two or four strokes. An orifice cannot be used reliably under these conditions, unless a very large damping volume is introduced between the orifice and the engine.

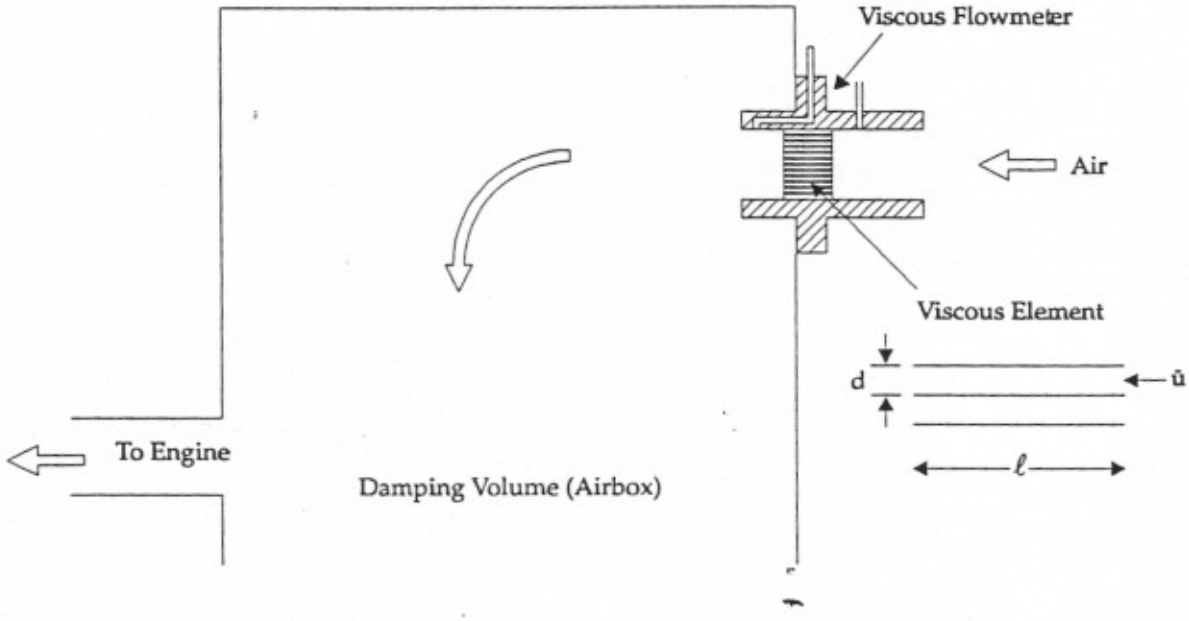

Figure 3.6. Measurement of Air Consumption.

Units are fitted with a viscous flow meter and, with this system, the large damping volume is eliminated. Figure 3.6 shows a sketch of the flow meter. Air is drawn in through an inlet and flows through an element consisting of thousands of small bore tubes before entering the damping volume. The size of the tubes is chosen so that the Reynolds Number (ud/ ν) is less than 2300. This ensures that airflow through the element is entirely viscous, in which case the pressure drop is given in Poiseuille's equation:

$$\Delta p = \frac{32\mu\ell\bar{u}}{d^2} \qquad 3.5$$

For a given air density the mass flow rate of air is proportional to the average velocity, so that the pressure drop across the viscous element is directly proportional to the flow rate, unlike the parabolic relationship associated with an orifice plate. The pressure drop is measured by an inclined tube

manometer, calibrated in millimetres of water. This should be zeroed before running the engine. The viscous flow meter is calibrated at the factory, and a calibration curve is supplied with the engine. Figure 3.7 shows a typical calibration curve for air at 1013mb and 20°C.

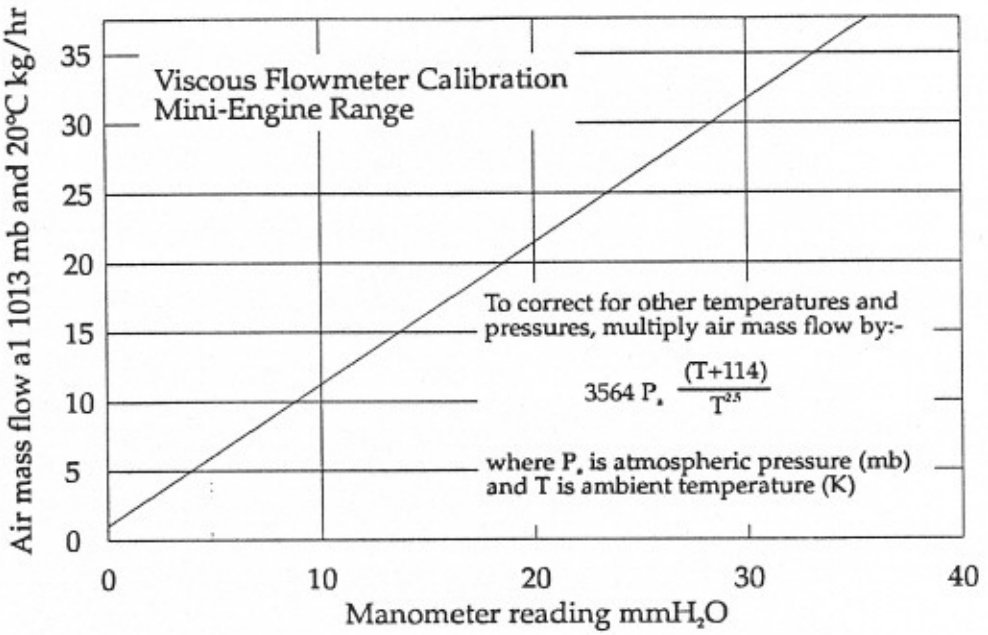

Figure 3.7. Viscous Flow Meter Calibration

Poiseuille's equation forms a basis for correcting flow rates measured at non-standard temperatures and pressures.

The mass flow of air through the pipe is given by:

$$\dot{m}_a = \rho \bar{u} \times \text{area of pipe} \qquad 3.6$$

so that for a given pipe and element:

$$\Delta p = \text{const.} \frac{\mu \dot{m}_a}{\rho} \qquad 3.7$$

Sutherland's formula gives the viscosity of air dependent on absolute temperature only:

$$\mu = \frac{AT^{\frac{3}{2}}}{T+B} \qquad 3.8$$

For air, the constants A and B have the values:

$A = 0.1465 \times 10^{-5}$
$B = 114$

The air density is a function of ambient pressure and temperature:

$$\rho = \frac{P}{RT} \qquad 3.9$$

Combining all of the above equations, the air mass flow is proportional to:

$$\frac{P(T+114)\Delta P}{T^{\frac{5}{2}}} \qquad 3.10$$

For a given pressure difference across the viscous flow meter, the mass flow given on the calibration curve must be factored by:

$$\frac{P_{actual}}{P_{cal}} \cdot \frac{T_{actual}+114}{T_{cal}+114} \cdot \left[\frac{T_{cal}}{T_{actual}}\right]^{\frac{5}{2}} \qquad 3.11$$

Measurement of Air/Fuel Ratio

The air/fuel ratio is calculated from values of air and fuel mass flows obtained from the airflow manometer reading and the time to consume, say, 8ml of fuel. Sections 3.5 and 3.6 explain how this is done.

Electrical Connections

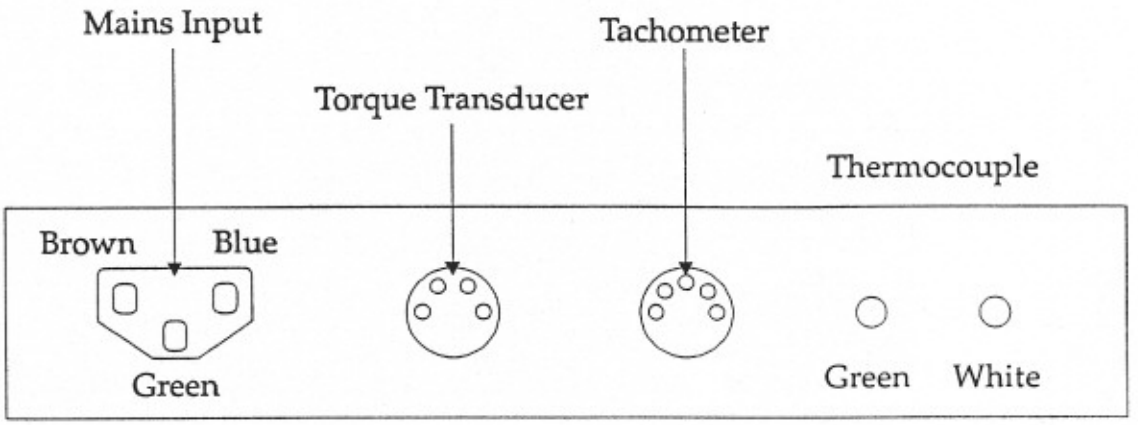

220/240 V a.c
110/120 V a.c
50/60 Hz

4 Way

5 Way

4mm Terminals

Figure 3.8 Electrical Connections to TD114 Instrumentation Unit

Figure 3.8 shows the location of the electrical connections which are situated underneath the front panel. The electronic tachometer and torquemeter are supplied from an internal transformer/rectifier unit, which derives its power from 220/240V or 110/120V, 50/60Hz single phase earthed supply.

The unit is switched on or off by a switch on the front panel, a neon light warning that the supply is switched on. A 1 amp cartridge fuse is located next to the warning lamp. If neither the tachometer nor the torquemeter function, even though the mains supply is switched on, the fuse should be taken out and checked.

The temperature meter does not require an electrical supply, and is powered directly from the emf generated by the thermocouple. Connection to the torque transducer on the dynamometer is made through a four pin Cannon plug/socket.

The tachometer optical head is connected to the instrumentation unit through a 5 pin Cannon plug/socket. It is not possible to connect the leads to the

The leads from the exhaust thermocouple terminate in colour coded terminals. These should be connected to the coloured terminals on the instrumentation unit as indicated below:

Instrumentation Terminal Colour	Thermocouple Lead Colour
White	White or Blue
Green	Green or Brown

EXPERIMENTAL PROCEDURE

Note:

There may be differences between individual experimental test rigs and instrumentation units, consequently discrepancies between the equipment and its description may occur in this manual.

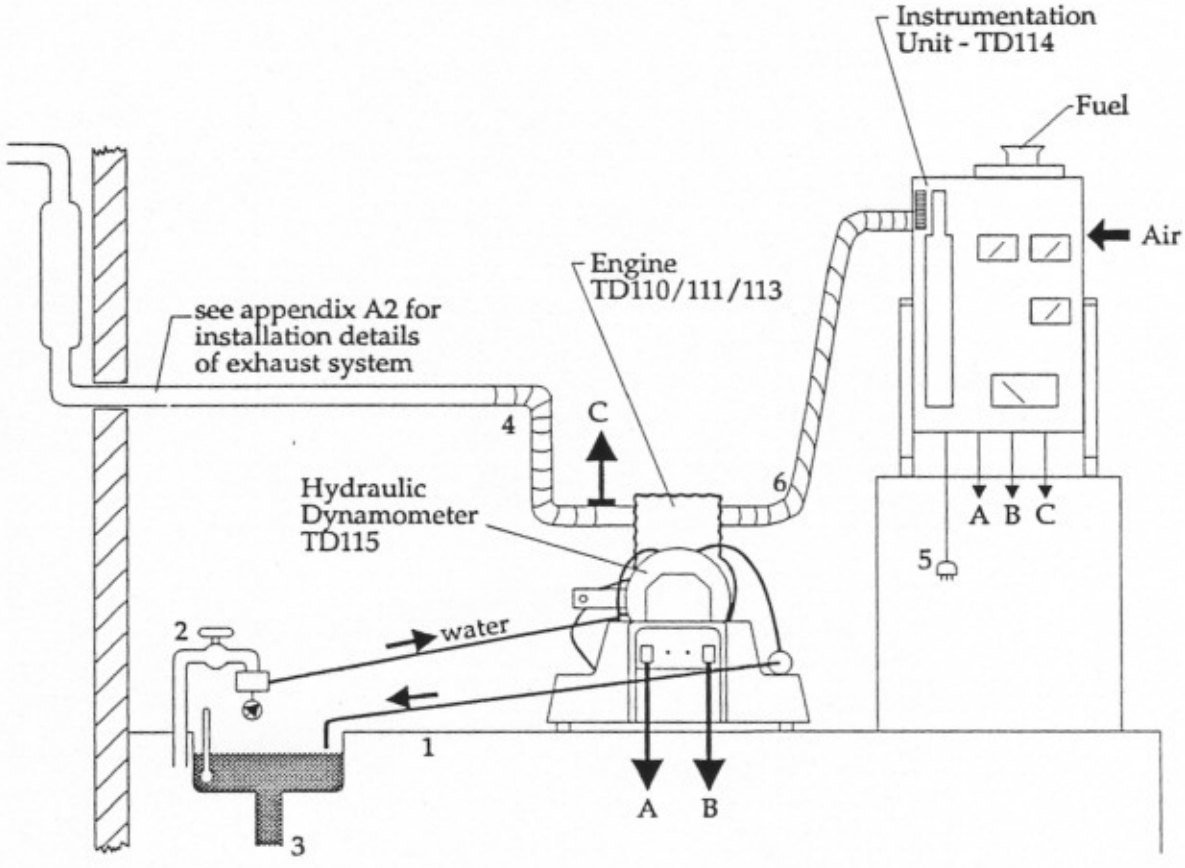

Figure 4.1 The complete mini-engine test rig.

Setting up the Equipment

It is assumed that an area of the laboratory has been equipped with a bench (1), water supply (2), drain (3), exhaust system (4) and an electrical power point (5) (as directed in 'INSTALLATION INSTRUCTIONS', page 8.1).

1. Place the engine to be tested and the TD115 Hydraulic Dynamometer on the bench. To prevent the transmission of vibration to the TD114 Instrumentation Unit, it is recommended that the TD114

Instrumentation Unit is then mounted on a separate bench to the engine and TD115 Hydraulic Dynamometer. The TD114 Instrumentation Unit must be mounted higher than the mini engine and the TD115 Hydraulic Dynamometer.

Note:

To ensure the TD114 Instrumentation Unit functions accurately, the lower 32ml bulb on the Instrumentation Unit must be higher than the reservoir on the carburettor.

2. Connect the engine to the exhaust system (4).

3. Connect the engine air intake to the Instrumentation Unit Airbox using as short a length of flexible pipe (6) as practicable.

4. Connect the torque transducer, tachometer optical head and exhaust thermocouple to the correct inputs on the Instrumentation Unit (A, B and C). If in doubt, refer to Section 3.8 for details of the electrical sockets used.

5. Connect the water supply (2) to the inlet of the needle valve mounted on the engine bed.

6. Push a length of flexible PVC pipe (not supplied) onto the drain pipe and ensure that the end discharges into a drain or collection tank and that it is not submerged when the water is flowing.

7. Check that the damper is full of oil and fill if necessary.

8. Place a thermometer in the drain to measure the temperature of the water discharged from the dynamometer.

9. Ensure that nobody is smoking. 'No smoking' signs should be displayed in a prominent position. (Not supplied).

10. If the engine under test requires different fuel from that in the tank, flush out the fuel system as described in Section 3.5. Fill the tank with the correct type of fuel.

11. (Four stroke engines only - TD110 and TD111).
Check that the engine sump is filled with the correct grade of oil. Do not overfill.

12. Switch on the Instrumentation Unit. Set the zero and span controls as detailed in Section 3.3.

13. Adjust the scale on the airflow manometer to read zero.

14. Turn on the water supply to the dynamometer. Adjust the needle valve so that the maximum flow of water is obtained. This ensures that the dynamometer seals are lubricated.

15. Now reduce the flow of water to a trickle so that the load on the engine is not too great when starting.

16. Remove all tools, weights and obstructions from around the engine to enable access to all controls.

17. Clear the area of personnel not involved in the test.

18. Check that you know how to stop the engine in an emergency. Locate the ignition switch or STOP/RUN lever. Fuel taps should be turned off.

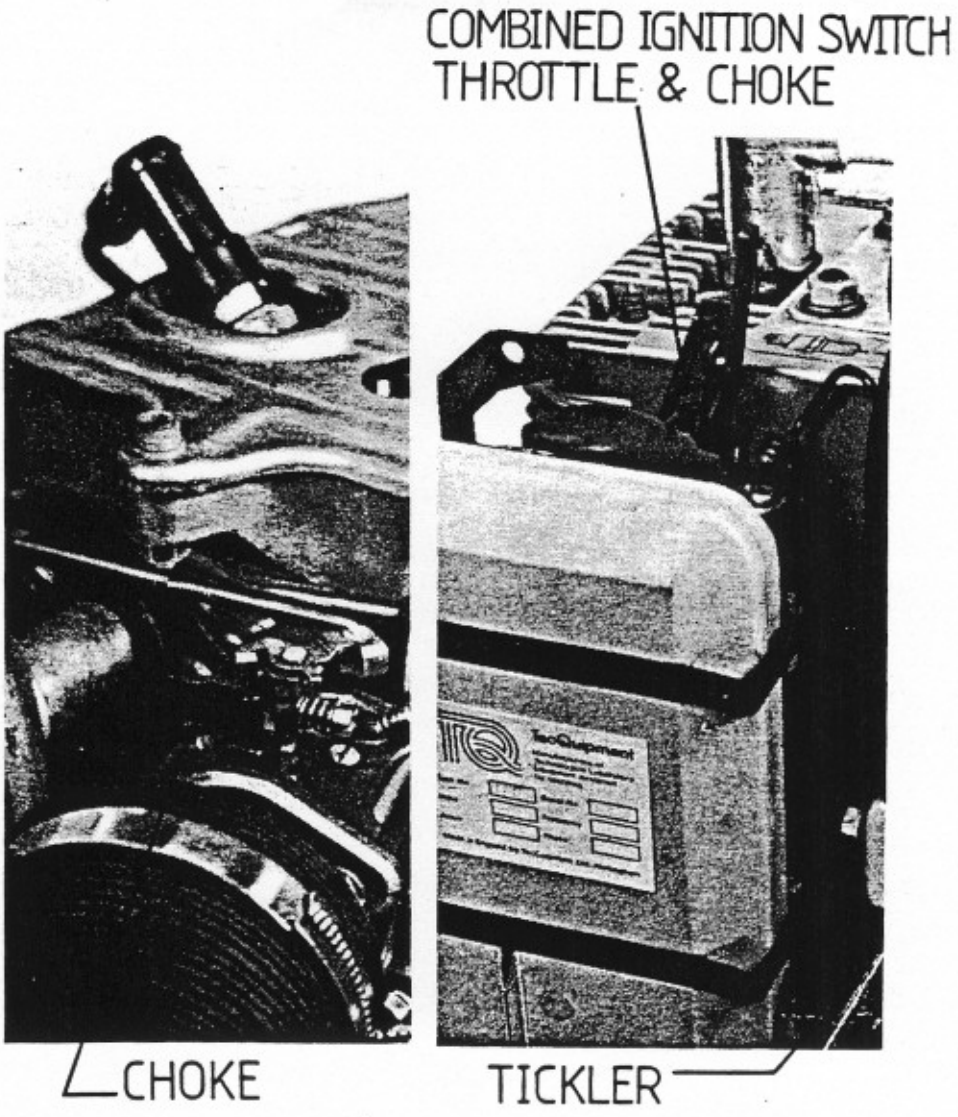

Figure 4.2 Petrol engine controls.

Starting the Engine

The method of starting differs slightly between diesel and petrol engines.

Petrol Engines

1. Turn on the tap of the fuel tank.

2. Ensure that the fuel has reached the carburettor from the fuel tank by depressing the "tickler" control on the carburettor (TD113 only).

3. Release the control as soon as petrol is seen to flow from the carburettor. Figure 4.2 shows the location of the controls on the carburettor of both the TD110 and TD113.

4. Open the throttle a small amount.

5. Switch on the ignition

6 Hold the base and pull the starting handle rapidly outwards. Repeat until the engine runs.

7. Allow the engine to warm up by running at half throttle for about 5 minutes. Return the choke to the 'open' position as soon as the engine will run smoothly without choke.

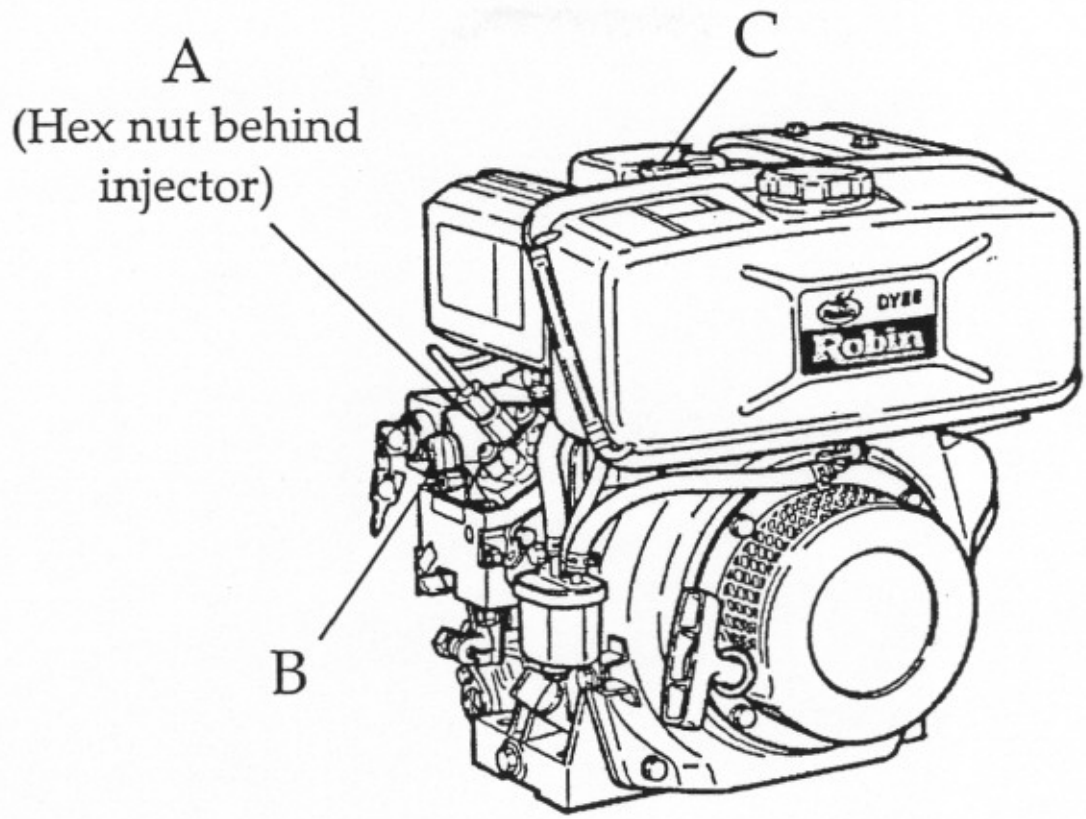

Figure 4.3 Diesel engine controls.

Diesel Engines

1. Turn on the tap of the fuel tank.

2. If the fuel system has been changed, air will have entered the fuel pipes and will prevent the injector pump from working. The air must be removed from the system. To do this (referring to Figure 4.3) loosen the bleed (hex) screw (A) on the top of the fuel pump until clean, bubble-free fuel leaks out. Retighten the screw.

3. Move the LOW/HIGH lever (B) to the 'HIGH' position. This sets the injector to pump an excess of fuel into the engine for starting and is analogous to the choke of a petrol engine.

4. If the engine is cold, it is essential to prime the engine for hand starting.
   (a) Remove the priming plunger (C).

(b) Fill the priming chamber with engine oil - NOT fuel.
This is to reduce leakage past the piston rings and to raise the compression ratio.

(c) Replace the priming plunger and press down.

5. Pull the starting rope to start the engine.

6. Should the engine fire and then stop, prime again (if cold) before attempting to start again.

7. Allow the engine to warm up for about 5 minutes. The excess fuel device resets automatically.

Test Procedure

1. Advance the throttle or rack control to its maximum position.

2. Note the maximum speed of the engine. (The dynamometer water flow should still be the trickle used for starting).

3. Keep the throttle or rack open and slowly adjust the needle valve to increase the flow of water through the dynamometer until the needle valve is fully open. Note the engine speed.

4. Assume, for the time being, that the engine will be tested over the speed range just established. Choose at least five speeds between the two extremes at which to take readings of engine performance.

5. Keep the throttle open and reduce the water flow to a trickle, so that the engine returns to its maximum speed.

6. When the engine has settled down to a steady output, record the readings of speed, torque, exhaust temperature and air consumption. Operate the fuel tap beneath the pipette so that the engine takes its fuel from the pipette. Time the consumption of 8ml of fuel. Turn the tap so that the pipette again fills. Enter the results in Table 4.1.

7. Check that the temperature of the water flowing out of the dynamometer is less than 80°C. If the temperature is higher than this, increase the water flow to cool the dynamometer bearing seals.

8. Increase the flow of water into the dynamometer until the engine speed drops to the next highest selected value. Because the time response of the dynamometer is fairly slow, the needle valve has to be operated slowly.

9. Allow time for the engine speed to stabilise before taking another set of results. If the dynamometer is too sensitive to obtain the desired speed, it will help if the drain tap is partially closed. Do NOT close fully.

10. Repeat paragraph 8 until the dynamometer needle valve is fully open.

11. Study the torque results. Engines normally produce a maximum torque at a certain speed. If your results suggest that the maximum is at a lower speed than you have reached, restrict the water flow from the dynamometer.

Stopping the Engine

1. Reduce the water flow through the dynamometer to a trickle.

2. Close the throttle or rack control until the engine is running at a fast idling speed.

3. Allow the engine to run for a few minutes.

4. Completely close the throttle or rack control. For petrol engines, switch off the ignition. If the engine is a diesel, move the STOP/RUN lever to the STOP position.

5. Close the main fuel tap at the fuel tank.

6. Obtain the values of ambient temperature and pressure and record in Table 4.1 for use in calculating the engine performance.

Special note for diesel engines:

Never stop a diesel engine by running the tank dry or using the decompressor lever. Also, never operate the excess fuel lever whilst the engine is running.

ANNEX 2: GX140 ENGINE MANUAL

1. SPECIFICATIONS

1. SPECIFICATIONS

MODEL / TYPE	WH15X	WH20X	
	C, D, DX	C, D, DX	DF
Overall length	430 mm (16.9 in)	435 mm (17.1 in)	520 mm (20.5 in)
Overall width	360 mm (14.2 in)	375 mm (14.8 in)	400 mm (15.7 in)
Overall height	400 mm (15.7 in)	400 mm (15.7 in)	450 mm (17.7 in)
Dry weight	22.0 kg (48.5 lb)	23.5 kg (51.8 lb)	27.0 kg (59.5 lb)
Operating weight (incld. gas, oil)	24.5 kg (54.0 lb)	26.5 kg (58.4 lb)	30.0 kg (66.1 lb)

ENGINE

		WH15X	WH20X
Model		HONDA engine GX110	HONDA engine GX140
Type		4-stroke, overhead valve single cylinder, inclined by 25°	←
Total displacement		107 cm^3 (6.6 cu in)	144 cm^3 (8.8 cu in)
Bore and stroke		57 × 42 mm (2.2 × 1.7 in)	64 × 45 mm (2.5 × 1.8 in)
Max. horsepower		2.6 kw/3600 min^{-1} (3.5 HP/3600 rpm)	3.8 kw/3600 min^{-1} (5.0 HP/3600 rpm)
Max. torque	Crank PTO	6.9 N.m (70 kg-cm, 5.1 ft-lb)/2500 rpm	9.8 N.m (100 kg-cm, 7.2 ft-lb)/2500 rpm
Compression ratio		8.75 : 1	←
Cooling system		Forced-air cooling	←
Ignition system		Transistorized magneto ignition	←
Ignition timing		25° B.T.D.C.	←
Spark plug		BP6 ES (NGK), W20EP-U (ND) BPR6 ES (NGK), W20EPR-U (ND)	←
Carburetor		Horizontal type, butterfly valve	←
Air cleaner		Semi-dry type	←
Governor		Centrifugal	←
Lubricating system		Forced splash type	←
Oil capacity		0.6ℓ (0.63 USqt, 0.53 Imp.qt)	←
Starting system		Recoil starter	←
Stopping system		Primary circuit ground	←
Fuel used		Regular gasoline (lead-free)	←
Fuel tank capacity		2.5ℓ (0.66 US gal, 0.55 Imp.gal)	3.6ℓ (0.95 US gal, 0.79 Imp. gal)
PTO shaft rotation		Counterclockwise (from PTO side)	

Date of Issue: Jan., 1985

WATER PUMP

	WH15X	WH20X
Type	Self-feed, suction pump	←
Drive system	Direct coupled	←
Suction apeature	40 mm (1.6 in)	50 mm (2 in)
Discharge apeature	40 mm (1.6 in)	50 mm (2 in)
Total head lift (max.)	50 m (164 ft)	←
Suction head lift (max.)	8 m (26.2 ft)	←
Maximum discharge capacity	400 ℓ (106 US gal)	500 ℓ (132 US gal)
Self-feed time	40 sec./5 m (15.4 ft)	60 sec./5 m (15.4 ft)
Rating speed	3,000 min^{-1} (rpm)	3,850
No load maximum speed	3,950 min^{-1} (rpm)	3,950 min^{-1} (rpm)
Fuel consumption	1.0 ℓ (0,26 US gal)/hr.	1.5 ℓ (0.4 US gal) /hr.
Priming water capacity	2.3 ℓ (0.6 US gal)	←

Date of Issue: Jan., 1985

MAINTENANCE STANDARDS

Part	Item	WH15X		WH20X	
		Standard	Service limit	Standard	Service limit
Engine	Max. rpm	3,950 ± 100 rpm	–	3,950 ± 100 rpm	
	Idle speed	1,400 $^{+200}_{-150}$ rpm	–	←	
	Cylinder compression	6.0~8.5 kg/cm³ (600 rpm)		←	
Cylinder	Sleeve ID	57.000 ~ 57.015mm (2.2441 ~ 2.2447 in)	57.165mm (2.2506 in)	64.0 ~ 64.015mm (2.5197 ~ 2.5202 in)	64.165mm (2.5262 in)
Piston	Skirt OD	56.965 ~ 56.985mm (2.2427~ 2.2435 in)	56.55mm (2.226in)	63.965 ~ 63.985mm (2.5183~ 2.5191 in)	63.55mm (2.502in)
	Piston-to-cylinder clearance	0.015 ~ 0.050 mm (0.0006 ~ 0.0020 in)	0.12mm (0.005 in)	←	←
	Piston pin bore ID	13.002 ~ 13.008mm (0.5119 ~ 0.5121 in)	13.048mm (0.5137 in)	18.002 ~ 18.008mm (0.7087 ~ 0.7090 in)	18.048mm (0.7105 in)
	Pin OD	12.994 ~ 13.0mm (0.5116~ 0.5118 in)	12.954mm (0.510in)	17.994 ~ 18.0mm (0.7084 ~ 0.7087in)	17.954mm (0.7068 in)
	Pin-to-pin bore clearance	0.002 ~ 0.014mm (0.0001 ~ 0.0006in)	0.08mm (0.0031in)	0.002 ~ 0.014mm (0.0001 ~ 0.0006in)	0.06mm (0.0024in)
Piston rings	Ring width top/second	1.5mm (0.06 in)	1.37mm (0.054in)	←	←
	Oil	2.5mm (0.10 in)	2.37mm (0.093in)	←	←
	Ring side clearance	0.015 ~ 0.045mm (0.0006 ~ 0.0018in)	0.15mm (0.006in)	←	←
	Ring end gap top/second	0.2 ~ 0.4mm (0.008 ~ 0.016in)	1.0mm (0.04 in)	←	←
	Oil	0.15 ~ 0.35mm (0.006 ~ 0.014in)	1.0mm (0.04 in)	←	←
Connecting rod	Small end ID	13.005 ~ 13.020mm (0.5120~ 0.5126 in)	13.07mm (0.5146 in)	18.005 ~ 18.020mm (0.7089 ~ 0.7094in)	18.07mm (0.711in)
	Connecting rod-to-piston pin clearance	0.005 ~ 0.026mm (0.0002 ~ 0.001in)	0.08mm (0.0031in)	←	←
	Big-end oil clearance	0.04 ~ 0.063mm (0.0016~ 0.0025 in)	0.12mm (0.0047in)	←	←
	Big-end axial clearance	0.1 ~ 0.7mm (0.004 ~ 0.028 in)	1.1mm (0.0433in)	←	←
Crankshaft	Crankpin OD	26.0mm (1.024in)	25.92mm (1.020in)	30.0mm (1.181in)	29.92mm (1.178in)
Valves	Tappet clearance IN	0.15 ± 0.02mm (0.006 ± 0.0008in)		←	
	EX	0.20 ± 0.02mm (0.008 ± 0.0008in)		←	
	Stem OD IN	5.468 ~ 5.480mm (0.2153 ~ 0.2157 in)	5.318mm (0.2094 in)	←	←
	EX	5.425 ~ 5.440mm (0.2136 ~ 0.2142 in)	5.275mm (0.2077 in)	←	←
	Guide ID IN/EX	5.500 ~ 5.512mm (0.2165 ~ 0.2170 in)	5.562mm (0.2190 in)	←	←
	Stem clearance IN	0.020 ~ 0.044mm (0.0008 ~ 0.0017 in)	0.10mm (0.004 in)	←	←
	EX	0.060 ~ 0.087mm (0.0024 ~ 0.0034in)	0.12mm (0.005 in)	←	←
	Seat width	0.8mm (0.031 in)	2.0mm (0.079in)	←	←
	Spring free length	34.0mm (1.339in)	32.5mm (1.280in)	←	←
Camshaft	Cam height IN	22.70 mm (1.091 in)	27.45mm (1.081in)	←	
	EX	27.75mm (1.093in)	27.50mm (1.083in)	←	
	Journal OD	14.00 mm (0.551 in)	13.916mm (0.5479 in)	←	←
Carburetor	Main jet	# 60	–	# 68	
	Float height	13.7 ± 1.5mm (0.54 ± 0.06in)		←	
	Pilot screw opening	2-1/4 turns	–	1 turn	
Spark plug	Gap	0.7 ~ 0.8 mm (0.028 ~ 0.031 in)		←	
Transistorized ignition coil	Secondary no load voltage	15kV/300rpm	13kV/300rpm	←	←
	Resistance values				
	Primary side	0.8 ± 0.1Ω		←	←
	Secondary side	7.0 ± 0.7 kΩ		←	←
	Clearance to flywheel (air gap)	0.4 ± 0.2mm (0.016 ± 0.008in)		←	

Date of Issue: June, 1986

TORQUE VALUES

Unit: N.m (kg-cm, ft-lb)

ITEM		THREAD DIAMETER	TORQUE
Connecting rod bolt		7 mm special bolt	11–13 (110–130, 8.0–9.4)
Cylinderhead bolt		8 mm bolt	22–26 (220–260, 15.9–18.8)
Flywheel nut		14 mm special bolt	70–80 (700–800, 50.6–57.9)
Pivot lock nut		6 mm special nut	8–12 (80–120, 5.8–8.7)
Pivot bolt		6 mm special bolt	8–12 (80–120, 5.8–8.7)
Crankcase cover bolt	WH15X	6 mm CT bolt	10–14 (100–140, 7.2–10.7)
	WH20X	8 mm bolt	22–26 (220–260, 15.9–18.8)
Fuel strainer joint nut		10 mm special nut	2–3 (20–30 , 1.4–2.2)
Muffler attachment nut		8 mm nut	22–26 (220–260, 15.9–18.8)
Inlet pipe		8 mm bolt	20–28 (200–280, 14.5–20.2)
Outlet pipe		8 mm bolt	20–28 (200–280, 14.5–20.2)
Impeller		16mm nut	20–30 (200–300, 14.5–21.7)
Volute case		6 mm cap nut	8–12 (80– 120, 5.8– 8.7)
Carrying handle nut		14 mm nut	20–30 (200–300, 14.5–21.7)
Standard torque		5 mm bolt, nut	4–7 (40–70 , 2.9–5.1)
		6 mm bolt, nut	8–12 (80–120, 5.8–8.7)
		8 mm bolt, nut	20–28 (200–280, 14.5–20.2)
		10 mm bolt, nut	35–40 (350–400, 25.3–28.9)

- Standard torque should be referred to in the case of bolts and nuts which are not specially specified.
- (CT) indicates a self-tapping bolt

Date of Issue: Jan., 1985